Chalcogen controlled redox behaviour in *peri*-substituted S, Se and Te naphthalene derivatives†

Tracey L. Roemmele, Fergus R. Knight, Ellis Crawford, Stuart D. Robertson, Bela E. Bode, Michael Bühl, Alexandra M. Z. Slawin, J. Derek Woollins and René T. Boeré

Electronic Supporting Information

Table of Contents

Chart S1 – Graphical Index to Compound Identities

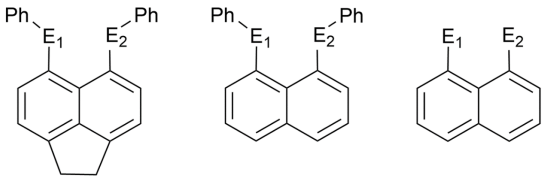

	E_1	E_2		E_1	E_2		E_1	E_2
A1	S	S	**N7**	S	S	**N13**	PhSe	Br
A2	Se	Se	**N8**	Se	Se	**N14**	PhSe	I
A3	Te	Te	**N9**	Te	Te	**N15**	PhTe	Br
A4	S	Se	**N10**	S	Se	**N16**	PhTe	I
A5	S	Te	**N11**	S	Te	**N17**	$Ph_2P(S)$	PhSe
A6	Se	Te	**N12**	Se	Te	N18	PhS(O)	PhS(O)

Index of syntheses and crystal structures (with Refcodes, special notes, *d*E···E):

A1 Aschenbach, *Dalton Trans.,* 2012 (incl. the Br and I analogs with ACEN of **15**-**18**). Xray WARKIL, AB *Z*'=2 3.274(4), 3.288(4).

A2 L. K. Aschenbach, F. R. Knight, R. A. M. Randall, D. B. Cordes, A. Baggott, M. B_hl, A. M. Z. Slawin, J. D. Woollins, *Dalton Trans*. 2012, 41, 3141 – 3153. Xray WARKOR AB 3.1834(7)

A3 Aschenbach, *Dalton*, 2012. Xray WARKUX AB 3.367(2)

A4 Aschenbach, *Dalton*, 2012. Xray WARLAE AB 3.113(4)

A5 Aschenbach, *Dalton*, 2012. Xray WARLEI AB 3.158(1)

A6 Aschenbach, *Dalton*, 2012. Xray WARLIM AB 3.248(2)

N7 Prepared by Nagy: P. Nagy, D. Szab_, I. Kapovits, Kucsman, G. Argay, A. Klmn, *J. Mol. Struct.* 2002, 606, 61.* Xray LUFCIY ($P2_1/c$) & LUFCIY01 ($P2_12_12_1$) both AB 3.0044(6); 3.021(2)

N8 S. Hayashi, W. Nakanishi, *Bull. Chem. Soc. Jpn.* 2008, 81, 1605.; S. Hayashi, W. Nakanishi, A. Furuta, J. Drabowicz, T. Sasamori, N. Tokitoh, New J. Chem. 2009, 33, 196. Xray POPCON AB 3.135(1)

N9 H.Fujihara, H.Ishitani, Y.Takaguchi, N.Furukawa, *Chem.Lett.* (1995), 571, doi:10.1246/cl.1995.571 ** Xray ZODNIP CCt 3.287 (2) (the torsion angles are +132.5, -124.8°)

N10 F. R. Knight, A. L. Fuller, M. Buhl, A. M. Z. Slawin, J. D. Woollins, *Chem. Eur. J.* 2010, 16, 7503 –7516 Xray MUWVOQ ($Pca2_1$), MUWVOQ01 ($P2_12_12_1$) both AB 3.063(2); 3.030(1)

N11 F. R. Knight, A. L. Fuller, M. Bühl, A. M. Z. Slawin, J. D. Woollins, *Chem. Eur. J.* 2010, 16, 7503 –7516. Xray MUWVUW AB Z'=2 3.098(1), 3.068(2)

N12 F. R. Knight, A. L. Fuller, M. Bühl, A. M. Z. Slawin, J. D. Woollins, *Chem. Eur. J.* 2010, 16, 7503 –7516. Xray MUWWAD AB Z'=2 3.158(2), 3.192(2)

N13 F. R. Knight, A. L. Fuller, M. Bühl, A. M. Z. Slawin, J. D. Woollins, *Chem. Eur. J.* 2010, 16, 7605 –7616. Xray CIKPUI B 3.1136(6) (but the torsion angle is 159.2°, so almost C).

N14 F. R. Knight, *e.a*., *Chem. Eur. J.* 2010, 16, 7605 –7616. Xray CUZDOR B 3.2524(8) (torsion 157°)

N15 F. R. Knight, A. L. Fuller, M. Buhl, A. M. Z. Slawin, J. D. Woollins, *Chem. Eur. J.* 2010, 16, 7605 –7616. Xray CUZDUX B 3.191(1) (torsion is 160 deg, so borderline C,B)

N16 F. R. Knight*, e.a.*, *Chem. Eur. J.* 2010, 16, 7605 –7616. Xray CUZFAF B 3.315(1) (torsion is 158.1, so C)

N17 Knight, CEJ, 2010, 7617. Xray MUXGOC AAc 3.2803(9); *d*(centroid-plane) = 3.383; 3.518

N18 Knight, CEJ, 2010, 7503. IP not given; estimated to be 9.16 eV from DeltaE thermal. Xray MUWWIL ACc 3.076(2) (torsion angles are 70.4 and 137.6°)

* The RadCat-$AlOR_4$ salt is Zhang 2014 *JACS*.

** $N9^{2+}$ prepared by these same authors but not structurally characterized.

Note that all these predominantly AB structures have the E substituents distorted towards *trans*. Never *cis*.

Section 1. Voltammetry Data and Methods

Solution electrochemical potentials for naphthalene and acenaphthene

Obtaining potentials for the parent polycyclic aromatics is not as easy as it seems. For the most common: naphthalene, anthracene etc., data are compiled in standard sources. For example, P. Vanysek, *Electrochemical Series* in Section 8, Analytical Chemistry, CRC Handbook of Chemistry and Physics, 85th Ed., D. R. Lide, Ed., CRC Press, Boca Raton, 2004. However, neither the method nor the medium is necessarily comparable to the experiments of interest. From the sources we have cited, the following results pertain:

Compound	**E^{red}, V**	**Conditions**	**E^{red}, $_{Fc+/0}$, V**	**E^{ox}, V**	**Conditions**	**E^{0x}, $_{Fc+/0}$, V**	**Ref.**
Naphthalene	-2.50	CH_3CN SCE, DME 0.1 M 0.1 M iPr_4NClO_4	-2.83	+1.54	CH_3CN SCE, Pt RDE, 0.1 M iPr_4NClO_4	+1.16	1
Naphthalene	-2.61	CH_3CN SCE	-2.99	+1.72	CH_3CN SCE	+1.72	2
Naphthalene	—	—	—	+1.65	Acetone/water Ag^+/AgCl	+1.47	3
Naphthalene (best est.)		CH_2Cl_2	-3.09		CH_2Cl_2	+1.37	
Acenaphthene	0	—	—	+1.39	Acetone/water Ag^+/AgCl	+1.39	3
Acenaphthene	-2.83	THF Ag wire	-3.24	—	—	—	Gray
Acenaphthene (best est.)		CH_2Cl_2	-3.34		CH_2Cl_2	+1.11	

* Diff. of +0.1 V between CH_2Cl_2 and CH_3CN for the $Fc^{+/0}$ redox couple.

Solution electrochemical potentials for Type I naphthalene[1,8-*cd*] (or acenaphthene[5,6-diyl] dichalcogenoles, I (E = S, Se, Te)* (compiled from the literature) [5 - 12]

	Redox couples	S,S	Se,Se	Te,Te
Napthalene series	+2/+1	0.53	0.40	0.02
	+1/+2	0.78	0.36	-0.13
	0/-1	-2.88/ -2.99	0.21	0.14
	-1/-2			
Acenapthenes	+2/+1	0.68	0.87	0.24
	+1/+2	0.42	0.53	0.12
	0/-1	-3.24	-1.36	0.22

* Original data converted to the $Fc^{+/0}$ scale.

References

1. A. Zweig and A. K. Hoffmann, *J. Org. Chem.*, 1965, **30**, 3997.
2. N. V. Vasilieva, I. G. Irtegova, T. A. Vaganova and V. D. Shteingarts, *J. Phys. Org. Chem.* 2008, **21**, 73.
3. R. E. Sioda and B. Frankowska, *J. Electroanal. Chem.*, 2008, **612**, 147.
4. D. G. Gray, *An investigation of electoanalytical techniques applicable to electrolytic polymerizations*, PhD Thesis, 1968 (University of Manitoba, Canada).
5. H. Fujihara, M. Yabe, J-J. Chiu and N. Furukawa, *Tetrahedron Lett.* 1991, **32**, 4345.
6. B. K. Teo, F. Wudl, J. H. Marshall and A. Krugger, *J. Am. Chem.Soc.*, 1977, **99**, 2349.
7. K. Bandyopadhyay, M. Sastry, V. Paul, and K. Vijayamohanan, *Langmuir*, 1997, **13**, 866.
8. T. Inamasu, D. Yoshitoku, Y. Sumi-otorii, H. Tani and N. Ono, *J. Electrochem. Soc.*, 2003, **150**, A128.

9. L. Zhang, S. M. Fakhouri, F. Liu, J. C. Timmons, N. A. Ran and A. L. Briseno, *J. Mater. Chem.*, 2011, **21**, 1329.
10. W. Ji, S. Jing, Z. Liu, J. Shen, J. Ma, D. Zhu, D. Cao, L. Zheng and M. Yao, *Inorg. Chem.*, 2013, **52**, 5786.
11. D. J. Press, T. G. Back, T. C. Sutherland, *Tetrahedron Lett.*, 2012, **53**, 1603.
12. T. Sarukawa and N. Oyama, *J. Electronal. Chem.*, 2010, **647**, 204.
13. F. B. Bramwell, R. C. Haddon, F. Wudl, M. L. Kaplan, J. H. Marshall, *J. Am. Chem. Soc.*, 1978, **100**, 4612.

Further details on voltammetry of the compounds A1 – N18

All compounds were sufficiently soluble in CH_2Cl_2 to give clear to yellow-coloured solutions at analytical concentrations in 0.4 M [^{n}Bu$_4$N][PF$_6$]. In each case there were at least one, and up to three, oxidation processes evident and no reduction processes up to the solvent electrolyte limit (−2.4 V). Similar behavior was seen for all eighteen compounds using both the glassy carbon (GC) and platinum (Pt) working electrodes. A representative CV trace is provided for each sample with the annotations employed in the Table 1 (main article). Exhaustive CVs exploring the full anodic and cathodic potential ranges, and the effect of increased scan rates up to 20 V/s have been undertaken. In addition, each compound and electrode was also investigated using Osteryoung Square Wave Voltammetry (SWV), which excels at resolving peaks that are closely overlapped. In those cases where the redox potentials are found too close to 0 V vs. $Fc^{+/0}$, cobaltocenium hexafluorophosphate was employed as an alternative standard, with the potentials recorded on the $Fc^{+/0}$ scale using reliable conversion factors.

In the case of **A1** three oxidation processes were present. The first oxidation process displayed a moderately large return wave which did not grow with increasing scan rate (Figure S1). The second oxidation process was irreversible at scan rates below 10 V s^{-1}. At scan rates of 10 V s^{-1} or higher a minor return wave appeared. The third oxidation process was irreversible at all scan rates.

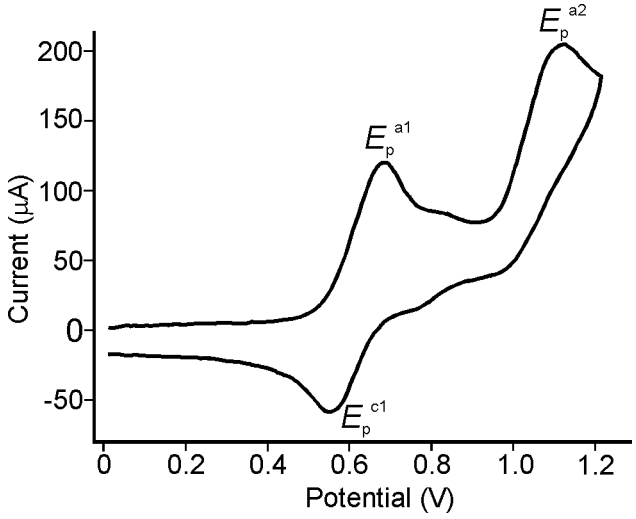

Figure S1. Cyclic voltammogram of a 5.4 mM solution of **A1** in CH_2Cl_2 (0.4 M [^{n}Bu$_4$N][PF$_6$]), ν = 0.2 V s^{-1}, T = 22.4 °C on a GC electrode.

Compound **A2** also displayed three oxidation processes. The first oxidation process had a large return wave over all scan rates, the second had a moderate return wave which grew slightly in peak current height with increasing scan rate, and the third process was irreversible at all scan rates and close to the solvent electrolyte limit (Figure S2). The electrochemical response was the same for both samples (old and new) but the second oxidation appears a bit sharper in the new sample even though the actual distance E_p^{a1} to E_p^{a2} is the same for both (280 mV).

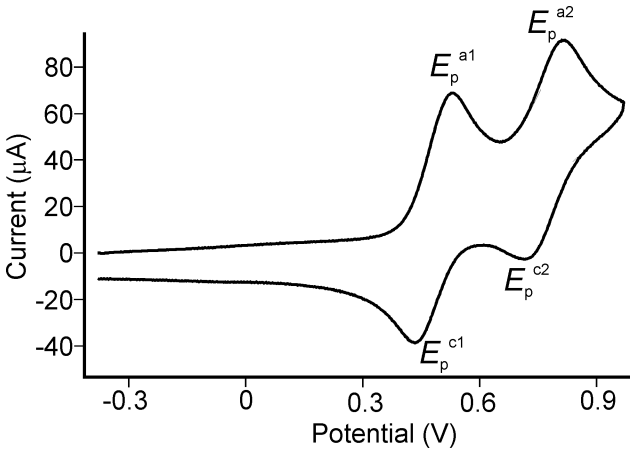

Figure S2. Cyclic voltammogram of a 2.7 mM solution of **A2** in CH_2Cl_2 (0.4 M [^{n}Bu$_4$N][PF_6]), ν = 0.2 V s^{-1}, T = 21.9 °C on a GC electrode.

Compound **A3** also displayed three oxidation processes, but the first two oxidations were very closely spaced. The first oxidation process had a large return wave at slow scan rates which did not increase in peak current height with increasing scan rate. The second oxidation is only 170 mV away and displays a minor return wave at slow scan rates that increases slightly with increasing scan rate. The third oxidation is irreversible and occurs very close to the solvent limit. In the old sample the first two oxidation processes were only visible as minor humps in the CV, followed by a third oxidation process that was no longer visible in the new sample CV.

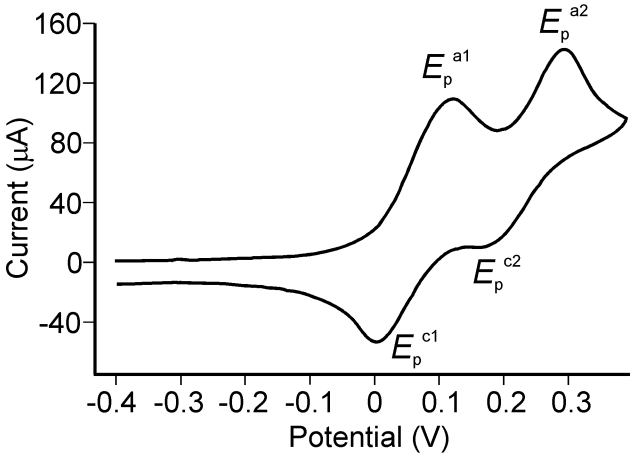

Figure S3. Cyclic voltammogram of a 5.5 mM solution of **A3** in CH_2Cl_2 (0.4 M [^{n}Bu$_4$N][PF_6]), ν = 0.2 V s^{-1}, T = 21.8 °C on a GC electrode.

Compound **A4** also displayed three oxidation processes. The first oxidation process had a large return wave at all scan rates, and the second and third oxidation processes were both irreversible over all scan rates (up to 10 V s^{-1}) (Figure 10S4 The only difference in the CV response between the old and new samples of **10** seems to be the shape of the second oxidation wave, which appears broader in the old sample but is still the same distance away from E_p^{a1}.

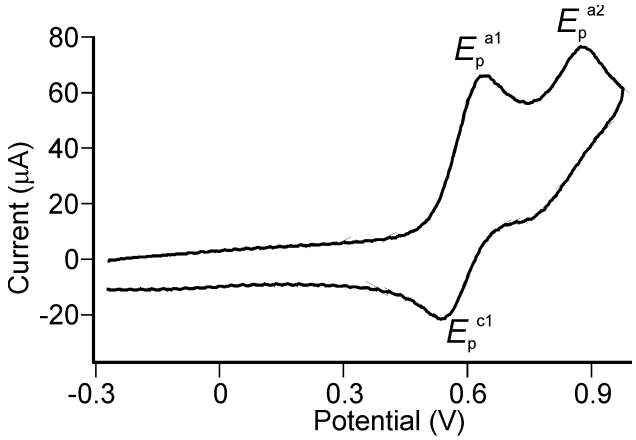

Figure S4. Cyclic voltammogram of a 2.0 mM solution of **A4** in CH_2Cl_2 (0.4 M [^{n}Bu$_4$N][PF_6]), ν = 0.2 V s^{-1}, T = 22.5 °C on a GC electrode.

Compound **A5** displayed three oxidation processes (Figure S5). The first had a minor return wave which did not increase in current size with scan rate. The other two were irreversible up to 10 V s^{-1}.

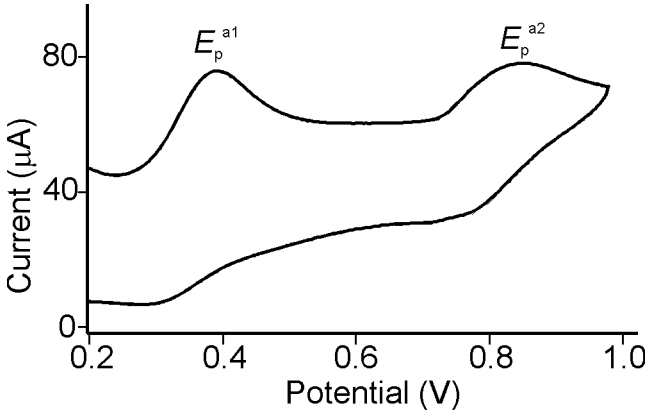

Figure S5. Cyclic voltammogram of a 2.2 mM solution of **A5** in CH_2Cl_2 (0.4 M [^{n}Bu$_4$N][PF_6]), ν = 0.2 V s^{-1}, T = 21.0 °C on a GC electrode.

Compound **A6** shows three oxidation processes and the first two had small return waves which did not increasing in size with increasing scan rate (Figure S6). Also, there were two offset return waves at −0.26 V and −0.66 V (not shown) likely stemming from the first two oxidation processes and suggesting that oxidation is causing decomposition of the molecule, which can then be re-reduced at more cathodic potentials.

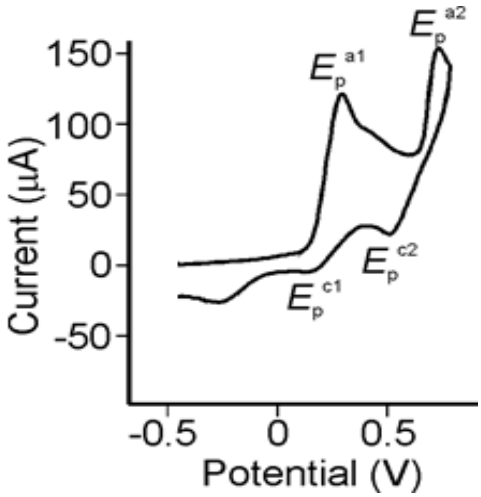

Figure S6. Cyclic voltammogram of a 6.1 mM solution of **A6** in CH_2Cl_2 (0.4 M [^{n}Bu$_4$N][PF_6]), ν = 0.2 V s^{-1}, T = 20.7 °C on a GC electrode.

In the case of **N7** three oxidation processes were present. The first oxidation process displayed a moderately large return wave at all scan rates (I_p^{c1}/I_p^{a1} = 0.54), which was closely followed by the second oxidation process which was irreversible at slow scan rates but became more chemically reversible (a return wave grew in) at scan rates of 5 V s^{-1} or faster (Figure S7). The third oxidation process was irreversible at all scan rates investigated.

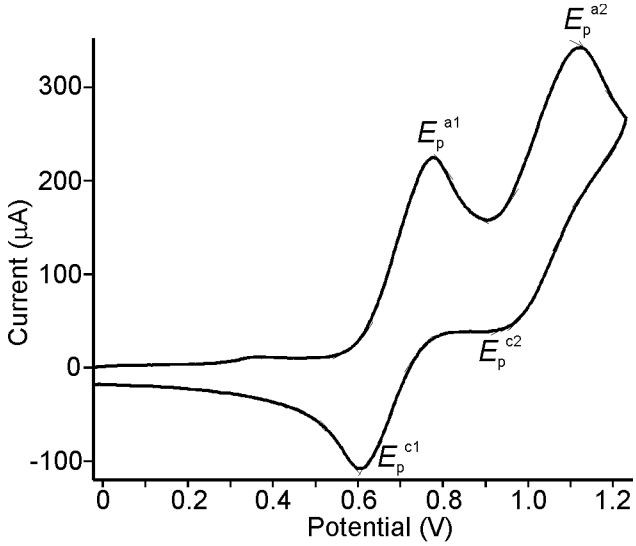

Figure S7. Cyclic voltammogram of a 10.2 mM solution of **N7** in CH_2Cl_2 (0.4 M [^{n}Bu$_4$N][PF_6]), ν = 0.2 V s^{-1}, T = 22.5 °C on a GC electrode.

For **N8** similar behavior was seen. The first two oxidation processes displayed large return waves (I_p^{c1}/I_p^{a1} = 0.66, I_p^{c2}/I_p^{a2} = 0.54) at all scan rates investigated (Figure S8). The third oxidation was irreversible at all scan rates and did not result in a diminished return wave for either of the first two oxidation processes when the potential was swept through this process.

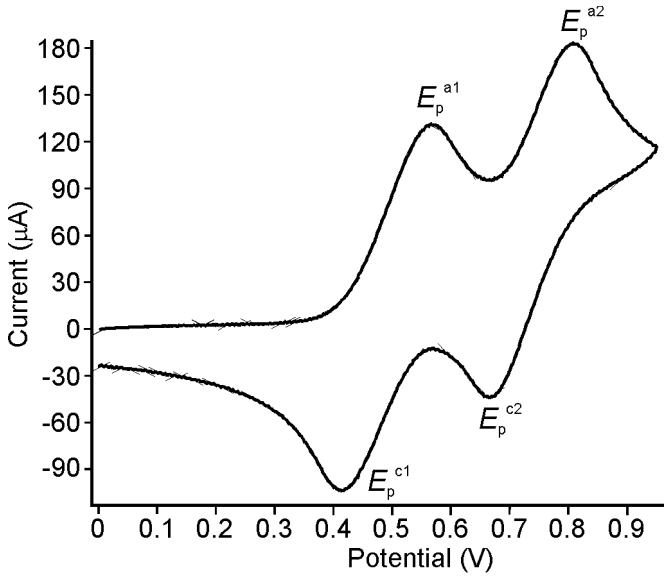

Figure S8. Cyclic voltammogram of a 6.6 mM solution of **N8** in CH_2Cl_2 (0.4 M [^{n}Bu$_4$N][PF_6]), ν = 0.2 V s^{-1}, T = 22.0 °C on a GC electrode.

In the case of **N9**, two oxidation processes were observed which were very closely spaced (only 50 mV apart, Figure S9). There was a minor return wave which appears to be associated with the first oxidation (switching the potential before the second peak gives a return wave), which did not increase in peak current height with increasing scan rate. The second process was of higher peak current height and irreversible (no second return wave grew in with increasing scan rate).

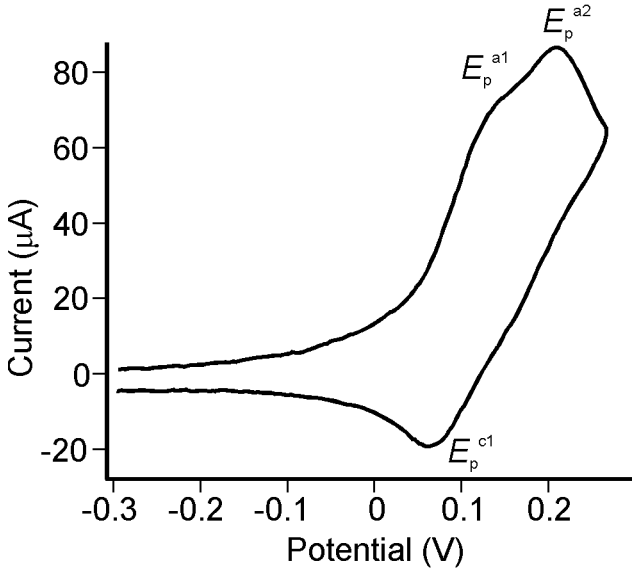

Figure S9. Cyclic voltammogram of a 3.0 mM solution of **N9** in CH_2Cl_2 (0.4 M [^{n}Bu$_4$N][PF_6]), ν = 0.2 V s^{-1}, T = 21.8 °C on a GC electrode.

In the case of **N10**, three oxidation processes were seen, with the first two being very closely spaced (only 100 mV apart) (Figure S10). The first process had a moderate sized return wave which did not grow with increasing scan rate. The second and third processes were irreversible over all scan rates investigated.

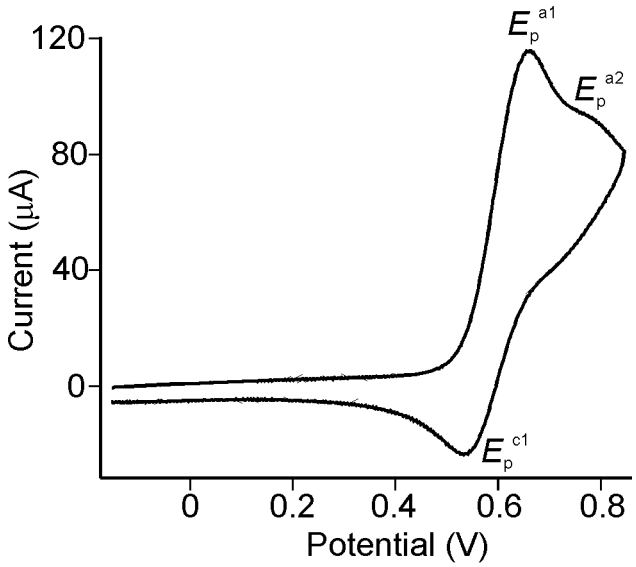

Figure S10. Cyclic voltammogram of a 3.7 mM solution of **N10** in CH_2Cl_2 (0.4 M [^{n}Bu$_4$N][PF_6]), ν = 0.2 V s^{-1}, T = 20.8 °C on a GC electrode.

For **N11**, three oxidation processes were again observed. The first oxidation process had a return wave that was offset and of slightly lower peak current height and the other two oxidations were irreversible over all scan rates (Figure S11). On Pt all three processes were irreversible at all scan rates.

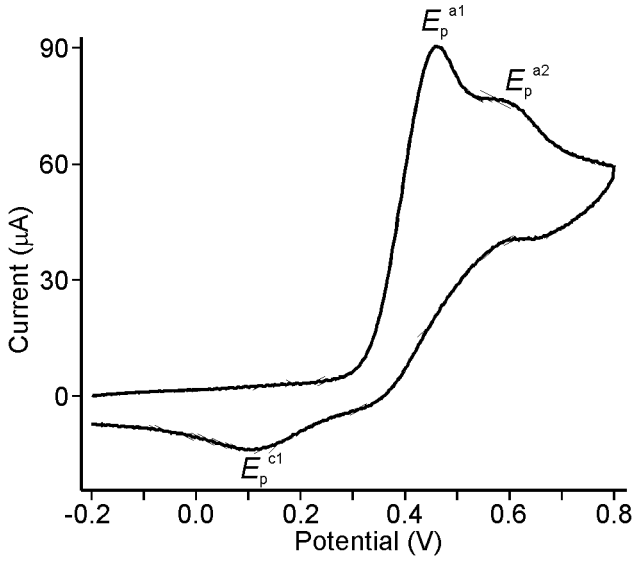

Figure S11. Cyclic voltammogram of a 3.8 mM solution of **N11** in CH_2Cl_2 (0.4 M [^{n}Bu$_4$N][PF_6]), ν = 0.2 V s^{-1}, T = 22.0 °C on a GC electrode.

In the case of **N12** three oxidations were observed with the first two being very close in potential. There was a minor, offset return wave for the first process and a very minor return wave for the second oxidation processes at slow scan rates (0.2 V s^{-1}). These did not grow in peak current height with increasing scan rate (Figure S12). The third oxidation process was irreversible at all scan rates investigated. All processes were irreversible on Pt at all scan rates.

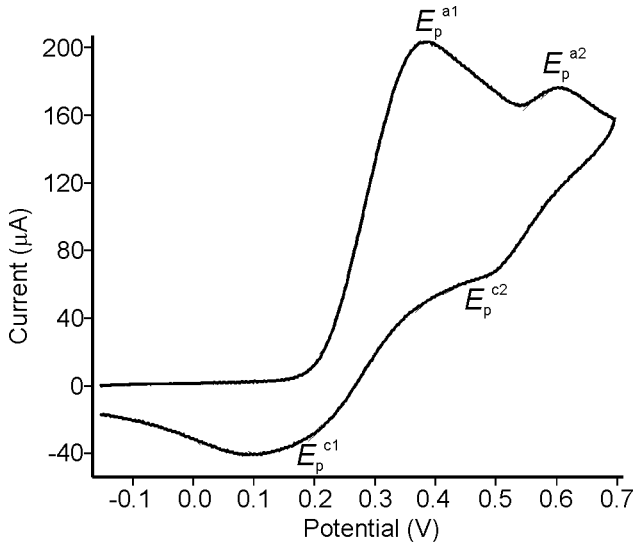

Figure S12. Cyclic voltammogram of an 8.1 mM solution of **N12** in CH_2Cl_2 (0.4 M [^{n}Bu$_4$N][PF_6]), ν = 0.2 V s^{-1}, T = 21.4 °C on a GC electrode.

N13 and **N14** displayed three oxidation processes. The first was a minor wave due to oxidation of the halogen (Bromine in **N13**, Figure S13 and Iodine in **N14**, Figure 9S14). The second process had a moderately large return wave and the third process was irreversible over all scan rates.

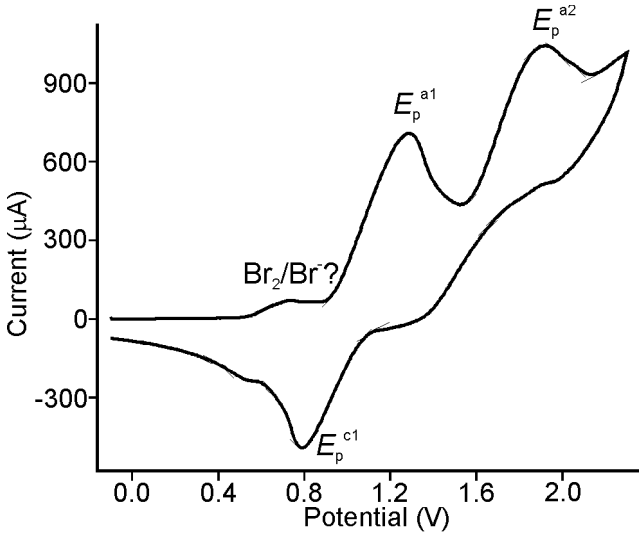

Figure S13. Cyclic voltammogram of a 42.4 mM solution of **N13** in CH_2Cl_2 (0.4 M [^{n}Bu$_4$N][PF_6]), ν = 0.2 V s^{-1}, T = 22.5 °C on a GC electrode.

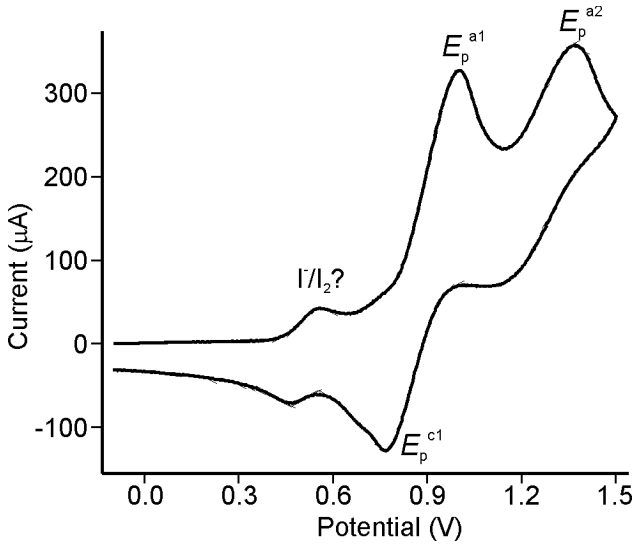

Figure S14. Cyclic voltammogram of a 12.1 mM solution of **N14** in CH_2Cl_2 (0.4 M [^{n}Bu$_4$N][PF_6]), ν = 0.2 V s^{-1}, T = 22.9 °C on a GC electrode.

In the case of **N15** there are two irreversible oxidations which lie in close proximity of one another (Figure S15). These do not have return waves at any of the scan rates investigated.

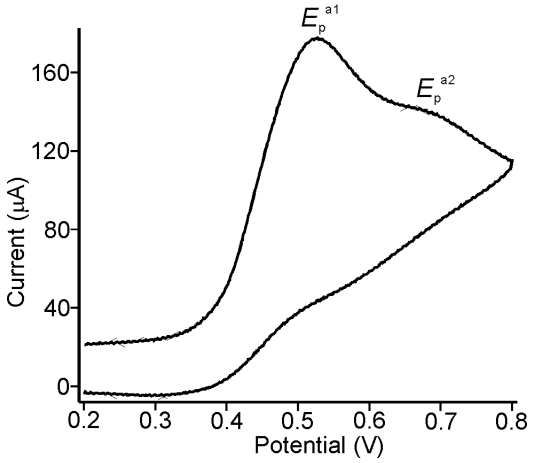

Figure S15. Cyclic voltammogram of a 5.3 mM solution of **N15** in CH_2Cl_2 (0.4 M [^{n}Bu$_4$N][PF_6]), ν = 0.2 V s^{-1}, T = 21.5 °C on a GC electrode.

For **N16** the first oxidation process has a very minor return wave which only grows slightly in peak current height up to 10 V s^{-1} (I_p^{c1}/I_p^{a1} = 0.29 at 0.2 V s^{-1} and 0.43 at 10 V s^{-1}) (Figure S16). There is also a second return wave which appears at −0.34 V and may originate from the reduction of an electrochemically generated oxidation product. The second oxidation is irreversible and minor in peak current height when compared with the first oxidation process.

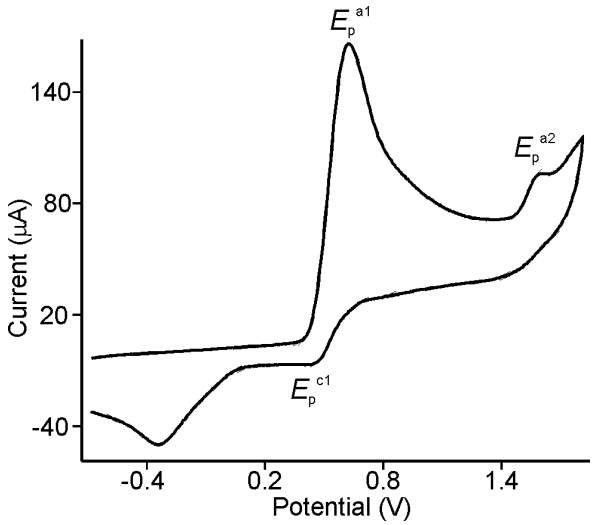

Figure S16. Cyclic voltammogram of a 6.1 mM solution of **N16** in CH_2Cl_2 (0.4 M [^{n}Bu$_4$N][PF_6]), ν = 0.2 V s^{-1}, T = 22.7 °C on a GC electrode.

N17 displayed two irreversible oxidation processes which were in very close proximity of each other causing the first oxidation to shoulder the second oxidation (Figure S17). On further anodic scanning, a third peak is detected and there are apparent return peaks for the first two oxidations.

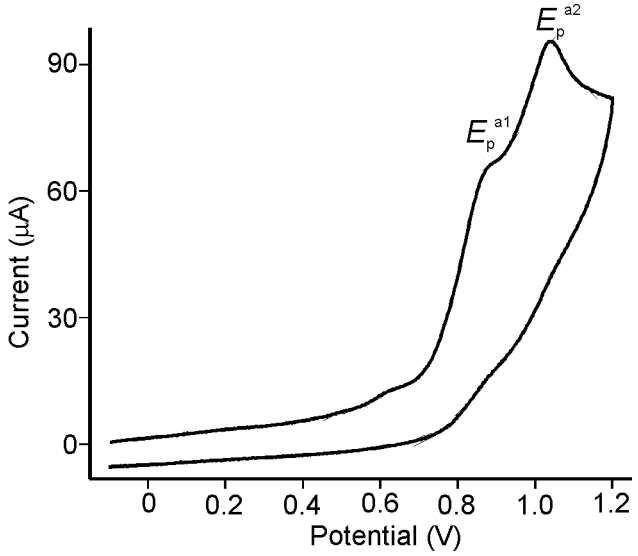

Figure S17. Cyclic voltammogram of a 4.1 mM solution of **N17** in CH_2Cl_2 (0.4 M [^{n}Bu$_4$N][PF_6]), ν = 0.2 V s^{-1}, T = 21.6 °C on a GC electrode.

In the case of **N18** there again appear to be two very closely separated oxidation processes, and all are irreversible at all scan rates and appeared very close to the solvent electrolyte window limit (Figure S18). A possible reduction processes could be detected, with a fully IRR response.

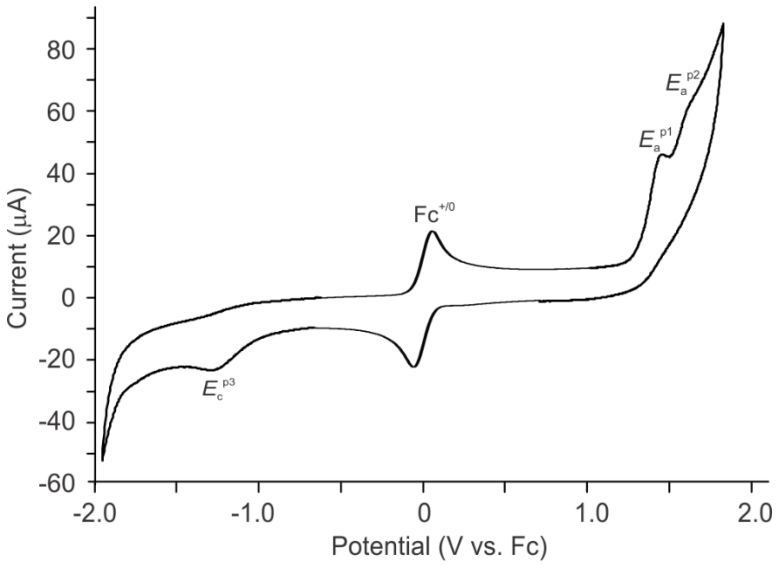

Figure S18. Cyclic voltammogram of a 4.1 mM solution of **N18**, plus included ferrocene internal standard, in CH_2Cl_2 (0.4 M [^{n}Bu$_4$N][PF$_6$]), ν = 0.2 V s^{-1}, T = 21.6 °C on a GC electrode.

Additional Voltammetry Data Analysis

Additional information such as comparison of voltammetry data obtained on Pt vs. GC solid interfacial electrodes is provided here.

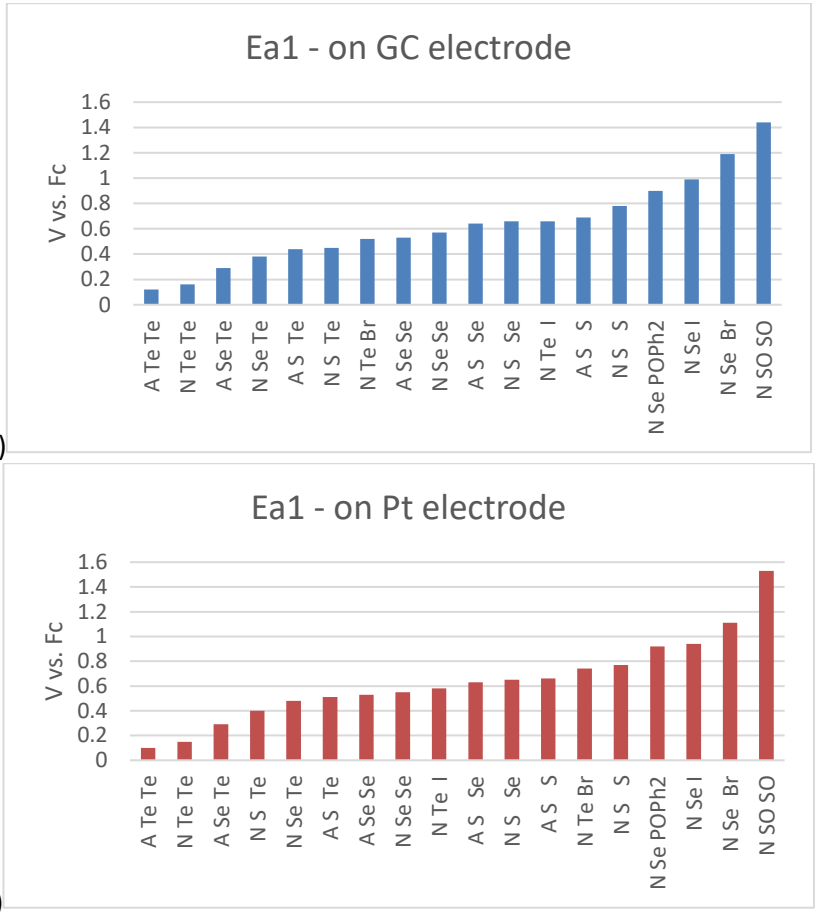

Figure S19. Bar graphs showing the large increase in E_p^{a1} values found for **1** – **12** as a function of E groups. (a) Measured at a GC electrode and (b) measured at a Pt electrode interface.

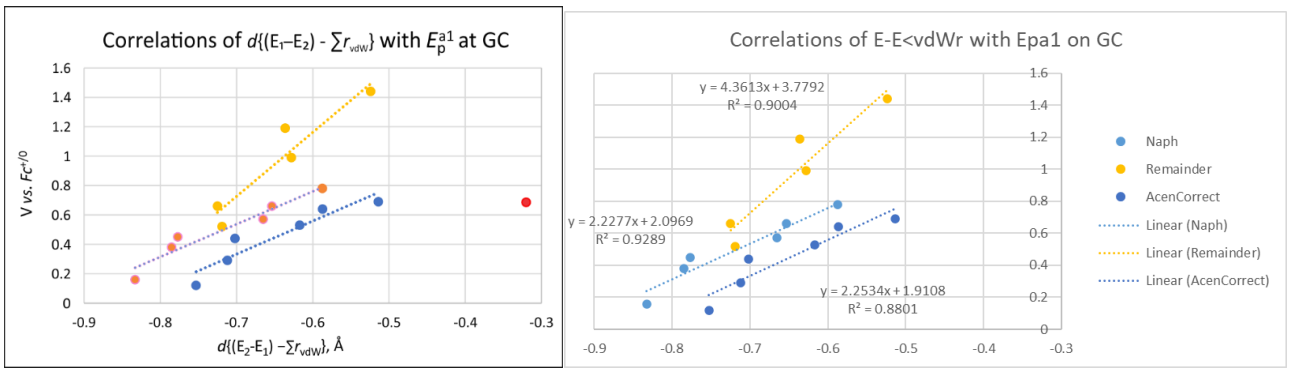

Figure S20. Correlation graphs comparing the E_p^{a1} values with {d(E_1-E_2)-∑(r_{vdW})} measured at GC (left) and Pt (right) electrodes. For the GC graph, the **A1-6** (blue dots) and **N7-12** (orange dots) series data are plotted separately, as are also the data for **N13** – **N17** (yellow dots). No suitable E–E distance could be defined for **N18**. The red dot indicates the coordinates for **A1** from crystallography (see text). Linear fits for **A1-6** y = 2.25x + 1.91, R^2 = 0.88; **N7-12** y = 2.23x + 2.10, R^2 = 0.93; **N13-17** y = 4.36x + 3.78, R^2 = 0.90.

For the twelve dichalcogenides (**A1** – **N12**) in oxidation state +2 where E_1 and E_2 are S, Se or Te, six results are available for each of the 1,8-naphthalene and 5,6-acenaphthene series. In a search for a causation of the trends in E_p^{a1} values, consideration was given to the analyses previously performed on the divergent geometries of neutral **A1** – **N12**.[59,62] The published crystal structures for this series were consulted, and the amount by which the E···E distances are *less than* the sums of the van der Waals radii of two atoms was used as a proxy for the degree of *peri* interaction (and hence of HOMO destabilization). In Fig. S20, correlations of the E_p^{a1} values with these distances are shown, which demonstrates that each half-dozen of samples show a different linear correlation (with the exception of **N18**, for which no suitable E–E distance could be defined).

Good linear correlations are found for the two *peri*-dichalcogen series **A2-6** and **N7-12**, which have very similar slopes of 2.25 and 2.23 V/Å, respectively (GC; see the ESI for the similar results at Pt) but different intercepts. The coordinates of compound **A1** are worthy of note; if the *d*(S···S) value from the crystal structure is used, as is the case for the other eleven compounds, the point indicated by the red dot in Fig. S20 is obtained, which does not fit the correlation. However, as Aschenbach *et al*. have shown, the crystal lattice of this compound contains a conformation "AA*t*" that is different from the others acenaphthenes designated "AB" (see Scheme 1 and definitions below).[59] These authors investigated the structural anomaly using a density functional theory (DFT) computational approach, concluding that the ground state of **A1** is the "AB" conformation, and that the observed crystal structure is a higher energy conformation that is probably induced by lattice packing forces. An estimated value of *d*(S···S) in the AB conformation, obtained by subtracting 0.05 Å from the computed distance to allow for typical DFT *vs.* crystallographic lengths, gives the coordinates used for the orange dot in the graphs in Fig. S20. Hence, the correlation between *d*(E···E) and E_p^{a1} fits on the assumption, that in solution, all twelve compounds have the same conformations with a defined *peri* interaction between a (perpendicular) E_1 l.p. donor orbital and a (parallel) E_2 $\sigma^*_{C–E}$ acceptor orbital. Moreover, the positions of the *mixed chalcogen* data points along these correlation lines clearly demonstrates that it is the cooperative interaction between E's that determines the measured values of E_p^{a1} for the whole series.

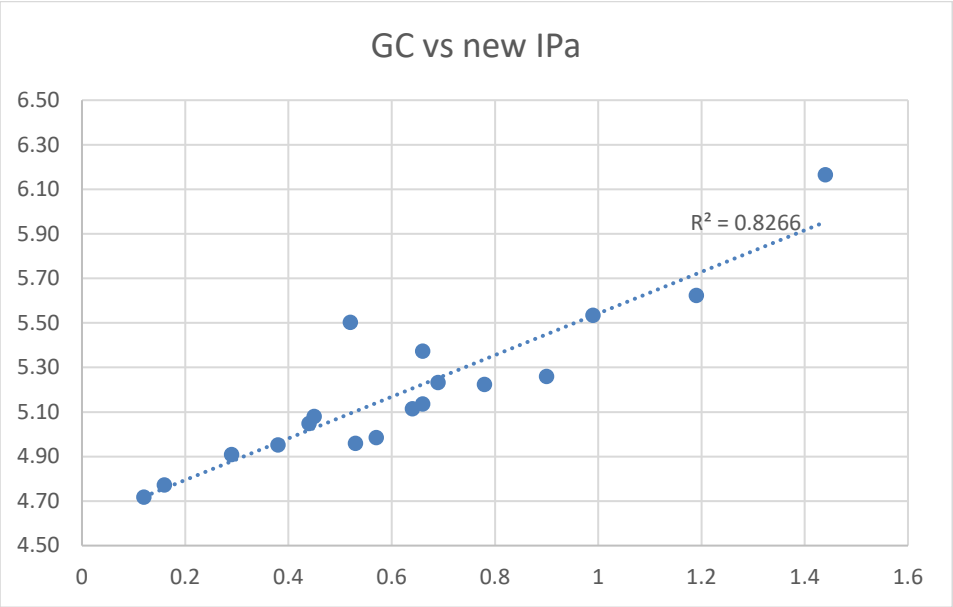

Figure S21. Correlation graph comparing the E_p^{a1} values at a GC electrode with DFT computed adiabatic first ionisation energies, relating the energies of neutral and monocationic **A1** – **N18**.

Experimental Section for Voltammetry

Reagents and General Procedures. Dichloromethane (BDH, reagent grade) was purified by distillation from CaH_2 and purged with dry argon prior to use. Electrochemical grade tetrabutylammonium hexafluorophosphate [^{n}Bu$_4$N][PF$_6$] (Fluka) was used as the supporting electrolyte and was stored in a dessicator. Ferrocene (Fc) was sublimed prior to use.

Voltammetry. Cyclic voltammograms (CV) were obtained at 21 ± 2°C in CH_2Cl_2 containing 0.4 M [^{n}Bu$_4$N][PF$_6$] as the supporting electrolyte. Solutions were purged with dry argon for 10 min directly before use and were kept under a blanket of argon during all experiments. CV measurements were performed with a Princeton Applied Research PARSTAT 2273 potentiostat. The voltammetry cell has been described previously.[1] Initial background scans characterized the size of the accessible electrochemical window and provided an estimate of the likely background current. The CVs were obtained over scan rates of 0.1 – 10 V s^{-1}. Potentials for compounds **A1** – **N18** are reported versus the operative formal potential, $E^{0/}$ for the $Fc^{0/+}$ redox couple, which was used as an internal standard. The working electrodes were either a 3.0 mm BASi glassy carbon (GC) or a 1.6 mm BASi platinum (Pt), and these were polished with an Al_2O_3 (Buehler, 0.05 um) slurry on a clean polishing cloth, rinsed with distilled water, and dried with tissue paper prior to use.

All compounds were fairly soluble in CH_2Cl_2 to give clear to yellow colored solutions. In the case of **N7-N11** there were three oxidation processes evident and no reduction processes up to the solvent electrolyte limit (−2.4 V). In the case of **N12** there is an additional irreversible reduction process which occurs at −1.8 V (vs. $Fc^{0/+}$). Similar responses were seen for all six compounds using both the glassy carbon (GC) and platinum (Pt) working electrodes.

Comp,	Neutral Confor.	Monocat. Confor.	Dication Confor.	First I.P. (e.V.)	Second I.P. (e.V.)
A1	AAt	AAc	CCc	5.23	6.30
A2	ABc	AAc	AAc	4.96	6.06
A3	ABt	AAc	AAc	4.72	5.62
A4	ABc	AAc	AAc	5.12	6.23
A5	ABt	AAc	AAc	5.05	6.03
A6	AB	AAc	AAc	4.91	5.84
N7	ACc	AAc	AAc	5.22	6.36
N8	ABt	AAc	AAc	4.99	6.03
N9	ABt	AAc	AAc	4.77	5.61
N10	ABt	AAc	AAc	5.14	6.20
N11	ABt	AAc	AAc	5.08	5.50
N12	ABt	AAc	AAc	4.95	5.83
N13	Bt	Ct	Ct	5.64	6.89
N14	Bt	At	C	5.53	6.77
N15	Bt	Ct	C	5.50	6.79
N16	Bt	At	A	5.37	6.56
N17	AAc [b]	AAc [b]	AAc [b]	5.26	5.56
N18	AAc	AAt	AAt c	6.173	5.96
N23	Flat	Flat	Flat		

Section 2: Quantum (DFT) Computations

Exhaustive Search of Conformational Space for Compounds in Neutral, Monocation and Dication States

A wide range of geometries were optimised for both monocationic and dicationic dichalcogen diphenyl derivatives (Fig. S22.) in the gas phase at the B3LYP[1] with use of Curtis and Binning's 962(d) basis set[2] on Se and the Stuttgart-Dresden effective core potential[3] applied to Te. For tellurium the relevant double zeta basis set was applied with the modification of d-polarisation functions with exponents of 0.237[4] whilst the 6-31+G(d) basis set was applied to all other atoms (carbon, hydrogen and sufur).

A key point of interest in exploring these systems was to observe, if any, the generation of bonding character between the chalcogen atoms upon oxidation with the expectation that monocation species may show a hemibond whilst the dications could exhibit full chalcogen-chalcogen bonding. To assess this, Wiberg bond indices[5] were obtained by means of natural bond analysis[6] at the same computational level and, coupled with chalcogen-chalcogen distances, provided a reasonable means to consider the nature of any bonds.

The search over compounds **N7** – **N12** will be presented first. Similar calculations have been reported previously for **A1** – **A6** in the ESI for our Communication [https://doi.org/10.1002/cphc.201300678].

Geometry optimisations were performed on a number of different starting structures. Where available, previously optimised neutral species were used as a starting point and, otherwise, initial geometries were generated by hand. Such a methodology was performed for both the monocation and dication species in order to determine that all energy minima had been found. Uncovering the likely global minima allowed for calculation of the adiabatic ionisation potential whilst single point calculations were performed to obtain the vertical ionisation potential. The former was taken as being the difference between the most stable geometric conformer of the higher oxidation state and the most stable geometric conformer of the lower oxidation state. Vertical ionisation potential involved calculation of the energy of a dication with the geometry of a stable monocation conformer. The energy associated with the stable monocation of the requisite geometry was then subtracted from the excited dication energy.

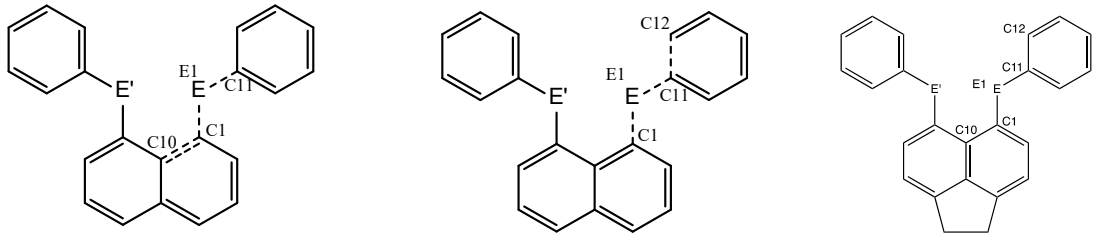

Figure S22: General structure of the species studied computationally where E = Chalcogen. The nature of E was varied between S, Se and Te. Also shown are the prominent dihedrals recorded (dashed bonds), respectively, θ (left) and γ. C_{12} and its counterpart C_{18} were always taken as being the atom furthest from the naphthalene ring.

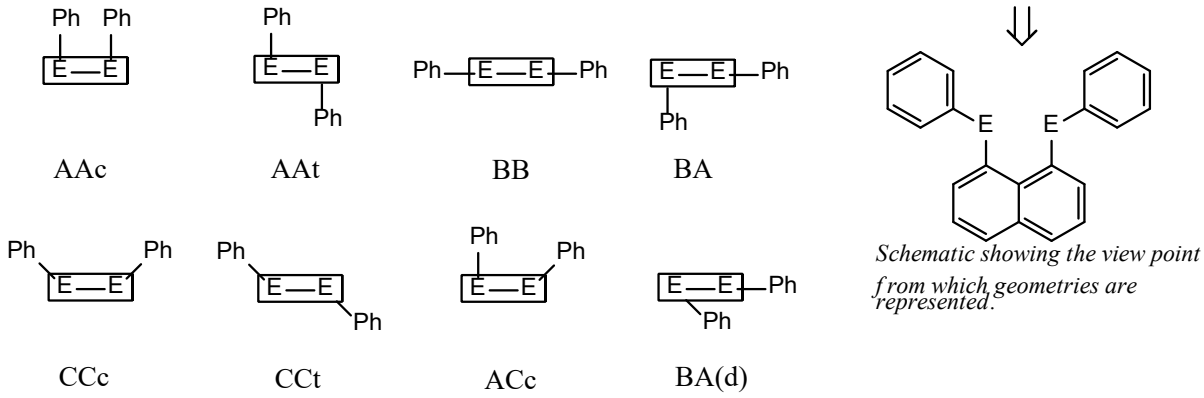

Figure S23: Representative geometries of the mono- and dication compounds investigated. Note that the rectangular box symbolises a "side-on" view of the naphthalene ring system.

As shown in Fig S23, a wide range of optimised geometries were found in the course of this study. Species which are denoted with "c" have both of the phenyl groups which are bound to the chalcogen atoms in a cis arrangement with respect to the naphthalene ring and those which are labelled "t" have the aromatic rings in a trans orientation. In order for a species to be classified as CC the C_{11}-E_1-E'_2 angle was required to fall within 120° to 165°. If these conditions were not met, the system was labelled as an A or B geometry. In general, it was found that interchangeability between the AA and CC based conformers was relatively facile aside from a small number of exceptions. The ACt, BA(d) and BB conformers were noted as being rare within the spectrum of systems examined and also energetically less favourable than either their AA or CC counterparts. All computations were performed using the Gaussian 03 suite of programs[7] whilst molecular orbitals were visualized using the VMD program[8] and Molden[9] was employed for following the shape of structures after each iteration.

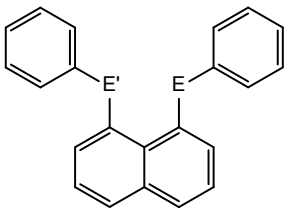

	N7	N8	N9	N10	N11	N12
E	S	Se	Te	Se	Te	Te
E'	S	Se	Te	S	S	Se

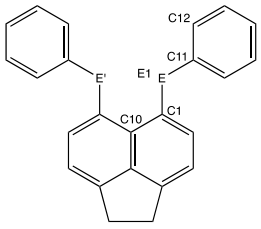

	(6) A1	(5) A2	(4) A3
E	S	Se	Te
E'	S	Se	Te

Figure S24. Labelling scheme for monocations and dications in the two diPhE series of *peri*-subsituted compounds..

Results

Proceeding results are labelled such that they are consistent with the descriptions provided for geometry in Figs S22 and S23 while chemical composition is outlined in Fig S24. Only geometries which were found to be energetic minima are presented.

Table S1: Selected optimised parameters, WBIs and relative energies of monocations of naphthalene derivatives **N7-N12** (B3LYP level).

Compound	**N7 AAt**	**N7 CCc**
EPh,E'Ph	SPh, SPh	SPh, SPh
Energy (Hartree)	-1644.13676	-1644.13786
Energy (kJ/mol)	-4316681.07	-4316683.95
Energy (rel)* / kj/mol	2.88	0
E(1)···E(2)	2.8628	2.9395
WBI E(1)···E(2)	0.1127	0.0781
E(1)-C(1)	1.7942	1.7792
E(2)-C(9)	1.7943	1.7792
C(10)-C(1)-E(1)-C(11); θ1 / °	100.290	140.181
C(10)-C(9)-E(2)-C(17); θ2 / °	100.441	-140.182
C(1)-E(1)-C(11)-C(12); γ1 / °	166.929	143.003
C(9)-E(2)-C(17)-C(18); γ2 / °	166.809	-143.009

Compound	**N8 AAc**	**N8 AAt**
EPh,E'Ph	SePh,SePh	SePh, SePh
Energy (Hartree)	-5650.46167	-5650.46269
Energy (kJ/mol)	-14835287.11	-14835289.81
Energy (rel)* / kj/mol	2.69	0
E(1)···E(2)	3.0285	2.9946
WBI E(1)···E(2)	0.1558	0.1706
E(1)-C(1)	1.9385	1.9385
E(2)-C(9)	1.9388	1.9385
C(10)-C(1)-E(1)-C(11); θ1 / °	110.099	95.523
C(10)-C(9)-E(2)-C(17); θ2 / °	-105.029	95.537
C(1)-E(1)-C(11)-C(12); γ1 / °	166.950	168.944
C(9)-E(2)-C(17)-C(18); γ2 / °	-170.447	168.937

Compound	**N9 AAc**	**N9 AAt**	**N9 BB**
EPh,E'Ph	TePh, TePh	TePh, TePh	TePh, TePh
Energy (Hartree)	-863.90680	-863.90888	-863.89743
Energy (kJ/mol)	-2268187.31	-2268192.77	-2268162.70
Energy (rel)* / kj/mol	5.46	0	30.07
E(1)···E(2)	3.2991	3.2596	3.2772
WBI E(1)···E(2)	0.1886	0.1990	0.1127
E(1)-C(1)	2.1357	2.1346	2.1290
E(2)-C(9)	2.1350	2.1346	2.1288
C(10)-C(1)-E(1)-C(11); θ1 / °	97.049	89.735	178.537
C(10)-C(9)-E(2)-C(17); θ2 / °	-104.661	89.774	-178.588
C(1)-E(1)-C(11)-C(12); γ1 / °	175.974	167.992	-91.344
C(9)-E(2)-C(17)-C(18); γ2 / °	-174.960	167.973	91.357

Compound	N10 AAt	N10 CCc
EPh,E'Ph	SePh, SPh	SePh, SPh
Energy (Hartree)	-3647.29995	-3647.29950
Energy (kJ/mol)	-9575986.03	-9575984.83
Energy (rel)* / kj/mol	0	1.19
E(1)···E(2)	2.9258	2.9838
WBI E(1)···E(2)	0.1511	0.1022
E(1)-C(1)	1.9361	1.9330
E(2)-C(9)	1.7961	1.7801
C(10)-C(1)-E(1)-C(11); θ1 / °	92.947	133.285
C(10)-C(9)-E(2)-C(17); θ2 / °	104.269	-135.780
C(1)-E(1)-C(11)-C(12); γ1 / °	171.327	147.333
C(9)-E(2)-C(17)-C(18); γ2 / °	162.208	-145.973

Compound	N11 AAc	N11 AAt	N11 CCc
EPh,E'Ph	TePh, SPh	TePh, SPh	TePh, SPh
Energy (Hartree)	-1254.02294	-1254.02422	-1254.02329
Energy (kJ/mol)	-3292437.23	-3292440.60	-3292438.14
Energy (rel)* / kj/mol	3.38	0	2.47
E(1)···E(2)	3.0721	3.0374	3.0562
WBI E(1)···E(2)	0.1461	0.1596	0.1152
E(1)-C(1)	2.1304	2.1275	2.1276
E(2)-C(9)	1.7949	1.7976	1.7825
C(10)-C(1)-E(1)-C(11); θ1 / °	106.113	86.333	135.839
C(10)-C(9)-E(2)-C(17); θ2 / °	-177.238	102.860	-133.656
C(1)-E(1)-C(11)-C(12); γ1 / °	171.918	176.638	146.539
C(9)-E(2)-C(17)-C(18); γ2 / °	-156.853	158.513	-144.816

Compound	N12 AAc	N12 AAt
EPh,E'Ph	TePh, SePh	TePh, SePh
Energy (Hartree)	-3257.18489	-3257.18653
Energy (kJ/mol)	-8551738.92	-8551743.23
Energy (rel)* / kj/mol	4.31	0
E(1)···E(2)	3.1543	3.1187
WBI E(1)···E(2)	0.1711	0.1820
E(1)-C(1)	2.1317	2.1308
E(2)-C(9)	1.9414	1.9406
C(10)-C(1)-E(1)-C(11); θ1 / °	102.635	-87.832
C(10)-C(9)-E(2)-C(17); θ2 / °	-104.202	-95.590
C(1)-E(1)-C(11)-C(12); γ1 / °	177.124	-173.280
C(9)-E(2)-C(17)-C(18); γ2 / °	-166.732	-165.440

Distances in Å, angles in degrees, energy values as specified.

Table S2: Adiabatic ionisation potentials (electron volts) of neutral species to monocations. Only the lowest energy conformers of the varying chemical compositions were considered and these are listed under "Geometry Neutral" and "Geometry Monocation".

Species	Geometry Neutral	Geometry Monocation	Adiabatic I.P. (eV)
N7	AB	CCc	6.553
N8	CCt	AAt	6.394
N9	CCt	AAt	6.214
N10	BA	AAt	6.531
N11	BA	AAt	6.484
N12	BA	AAt	6.360

Table S3: Selected optimised parameters, WBIs and relative energies of dications of naphthalene derivatives **N7-N12** (B3LYP level).

Compound	**N7 AAt**	**N7 ACc**	**N7 BA(d)**	**N7 CCc**
EPh,E'Ph	SPh, SPh	SPh, SPh	SPh, SPh	SPh, SPh
Energy (Hartree)	-1643.75719	-1643.75752	-1643.74442	-1643.76591
Energy (kJ/mol)	-4315684.50	-4315685.36	-4315650.98	-4315707.39
Energy (rel)* / kj/mol	22.89	22.03	56.41	0.00
E(1)···E(2)	2.4963	2.6647	3.2260	2.8072
WBI E(1)···E(2)	0.5013	0.3537	0.1340	0.2415
E(1)-C(1)	1.7938	1.7792	1.7460	1.7600
E(2)-C(9)	1.7938	1.7757	1.7616	1.7600
C(10)-C(1)-E(1)-C(11); θ1 / °	-106.416	-85.615	174.155	139.778
C(10)-C(9)-E(2)-C(17); θ2 / °	-106.967	-127.181	-41.749	-139.766
C(1)-E(1)-C(11)-C(12); γ1 / °	-160.881	-170.476	131.626	150.023
C(9)-E(2)-C(17)-C(18); γ2 / °	-160.712	-155.384	162.299	-150.061

Compound	**N8 AAt**	**N8 CCc**
EPh,E'Ph	SePh, SePh	SePh, SePh
Energy (Hartree)	-5650.09478	-5650.09493
Energy (kJ/mol)	-14834323.84	-14834324.24
Energy (rel)* / kj/mol	0.40	0.00
E(1)···E(2)	2.6117	2.7945
WBI E(1)···E(2)	0.6459	0.4497
E(1)-C(1)	1.9390	1.9195
E(2)-C(9)	1.9390	1.9195
C(10)-C(1)-E(1)-C(11); θ1 / °	-100.930	126.360
C(10)-C(9)-E(2)-C(17); θ2 / °	-100.914	-126.340
C(1)-E(1)-C(11)-C(12); γ1 / °	-162.043	156.713
C(9)-E(2)-C(17)-C(18); γ2 / °	-162.075	-156.730

Compound	**N9 AAc**	**N9 AAt**
EPh,E'Ph	TePh, TePh	TePh, TePh
Energy (Hartree)	-863.55282	-863.55525
Energy (kJ/mol)	-2267257.93	-2267264.32
Energy (rel)* / kj/mol	6.39	0.00
E(1)···E(2)	2.9337	2.8938
WBI E(1)···E(2)	0.7083	0.7577
E(1)-C(1)	2.1273	2.1293
E(2)-C(9)	2.1281	2.1293
C(10)-C(1)-E(1)-C(11); θ1 / °	111.539	95.546
C(10)-C(9)-E(2)-C(17); θ2 / °	-106.303	95.555
C(1)-E(1)-C(11)-C(12); γ1 / °	163.058	163.322
C(9)-E(2)-C(17)-C(18); γ2 / °	-164.976	163.291

Compound	**N10 AAt**	**N10 CCc**
EPh,E'Ph	SePh, SPh	SePh, SPh
Energy (Hartree)	-3646.92620	-3646.93008
Energy (kJ/mol)	-9575004.74	-9575014.93
Energy (rel)* / kj/mol	10.19	0.00
E(1)···E(2)	2.5548	2.8247
WBI E(1)···E(2)	0.5617	0.3145
E(1)-C(1)	1.9309	1.9086
E(2)-C(9)	1.7988	1.7650
C(10)-C(1)-E(1)-C(11); θ1 / °	-96.737	133.546
C(10)-C(9)-E(2)-C(17); θ2 / °	-112.033	-138.272
C(1)-E(1)-C(11)-C(12); γ1 / °	-165.548	154.502
C(9)-E(2)-C(17)-C(18); γ2 / °	-156.505	-149.823

Compound	**N11 AAt**	**N11 CCc**
EPh,E'Ph	TePh, SPh	TePh, SPh
Energy (Hartree)	-1253.65689	-1253.65719
Energy (kJ/mol)	-3291476.15	-3291476.97
Energy (rel)* / kj/mol	0.81	0.00

E(1)···E(2)	2.6650	2.8675
WBI E(1)···E(2)	0.6134	0.4131
E(1)-C(1)	2.1141	2.1044
E(2)-C(9)	1.8066	1.7756
C(10)-C(1)-E(1)-C(11); θ1 / °	92.610	123.815
C(10)-C(9)-E(2)-C(17); θ2 / °	108.372	-138.846
C(1)-E(1)-C(11)-C(12); γ1 / °	168.745	160.575
C(9)-E(2)-C(17)-C(18); γ2 / °	153.237	-148.240
Compound	**N12 AAc**	**N12 AAt**
EPh,E'Ph	TePh, SePh	TePh, SePh
Energy (Hartree)	-3256.82390	-3256.82557
Energy (kJ/mol)	-8550791.16	-8550795.54
Energy (rel)* / kj/mol	4.38	0.00
E(1)···E(2)	2.8122	2.7431
WBI E(1)···E(2)	0.6178	0.6975
E(1)-C(1)	2.1184	2.1215
E(2)-C(9)	1.9385	1.9461
C(10)-C(1)-E(1)-C(11); θ1 / °	109.360	-95.488
C(10)-C(9)-E(2)-C(17); θ2 / °	-119.250	-100.862
C(1)-E(1)-C(11)-C(12); γ1 / °	165.161	-165.852
C(9)-E(2)-C(17)-C(18); γ2 / °	-156.981	-158.832

Distances in Å, angles in degrees, energy values as specified.

Table S4: Adiabatic ionisation potentials (electron volts) of monocation species to dications. Only the lowest energy conformers of the varying chemical compositions were considered and these are listed under "Geometry Neutral" and "Geometry Monocation".

Species	Geometry Monocation	Geometry Dication	Adiabatic I.P. (eV)
N7	CCc	CCc	10.121
N8	AAt	CCc	10.007
N9	AAt	AAt	9.619
N10	AAt	CCc	10.065
N11	AAt	AAt	9.987
N12	AAt	AAt	9.822

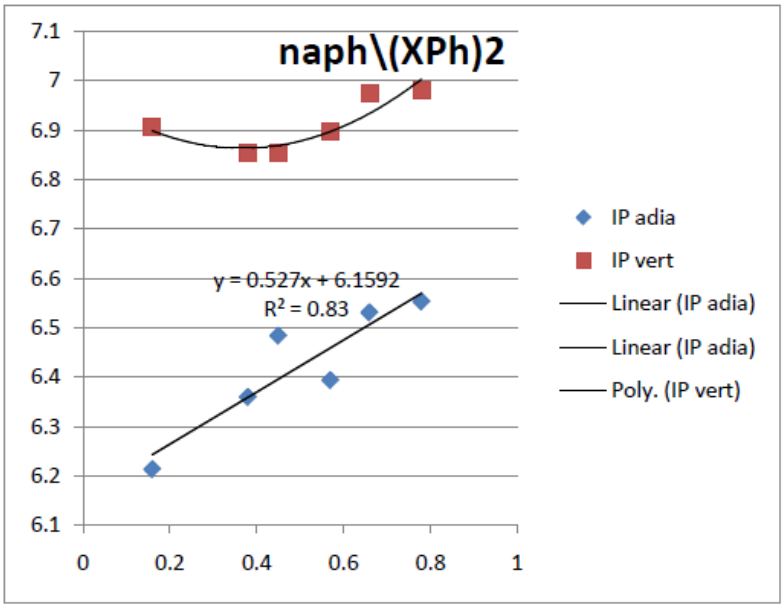

Figure S25. Correlations of Epa1 from solution voltammetry with Vertical and Adiabatic IPs, demonstrating the parabolic behaviour of the correlation for VIP versus approximately linear fits to the AIP.

Table S5: Vertical ionisation potentials of all geometries associated with a local energy minima for neutral and monocation species. The vertical ionisation involved for neutral species involves formation of a monocation with no subsequent relaxation. Similarly, for the monocations, vertical ionisation involves the removal of an additional electron from monocation geometry with no relaxation.

Compound	Neutral Geometry	V. IP (eV)	Monocation Geometry	V. IP (eV)
N7	AAt	6.908	AAt	10.588
	AB	6.982	CCc	10.223
	CCt	6.872		
N8	AAt	6.839	AAc	11.183
	AB	6.687	AAt	10.337
	CCt	6.896		
N9	CCc	6.699	AAc	9.953
	CCt	6.906	AAt	9.986
			BB	10.295
N10	AAt	6.817	CCc	10.177
	BA	6.975	AAt	10.451
			AAt	10.301
N11	BA	6.854	AAc	10.195
			CCc	10.142
N12	BA	6.853	AAc	10.125
			AAt	10.169

V. IP = Vertical ionisation potential.

Discussion

Compared with the chalcogen – chalcogen distances observed for the neutral species, this distance decreases after both the initial and secondary oxidation event. Additionally, the Wiberg bond index (WBI) increases between the two chalcogens as oxidation occurs. As presented within the results section, the first oxidation occurs with greater ease than the second for all systems and the heavier chalcogens prove easier to remove an electron from in terms of the adiabatic ionisation potential (Tab S2. and Tab S4.). This is in-line with expectations given the more diffuse nature of the highest energy level of an atom down a periodic group.

Furthermore, as larger chalcogen atoms are placed in the peri position, the preference for geometries which support a higher WBI and smaller interchalcogen distance increases. Since the chalcogens are held in relatively inflexible positions due to the rigid structure of the naphthalene ring this is thought to be due to a greater orbital overlap which may allow the formation of bonds or hemibonds with greater ease.

Sulfur-Sulfur

Within the neutral geometry, the **N7** systems show a relatively weak preference for the AB conformer relative to CCt (+0.69 kJ/mol) and AAt (+5.93 kJ/mol). The large interchalcogen distance of 3.05 to 3.25 Å coupled with low WBI values of less than 0.05 suggest that there is little bonding character between the sulfur atoms. It is interesting to note that within the neutral **N7** species the AAt geometry shows the lowest bonding character as per the previously mentioned parameters.

Following the first oxidation event, the AB geometry which was previously the most stable conformer now appears to exist at a local energy maxima and only AAt and CCc were found from a range of starting geometries. For $\mathbf{N7}^{1+}$, CCc presents the most stable conformer though this has a lower bonding character (Tab. S1) relative to AAt. This first oxidation event is not predicted to form a hemibond within the

gaseous species at the level of theory employed and, as shown in the results section, the WBI for these systems is relatively low; 0.1127 for AAt and 0.0781 for CCc.

Removing a further electron again decreases the bond length between atoms (Tab. S3) though now the CCc conformer is heavily favoured, even over AAt (WBI of 0.5013; peri – S-S distance of 2.4963) which would be expected to present a hemibond. Two other geometries were found for **N7**$^{2+}$, namely ACc and BA(d). ACc presents a conformer which is approximately the same energy as AAt (within 1 kJ/mol) though shows a lower bonding character. The BA(d) geometry has both the lowest WBI, longest S-S distance and the highest relative energy, likely stemming from steric repulsion between the phenyls which would be increased within this geometry.

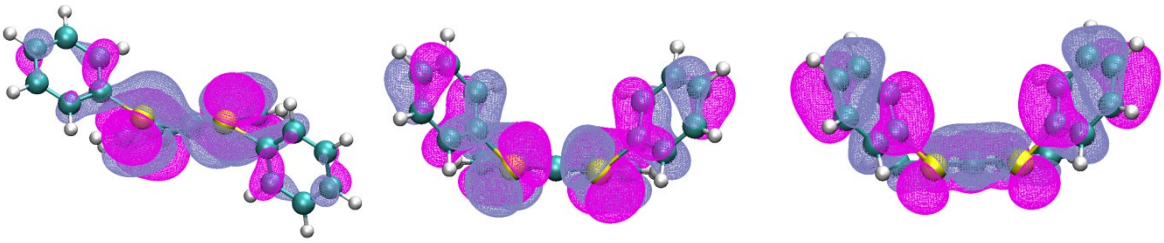

Figure S26*:* Molecular orbital diagrams of the HOMO (or SOMO) of the most stable **N7** conformers from neutral (left) to dication (right). A chalcogen-chalcogen interaction appears to be present at the HOMO for **N7**$^{2+}$.

Past the neutral oxidation state, sulfur shows a preference for CCc which grows in line with increasing positive charge on the **N7** species.

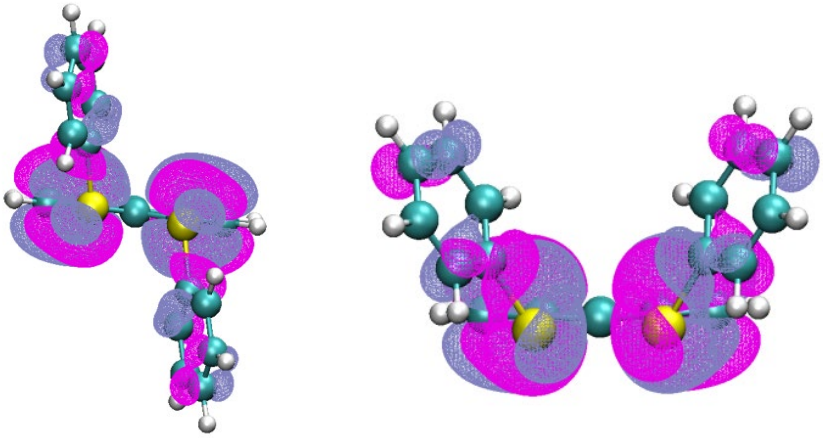

Figure S27: HOMOs of the two **N8**$^{2+}$ geometries – AAt (left) and CCc. The CCc conformer is preferred by 0.40 kJ/mol at the applied level of theory though shows less bonding character between the selenium atoms.

Selenium-Selenium

As a neutral molecule, this system shows a strong favorance for CCt with the AAt geometry resting 15.18 kJ/mol higher in energy. Upon oxidation, AAt becomes slightly favoured (Tab 1.) and this is postulated to be prominently due to minimising repulsion between the π clouds of the phenyl rings (compared with AAc) coupled with a slight increase in bonding character between the chalcogens. The data collected for the dicationic **N8** species (Tab 3.) surprisingly suggests a greater conformational preference for CCc by 0.40 kJ/mol over AAt even though the former has a lower bonding character and AAt may also be considered to minimize phenyl-phenyl steric repulsion to the same extent as CCc.

Tellurium-Tellurium

The geometric preferences of the Te-Te systems (**N9**) are dictated at both studied oxidation states by the attainment of greater bonding between the two chalcogen atoms. For the neutral systems though, CCt is 3.25 kJ/mol more favourable compared with the CCc conformer though this appears to be due to reduced steric repulsion between the phenyl rings rather than any increased bonding character with the WBI of these two conformers showing a negligible difference of 0.009.

Oxidising the **N9** species is predicted to favour the AAt geometry which also provides the greatest bonding character in terms of Te-Te distance and WBI. Geometry optimisations also uncovered the relatively unusual BB conformer which was only found for the Te-Te monocation systems. This peculiar geometry was found to be considerably higher in energy (~ 30 kJ/mol) than either AAc or AAt and also presented a markedly different SOMO (Figure S28).

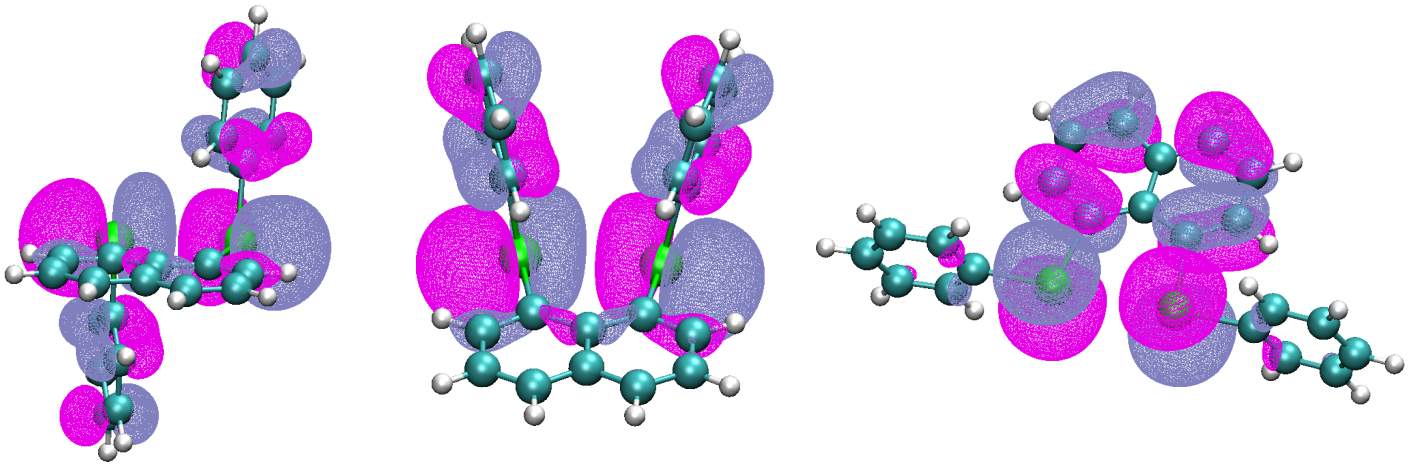

Figure S28: SOMOs of the $\mathbf{N9}^{1+}$ conformers, viewpoints taken so as to express the differences between AAc (left), AAt (centre) and BB (right). The BB conformer, which is less favoured (+30 kJ/mol), exhibits electron density on the naphthalene whereas electron density at this level in AAt and AAc is concentrated on the phenyl rings.

$\mathbf{N9}^{2+}$ shows a favorance for AAt over AAc and this appears to be due to decreased steric repulsion between the phenyl groups in addition to an increased bonding character between the tellurium atoms (Table 3.). Indeed, both of these oxidised geometries would be expected to display a full bond between the chalcogens. A WBI of 0.7577 is recorded for the preferred AAt conformer and a Te-Te distance which is 30% smaller than the sum of the VdW radii is also observed.

Mixed Species

The mixed compounds (**N10**, **N11** and **N12**) show values which are intermediate between those of the two identical chalcogen systems in question. Thus, **N10**, presents characteristics between **N7** and **N8** whilst **N12** displays attributes which are a mix of **N8** and **N9** in terms of WBI and interchalcogen (E···E') distances. The neutral mixed compounds all show preference for the BA geometry and the monocations are all most stable in the AAt geometry.

For the dications, $\mathbf{N10}^{2+}$ shows a considerably more stable CCc geometry compared with other conformers found to rest within energy minima (Table S3.) and this is likely guided by the sulfur atom as $\mathbf{N7}^{2+}$ dications

show a considerably more stable CCc geometry. The preference of $\mathbf{N10^{2+}}$ for CCc over AAt (10.19 kJ/mol) is just under half the relative stability of these conformers in the $\mathbf{N7^{2+}}$ systems and selenium has been shown to have a slim inclination as to the geometry it will adopt which further adheres to the notion that $\mathbf{N10^{2+}}$ geometry is confirmed primarily by sulfur. For $\mathbf{N11^{2+}}$, again, CCc is advanced as the more stable conformer by DFT calculations though now the relative difference over AAt is diminished compared with $\mathbf{N10^{2+}}$. This is likely due to sulfur's CCc directing ability in dications being opposed by the strong desire of tellurium to obtain bonding at this oxidation level. A conclusion such as this is supported by AAt exhibiting a considerably larger WBI over CCc (0.6134 against 0.4131 respectively) in addition to the former having an interchalcogen distance which is lower by 0.2 Å.

Finally, $\mathbf{N12^{2+}}$ shows a likening towards AAt with tellurium directing towards the conformer which can support greater bonding character (Tab 3.). A preference of 4.38 kJ/mol over AAc is observed and this smaller value compared with relative energies for $\mathbf{N9^{2+}}$ is potentially due to poorer orbital overlap between tellurium and selenium in contrast to the Te-Te overlap.

References for this initial part of the Computational Section

1. A. D. Becke, *J. Chem. Phys.,* 1993, **98**, 5648-5652; C. Lee, W. Yang and R. G. Parr, *Phys. Rev. B,* 1988, **37**, 785-789.
2. R. C. Binning and L. A. Curtiss, *J. Comput. Chem.,* 1990*,* **11**, 1206-1216.
3. M. Dolq, H. Stoll, H. Preuss and R.M Pitzer, *J. Phys. Chem*., 1993, **97**, 5852
4. S. Huzinaga, J. Anzelm, M. Klobukowski, E. Radzio-Andzelm, Y. Sakai and H. Tatewaki, in: *Gaussian Basis Sets for Molecular Calculations*, Elsevier, Amsterdam, 1984.
5. K. B. Wiberg, *Tetrahedron*, 1968, **24**, 1083-1096.
6. A. E. Reed, L. A. Curtiss and F. Weinhold, *Chem. Rev.*, 1998, **88**, 899-926.
7. M. J. Frisch, G. W. Trucks, H. B. Schlegel, G. E. Scuseria, M. A. Robb, J. R. Cheeseman, J. A. Montgomery, Jr., T. Vreven, K. N. Kudin, J. C. Burant, J. M. Millam, S. S. Iyengar, J. Tomasi, V. Barone, B. Mennucci, M. Cossi, G. Scalmani, N. Rega, G. A. Petersson, H. Nakatsuji, M. Hada, M. Ehara, K. Toyota, R. Fukuda, J.Hasegawa, M. Ishida, T. Nakajima, Y. Honda, O. Kitao, H. Nakai, M. Klene, X. Li, J. E. Knox, H. P. Hratchian, J. B. Cross, V. Bakken, C. Adamo, J. Jaramillo, R. Gomperts, R. E. Stratmann, O. Yazyev, A. J. Austin, R. Cammi, C. Pomelli, J. W. Ochterski, P. Y. Ayala, K. Morokuma, G. A. Voth, P. Salvador, J. J. Dannenberg, V. G. Zakrzewski, S. Dapprich, A. D. Daniels, M. C. Strain, O. Farkas, D. K. Malick, A. D. Rabuck, K. Raghavachari, J. B. Foresman, J. V. Ortiz, Q. Cui, A. G. Baboul, S. Clifford, J. Cioslowski, B. B. Stefanov, G. Liu, A. Liashenko, P. Piskorz, I. Komaromi, R. L. Martin, D. J. Fox, T. Keith, M. A. Al-Laham, C. Y. Peng, A. Nanayakkara, M. Challacombe, P. M. W. Gill, B. Johnson, W. Chen, M. W. Wong, C. Gonzalez and J. A. Pople, Gaussian 03, Revision E.01, Gaussian, Inc., Wallingford CT, 2004.
8. W. Humphrey, A. Dalke and K. Schulten, *J. Molec. Graphics.,* 1996, **14**, 33-38.
9. G. Schaftenaar and J.H. Noordik, *J. Comput.-Aided Mol. Design,* 2000, **14**, 123.

PCM applied to the Ionisation Potential of Diphenyl Dichalcogen Naphthalene Systems

The data relating to the conformational preference of the species investigated and adiabatic ionisation potentials has been updated using the DFT-D3 correction for dispersion, an attractive effect which is not readily accounted for by the employed B3LYP functional. Additionally, the effect of solvation, has been approximated using a polarisable continuum model (PCM). Two solvents were investigated, water (ε = 78.3553) and tetrahydrofuran (ε = 7.4257), to assess the effect of solvent polarity on preferred conformer and thus the adiabatic ionisation potential.

Neutral Species

Table S6: Energetic values for neutral species **N7-N12** (B3LYP and B3LYP-D). Dielectric values for PCM calculations were those corresponding to water and THF.

Gaseous

Compound	**N7 AAt**	**N7 AB**	**N7 CCt**
EPh,E'Ph	SPh, SPh	SPh, SPh	SPh, SPh
B3LYP Energy (Hartree)	-1644.37642	-1644.378673	-1644.378413
B3LYP Energy (kJ/mol)	-4317310.292	-4317316.206	-4317315.524
B3LYP Energy (rel)* / kj/mol	5.91	0.00	0.68
Disperson Correction (Hatree)	-0.04413	-0.04174	-0.03995
B3LYP-D Energy (Hartree)	-1644.42055	-1644.42041	-1644.41836
B3LYP-D Energy (kJ/mol)	-4317426.15	-4317425.78	-4317420.41
B3LYP-D Energy (rel)* / kj/mol	0.00	0.36	5.74

Water

Compound	**N7 AAt**	**N7 AB**	**N7 CCt**
EPh,E'Ph	SPh, SPh	SPh, SPh	SPh, SPh
B3LYP Energy (Hartree)	-1644.395102	-1644.396451	-1644.397208
B3LYP Energy (kJ/mol)	-4317359.341	-4317362.882	-4317364.871
B3LYP Energy (rel)* / kj/mol	5.53	1.99	0.00
Disperson Correction (Hatree)	-0.04413	-0.04174	-0.03995
B3LYP-D Energy (Hartree)	-1644.43923	-1644.43819	-1644.43716
B3LYP-D Energy (kJ/mol)	-4317475.20	-4317472.46	-4317469.76
B3LYP-D Energy (rel)* / kj/mol	0.00	2.74	5.44

THF

Compound	**N7 AAt**	**N7 AB**	**N7 CCt**
EPh,E'Ph	SPh, SPh	SPh, SPh	SPh, SPh
B3LYP Energy (Hartree)	-1644.390337	-1644.391974	-1644.392539
B3LYP Energy (kJ/mol)	-4317346.829	-4317351.127	-4317352.611
B3LYP Energy (rel)* / kj/mol	5.78	1.48	0.00
Disperson Correction (Hatree)	-0.04413	-0.04174	-0.03995
B3LYP-D Energy (Hartree)	-1644.43446	-1644.43371	-1644.43249
B3LYP-D Energy (kJ/mol)	-4317462.68	-4317460.70	-4317457.50
B3LYP-D Energy (rel)* / kj/mol	0.00	1.98	5.19

Gaseous

Compound	**N8 AB**	**N8 AAt**	**N8 CCt**
EPh,E'Ph	SePh, SePh	SePh, SePh	SePh, SePh
B3LYP Energy (Hartree)	-5650.69709	-5650.691889	-5650.69767

B3LYP Energy (kJ/mol)	-14835905.21	-14835891.55	-14835906.73
B3LYP Energy (rel)* / kj/mol	1.52	15.18	0.00
Disperson Correction (Hatree)	-0.04289	-0.04646	-0.04153
B3LYP-D Energy (Hartree)	-5650.73998	-5650.73834	-5650.73920
B3LYP-D Energy (kJ/mol)	-14836017.82	-14836013.52	-14836015.78
B3LYP-D Energy (rel)* / kj/mol	0.00	4.30	2.05

Water

Compound	**N8 AB**	**N8 AAt**	**N8 CCt**
EPh,E'Ph	SePh, SePh	SePh, SePh	SePh, SePh
B3LYP Energy (Hartree)	-5650.715056	-5650.709883	-5650.696199
B3LYP Energy (kJ/mol)	-14835952.38	-14835938.8	-14835902.87
B3LYP Energy (rel)* / kj/mol	0.00	13.58	49.51
Disperson Correction (Hatree)	-0.04289	-0.04646	-0.04153
B3LYP-D Energy (Hartree)	-5650.75795	-5650.75634	-5650.73773
B3LYP-D Energy (kJ/mol)	-14836064.99	-14836060.77	-14836011.91
B3LYP-D Energy (rel)* / kj/mol	0.00	4.22	53.08

THF

Compound	**N8 AB**	**N8 AAt**	**N8 CCt**
EPh,E'Ph	SePh, SePh	SePh, SePh	SePh, SePh
B3LYP Energy (Hartree)	-5650.710487	-5650.705165	-5650.691527
B3LYP Energy (kJ/mol)	-14835940.38	-14835926.41	-14835890.6
B3LYP Energy (rel)* / kj/mol	0.00	13.97	49.78
Disperson Correction (Hatree)	-0.04289	-0.04646	-0.04153
B3LYP-D Energy (Hartree)	-5650.75338	-5650.75162	-5650.73306
B3LYP-D Energy (kJ/mol)	-14836052.99	-14836048.38	-14835999.65
B3LYP-D Energy (rel)* / kj/mol	0.00	4.61	53.35

Gaseous

Compound	**N9 CCc**	**N9 CCt**
EPh,E'Ph	TePh, TePh	TePh, TePh
B3LYP Energy (Hartree)	-864.1360815	-864.1372566
B3LYP Energy (kJ/mol)	-2268789.282	-2268792.367
B3LYP Energy (rel)* / kj/mol	3.09	0.00
Disperson Correction (Hatree)	-0.04299	-0.04197
B3LYP-D Energy (Hartree)	-864.17908	-864.17923
B3LYP-D Energy (kJ/mol)	-2268902.16	-2268902.57
B3LYP-D Energy (rel)* / kj/mol	0.40	0.00

Water

Compound	**N9 CCc**	**N9 CCt**
EPh,E'Ph	TePh, TePh	TePh, TePh
B3LYP Energy (Hartree)	-864.1535651	-864.1551414
B3LYP Energy (kJ/mol)	-2268835.185	-2268839.324
B3LYP Energy (rel)* / kj/mol	4.14	0.00

Disperson Correction (Hatree)	-0.04299	-0.04197
B3LYP-D Energy (Hartree)	-864.19656	-864.19711
B3LYP-D Energy (kJ/mol)	-2268948.07	-2268949.52
B3LYP-D Energy (rel)* / kj/mol	1.46	0.00

THF

Compound	**N9 CCc**	**N9 CCt**
EPh,E'Ph	TePh, TePh	TePh, TePh
B3LYP Energy (Hartree)	-864.1491936	-864.1508008
B3LYP Energy (kJ/mol)	-2268823.708	-2268827.927
B3LYP Energy (rel)* / kj/mol	4.22	0.00
Disperson Correction (Hatree)	-0.04299	-0.04197
B3LYP-D Energy (Hartree)	-864.19219	-864.19277
B3LYP-D Energy (kJ/mol)	-2268936.59	-2268938.13
B3LYP-D Energy (rel)* / kj/mol	1.54	0.00

Gaseous

Compound	**N10 AAt**	**N10 BA**
EPh,E'Ph	SePh, SPh	SePh, SPh
B3LYP Energy (Hartree)	-3647.534214	-3647.53997
B3LYP Energy (kJ/mol)	-9576601.078	-9576616.19
B3LYP Energy (rel)* / kj/mol	15.11	0.00
Disperson Correction (Hatree)	-0.04541	-0.04207
B3LYP-D Energy (Hartree)	-3647.57962	-3647.58204
B3LYP-D Energy (kJ/mol)	-9576720.30	-9576726.65
B3LYP-D Energy (rel)* / kj/mol	6.35	0.00

Water

Compound	**N10 AAt**	**N10 BA**
EPh,E'Ph	SePh, SPh	SePh, SPh
B3LYP Energy (Hartree)	-3647.552339	-3647.558137
B3LYP Energy (kJ/mol)	-9576648.665	-9576663.888
B3LYP Energy (rel)* / kj/mol	15.22	0.00
Disperson Correction (Hatree)	-0.04541	-0.04207
B3LYP-D Energy (Hartree)	-3647.59775	-3647.60021
B3LYP-D Energy (kJ/mol)	-9576767.89	-9576774.35
B3LYP-D Energy (rel)* / kj/mol	6.46	0.00

THF

Compound	**N10 AAt**	**N10 BA**
EPh,E'Ph	SePh, SPh	SePh, SPh
B3LYP Energy (Hartree)	-3647.547717	-3647.553562
B3LYP Energy (kJ/mol)	-9576636.53	-9576651.878
B3LYP Energy (rel)* / kj/mol	15.35	0.00
Disperson Correction (Hatree)	-0.04541	-0.04207
B3LYP-D Energy (Hartree)	-3647.59313	-3647.59563

B3LYP-D Energy (kJ/mol)	-9576755.75	-9576762.34
B3LYP-D Energy (rel)* / kj/mol	6.58	0.00

Gaseous

Compound	**N11 BA**
EPh,E'Ph	TePh, SPh
B3LYP Energy (Hartree)	-1254.262508
B3LYP Energy (kJ/mol)	-3293066.214
B3LYP Energy (rel)* / kj/mol	N/A
Disperson Correction (Hatree)	-0.04251
B3LYP-D Energy (Hartree)	-1254.30502
B3LYP-D Energy (kJ/mol)	-3293177.82
B3LYP-D Energy (rel)* / kj/mol	N/A

Water

Compound	**N11 BA**
EPh,E'Ph	TePh, SPh
B3LYP Energy (Hartree)	-1254.280317
B3LYP Energy (kJ/mol)	-3293112.972
B3LYP Energy (rel)* / kj/mol	N/A
Disperson Correction (Hatree)	-0.04251
B3LYP-D Energy (Hartree)	-1254.32283
B3LYP-D Energy (kJ/mol)	-3293224.58
B3LYP-D Energy (rel)* / kj/mol	N/A

THF

Compound	**N11 BA**
EPh,E'Ph	TePh, SPh
B3LYP Energy (Hartree)	-1254.275919
B3LYP Energy (kJ/mol)	-3293101.425
B3LYP Energy (rel)* / kj/mol	N/A
Disperson Correction (Hatree)	-0.04251
B3LYP-D Energy (Hartree)	-1254.31843
B3LYP-D Energy (kJ/mol)	-3293213.04
B3LYP-D Energy (rel)* / kj/mol	N/A

Gaseous

Compound	**N12 BA**
EPh,E'Ph	TePh, SePh
B3LYP Energy (Hartree)	-3257.420256
B3LYP Energy (kJ/mol)	-8552356.881
B3LYP Energy (rel)* / kj/mol	N/A
Disperson Correction (Hatree)	-0.04302
B3LYP-D Energy (Hartree)	-3257.46328
B3LYP-D Energy (kJ/mol)	-8552469.84
B3LYP-D Energy (rel)* / kj/mol	N/A

Water

Compound	**N12 BA**
EPh,E'Ph	TePh, SePh
B3LYP Energy (Hartree)	-3257.437899
B3LYP Energy (kJ/mol)	-8552403.205
B3LYP Energy (rel)* / kj/mol	N/A
Disperson Correction (Hatree)	-0.04302
B3LYP-D Energy (Hartree)	-3257.48092
B3LYP-D Energy (kJ/mol)	-8552516.16
B3LYP-D Energy (rel)* / kj/mol	N/A

THF

Compound	**N12 BA**
EPh,E'Ph	TePh, SePh
B3LYP Energy (Hartree)	-3257.433641
B3LYP Energy (kJ/mol)	-8552392.023
B3LYP Energy (rel)* / kj/mol	N/A
Disperson Correction (Hatree)	-0.04302
B3LYP-D Energy (Hartree)	-3257.47666
B3LYP-D Energy (kJ/mol)	-8552504.98
B3LYP-D Energy (rel)* / kj/mol	N/A

Monocations

Table S7: Energetic values for monocationic species **N7-N12** (B3LYP and B3LYP-D).

Gaseous		
Compound	**N7 AAt**	**N7 CCc**
EPh,E'Ph	SPh, SPh	SPh, SPh
B3LYP Energy (Hartree)	-1644.13676	-1644.13786
B3LYP Energy (kJ/mol)	-4316681.07	-4316683.95
B3LYP Energy (rel)* / kj/mol	2.88	0
Dispersion correction (Hartree)	-0.04222	-0.04045
B3LYP-D Energy (Hartree)	-1644.17898	-1644.17831
B3LYP-D Energy (kJ/mol)	-4316791.91	-4316790.16
B3LYP-D Energy (rel)* / kj/mol	0.00	1.75

Water		
Compound	**N7 AAt**	**N7 CCc**
EPh,E'Ph	SPh, SPh	SPh, SPh
B3LYP Energy (Hartree)	-1644.20580	-1644.206961
B3LYP Energy (kJ/mol)	-4316862.32	-4316865.38
B3LYP Energy (rel)* / kj/mol	3.06	0
Dispersion correction (Hartree)	-0.04222	-0.04045
B3LYP-D Energy (Hartree)	-1644.24801	-1644.24741
B3LYP-D Energy (kJ/mol)	-4316973.16	-4316971.59
B3LYP-D Energy (rel)* / kj/mol	0.00	1.58

THF		
Compound	**N7 AAt**	**N7 CCc**
EPh,E'Ph	SPh, SPh	SPh, SPh
B3LYP Energy (Hartree)	-1644.195037	-1644.196137
B3LYP Energy (kJ/mol)	-4316834.07	-4316836.96
B3LYP Energy (rel)* / kj/mol	2.89	0
Dispersion correction (Hartree)	-0.04222	-0.04045
B3LYP-D Energy (Hartree)	-1644.23726	-1644.23659
B3LYP-D Energy (kJ/mol)	-4316944.91	-4316943.17
B3LYP-D Energy (rel)* / kj/mol	0.00	1.75

Gaseous		
Compound	**N8 AAc**	**N8 AAt**
EPh,E'Ph	SePh,SePh	SePh, SePh
B3LYP Energy (Hartree)	-5650.46167	-5650.46269
B3LYP Energy (kJ/mol)	-14835287.11	-14835289.81
B3LYP Energy (rel)* / kj/mol	2.69	0
Disperson Correction (Hatree)	-0.04512	-0.04421
B3LYP-D Energy (Hartree)	-5650.50679	-5650.50691
B3LYP-D Energy (kJ/mol)	-14835405.57	-14835405.88
B3LYP-D Energy (rel)* / kj/mol	0.31	0.00

Water

Compound	**N8 AAc**	**N8 AAt**
EPh,E'Ph	SePh,SePh	SePh, SePh
B3LYP Energy (Hartree)	-5650.532534	-5650.532402
B3LYP Energy (kJ/mol)	-5650.532534	-5650.532402
B3LYP Energy (rel)* / kj/mol	0.00	0
Disperson Correction (Hatree)	-0.04512	-0.04421
B3LYP-D Energy (Hartree)	-5650.57765	-5650.57661
B3LYP-D Energy (kJ/mol)	-14835591.63	-14835588.90
B3LYP-D Energy (rel)* / kj/mol	-2.73	0.00

THF

Compound	**N8 AAc**	**N8 AAt**
EPh,E'Ph	SePh,SePh	SePh, SePh
B3LYP Energy (Hartree)	-5650.521565	-5650.521349
B3LYP Energy (kJ/mol)	-14835444.37	-14835443.80
B3LYP Energy (rel)* / kj/mol	-0.57	0
Disperson Correction (Hatree)	-0.04512	-0.04421
B3LYP-D Energy (Hartree)	-5650.56668	-5650.56556
B3LYP-D Energy (kJ/mol)	-14835562.83	-14835559.87
B3LYP-D Energy (rel)* / kj/mol	-2.96	0.00

Gaseous

Compound	**N9 AAc**	**N9 AAt**	**N9 BB**
EPh,E'Ph	TePh, TePh	TePh, TePh	TePh, TePh
B3LYP Energy (Hartree)	-863.90680	-863.90888	-863.89743
B3LYP Energy (kJ/mol)	-2268187.31	-2268192.77	-2268162.70
B3LYP Energy (rel)* / kj/mol	5.46	0	30.07
Disperson Correction (Hatree)	-0.04611	-0.04503	-0.04117
B3LYP-D Energy (Hartree)	-863.95291	-863.95391	-863.93860
B3LYP-D Energy (kJ/mol)	-2268308.38	-2268310.98	-2268270.79
B3LYP-D Energy (rel)* / kj/mol	2.61	0.00	40.19

Water

Compound	**N9 AAc**	**N9 AAt**	**N9 BB**
EPh,E'Ph	TePh, TePh	TePh, TePh	TePh, TePh
B3LYP Energy (Hartree)	-863.980051	-863.9809118	-863.9649427
B3LYP Energy (kJ/mol)	-2268379.62	-2268381.88	-2268339.96
B3LYP Energy (rel)* / kj/mol	2.26	0	41.93
Disperson Correction (Hatree)	-0.04611	-0.04503	-0.04117
B3LYP-D Energy (Hartree)	-864.02616	-864.02594	-864.00611
B3LYP-D Energy (kJ/mol)	-2268500.70	-2268500.10	-2268448.05
B3LYP-D Energy (rel)* / kj/mol	-0.60	0.00	52.04

THF

Compound	**N9 AAc**	**N9 AAt**	**N9 BB**
EPh,E'Ph	TePh, TePh	TePh, TePh	TePh, TePh
B3LYP Energy (Hartree)	-863.9681875	-863.9690226	-863.9546427
B3LYP Energy (kJ/mol)	-2268348.48	-2268350.67	-2268312.91
B3LYP Energy (rel)* / kj/mol	2.19	0	37.75
Disperson Correction (Hatree)	-0.04611	-0.04503	-0.04117
B3LYP-D Energy (Hartree)	-864.01430	-864.01405	-863.99581
B3LYP-D Energy (kJ/mol)	-2268469.55	-2268468.88	-2268421.01
B3LYP-D Energy (rel)* / kj/mol	-0.66	0.00	47.87

Gaseous

Compound	**N10 AAt**	**N10 CCc**
EPh,E'Ph	SePh, SPh	SePh, SPh
B3LYP Energy (Hartree)	-3647.29995	-3647.29950
B3LYP Energy (kJ/mol)	-9575986.03	-9575984.83
B3LYP Energy (rel)* / kj/mol	0	1.19
Disperson Correction (Hatree)	-0.04320	-0.04161
B3LYP-D Energy (Hartree)	-3647.34316	-3647.34111
B3LYP-D Energy (kJ/mol)	-9576099.46	-9576094.08
B3LYP-D Energy (rel)* / kj/mol	0.00	5.37

Water

Compound	**N10 AAt**	**N10 CCc**
EPh,E'Ph	SePh, SPh	SePh, SPh
B3LYP Energy (Hartree)	-3647.36941	-3647.368975
B3LYP Energy (kJ/mol)	-9576168.39	-9576167.24
B3LYP Energy (rel)* / kj/mol	0	1.14
Disperson Correction (Hatree)	-0.04320	-0.04161
B3LYP-D Energy (Hartree)	-3647.41261	-3647.41059
B3LYP-D Energy (kJ/mol)	-9576281.82	-9576276.49
B3LYP-D Energy (rel)* / kj/mol	0.00	5.32

THF

Compound	**N10 AAt**	**N10 CCc**
EPh,E'Ph	SePh, SPh	SePh, SPh
B3LYP Energy (Hartree)	-3647.358496	-3647.35782
B3LYP Energy (kJ/mol)	-9576139.73	-9576137.96
B3LYP Energy (rel)* / kj/mol	0	1.77
Disperson Correction (Hatree)	-0.04320	-0.04161
B3LYP-D Energy (Hartree)	-3647.40170	-3647.39943
B3LYP-D Energy (kJ/mol)	-9576253.16	-9576247.21
B3LYP-D Energy (rel)* / kj/mol	0.00	5.95

Gaseous

Compound	**N11 AAc**	**N11 AAt**	**N11 CCc**
EPh,E'Ph	TePh, SPh	TePh, SPh	TePh, SPh
B3LYP Energy (Hartree)	-1254.02294	-1254.02422	-1254.02329
B3LYP Energy (kJ/mol)	-3292437.23	-3292440.60	-3292438.14
B3LYP Energy (rel)* / kj/mol	3.38	0	2.47
Disperson Correction (Hatree)	-0.04388	-0.04378	-0.04218
B3LYP-D Energy (Hartree)	-1254.06682	-1254.06801	-1254.06547
B3LYP-D Energy (kJ/mol)	-3292552.43	-3292555.56	-3292548.88
B3LYP-D Energy (rel)* / kj/mol	3.13	0.00	6.68

Water

Compound	**N11 AAc**	**N11 AAt**	**N11 CCc**
EPh,E'Ph	TePh, SPh	TePh, SPh	TePh, SPh
B3LYP Energy (Hartree)	-1254.095118	-1254.095523	-1254.093988
B3LYP Energy (kJ/mol)	-3292626.73	-3292627.79	-3292623.77
B3LYP Energy (rel)* / kj/mol	1.06	0	4.03
Disperson Correction (Hatree)	-0.04388	-0.04378	-0.04218
B3LYP-D Energy (Hartree)	-1254.13899	-1254.13931	-1254.13617
B3LYP-D Energy (kJ/mol)	-3292741.93	-3292742.75	-3292734.51
B3LYP-D Energy (rel)* / kj/mol	0.82	0.00	8.24

THF

Compound	**N11 AAc**	**N11 AAt**	**N11 CCc**
EPh,E'Ph	TePh, SPh	TePh, SPh	TePh, SPh
B3LYP Energy (Hartree)	-1254.083306	-1254.08381	-1254.082227
B3LYP Energy (kJ/mol)	-3292595.72	-3292597.04	-3292592.89
B3LYP Energy (rel)* / kj/mol	1.32	0	4.16
Disperson Correction (Hatree)	-0.04388	-0.04378	-0.04218
B3LYP-D Energy (Hartree)	-1254.12718	-1254.12759	-1254.12441
B3LYP-D Energy (kJ/mol)	-3292710.92	-3292712.00	-3292703.63
B3LYP-D Energy (rel)* / kj/mol	1.08	0.00	8.37

Gaseous

Compound	**N12 AAc**	**N12 AAt**
EPh,E'Ph	TePh, SePh	TePh, SePh
B3LYP Energy (Hartree)	-3257.18489	-3257.18653
B3LYP Energy (kJ/mol)	-8551738.92	-8551743.23
B3LYP Energy (rel)* / kj/mol	4.31	0
Disperson Correction (Hatree)	-0.04596	-0.04474
B3LYP-D Energy (Hartree)	-3257.23084	-3257.23127
B3LYP-D Energy (kJ/mol)	-8551859.58	-8551860.70
B3LYP-D Energy (rel)* / kj/mol	1.13	0

Water

Compound	**N12 AAc**	**N12 AAt**

EPh,E'Ph	TePh, SePh	TePh, SePh
B3LYP Energy (Hartree)	-3257.257056	-3257.257607
B3LYP Energy (kJ/mol)	-8551928.40	-8551929.85
B3LYP Energy (rel)* / kj/mol	1.45	0
Disperson Correction (Hatree)	-0.04596	-0.04474
B3LYP-D Energy (Hartree)	-3257.30301	-3257.30235
B3LYP-D Energy (kJ/mol)	-8552049.06	-8552047.32
B3LYP-D Energy (rel)* / kj/mol	-1.74	0

THF

Compound	**N12 AAc**	**N12 AAt**
EPh,E'Ph	TePh, SePh	TePh, SePh
B3LYP Energy (Hartree)	-3257.245918	-3257.245943
B3LYP Energy (kJ/mol)	-8551899.16	-8551899.22
B3LYP Energy (rel)* / kj/mol	0.06	0
Disperson Correction (Hatree)	-0.04596	-0.04474
B3LYP-D Energy (Hartree)	-3257.29187	-3257.29069
B3LYP-D Energy (kJ/mol)	-8552019.82	-8552016.69
B3LYP-D Energy (rel)* / kj/mol	-3.12	0

Dications

Table S8: Energetic values for dicationic species **N7-N12** (B3LYP and B3LYP-D).

Gaseous				
Compound	**N7 AAt**	**N7 ACc**	**N7 BA(d)**	**N7 CCc**
EPh,E'Ph	SPh, SPh	SPh, SPh	SPh, SPh	SPh, SPh
B3LYP Energy (Hartree)	-1643.75719	-1643.75752	-1643.74442	-1643.76591
B3LYP Energy (kJ/mol)	-4315684.50	-4315685.36	-4315650.98	-4315707.39
B3LYP Energy (rel)* / kj/mol	22.89	22.03	56.41	0.00
Disperson Correction (Hatree)	-0.04243	-0.04245	-0.04430	-0.04081
B3LYP-D Energy (Hartree)	-1643.79962	-1643.79997	-1643.78872	-1643.80672
B3LYP-D Energy (kJ/mol)	-4315795.91	-4315796.81	-4315767.28	-4315814.55
B3LYP-D Energy (rel)* / kj/mol	18.63	17.74	47.27	0.00

Water				
Compound	**N7 AAt**	**N7 ACc**	**N7 BA(d)**	**N7 CCc**
EPh,E'Ph	SPh, SPh	SPh, SPh	SPh, SPh	SPh, SPh
B3LYP Energy (Hartree)	-1643.987135	-1643.985943	-1643.974543	-1643.99417
B3LYP Energy (kJ/mol)	-4316288.22	-4316285.09	-4316255.16	-4316306.69
B3LYP Energy (rel)* / kj/mol	18.47	21.60	51.53	0.00
Disperson Correction (Hatree)	-0.04243	-0.04245	-0.04430	-0.04081
B3LYP-D Energy (Hartree)	-1644.02957	-1644.02839	-1644.01884	-1644.03498
B3LYP-D Energy (kJ/mol)	-4316399.63	-4316396.54	-4316371.46	-4316413.85
B3LYP-D Energy (rel)* / kj/mol	14.22	17.31	42.39	0.00

THF				
Compound	**N7 AAt**	**N7 ACc**	**N7 BA(d)**	**N7 CCc**
EPh,E'Ph	SPh, SPh	SPh, SPh	SPh, SPh	SPh, SPh
B3LYP Energy (Hartree)	-1643.953758	-1643.953428	-1643.943142	-1643.961743
B3LYP Energy (kJ/mol)	-4316200.59	-4316199.73	-4316172.72	-4316221.56
B3LYP Energy (rel)* / kj/mol	20.96	21.83	48.84	0.00
Disperson Correction (Hatree)	-0.04243	-0.04245	-0.04430	-0.04081
B3LYP-D Energy (Hartree)	-1643.99619	-1643.99588	-1643.98744	-1644.00256
B3LYP-D Energy (kJ/mol)	-4316312.00	-4316311.18	-4316289.02	-4316328.71
B3LYP-D Energy (rel)* / kj/mol	16.71	17.54	39.69	0.00

Gaseous		
Compound	**N8 AAt**	**N8 CCc**
EPh,E'Ph	SePh, SePh	SePh, SePh
B3LYP Energy (Hartree)	-5650.09478	-5650.09493
B3LYP Energy (kJ/mol)	-14834323.84	-14834324.24
B3LYP Energy (rel)* / kj/mol	0.40	0.00
Disperson Correction (Hatree)	-0.04435	-0.04323
B3LYP-D Energy (Hartree)	-5650.13913	-5650.13817
B3LYP-D Energy (kJ/mol)	-14834440.30	-14834437.75
B3LYP-D Energy (rel)* / kj/mol	0.00	2.54

Water

Compound	**N8 AAt**	**N8 CCc**
EPh,E'Ph	SePh, SePh	SePh, SePh
B3LYP Energy (Hartree)	-5650.327928	-5650.327141
B3LYP Energy (kJ/mol)	-14834935.98	-14834933.91
B3LYP Energy (rel)* / kj/mol	-2.07	0.00
Disperson Correction (Hatree)	-0.04435	-0.04323
B3LYP-D Energy (Hartree)	-5650.37228	-5650.37037
B3LYP-D Energy (kJ/mol)	-14835052.43	-14835047.42
B3LYP-D Energy (rel)* / kj/mol	0.00	5.01

THF

Compound	**N8 AAt**	**N8 CCc**
EPh,E'Ph	SePh, SePh	SePh, SePh
B3LYP Energy (Hartree)	-5650.293608	-5650.293605
B3LYP Energy (kJ/mol)	-14834845.87	-14834845.86
B3LYP Energy (rel)* / kj/mol	0.00	0.01
Disperson Correction (Hatree)	-0.04435	-0.04323
B3LYP-D Energy (Hartree)	-5650.33796	-5650.33684
B3LYP-D Energy (kJ/mol)	-14834962.32	-14834959.37
B3LYP-D Energy (rel)* / kj/mol	0.00	2.95

Gaseous

Compound	**N9 AAc**	**N9 AAt**
EPh,E'Ph	TePh, TePh	TePh, TePh
B3LYP Energy (Hartree)	-863.55282	-863.55525
B3LYP Energy (kJ/mol)	-2267257.93	-2267264.32
B3LYP Energy (rel)* / kj/mol	6.39	0.00
Disperson Correction (Hatree)	-0.04560	-0.04474
B3LYP-D Energy (Hartree)	-863.59842	-863.60000
B3LYP-D Energy (kJ/mol)	-2267377.65	-2267381.79
B3LYP-D Energy (rel)* / kj/mol	4.14	0.00

Water

Compound	**N9 AAc**	**N9 AAt**
EPh,E'Ph	TePh, TePh	TePh, TePh
B3LYP Energy (Hartree)	-863.7945982	-863.7946833
B3LYP Energy (kJ/mol)	-2267892.72	-2267892.94
B3LYP Energy (rel)* / kj/mol	0.22	0.00
Disperson Correction (Hatree)	-0.04560	-0.04474
B3LYP-D Energy (Hartree)	-863.84020	-863.83943
B3LYP-D Energy (kJ/mol)	-2268012.44	-2268010.41
B3LYP-D Energy (rel)* / kj/mol	0.00	2.02

THF

Compound	**N9 AAc**	**N9 AAt**

EPh,E'Ph	TePh, TePh	TePh, TePh
B3LYP Energy (Hartree)	-863.7590289	-863.7577816
B3LYP Energy (kJ/mol)	-2267799.33	-2267796.06
B3LYP Energy (rel)* / kj/mol	-3.27	0.00
Disperson Correction (Hatree)	-0.04560	-0.04474
B3LYP-D Energy (Hartree)	-863.80463	-863.80252
B3LYP-D Energy (kJ/mol)	-2267919.05	-2267913.53
B3LYP-D Energy (rel)* / kj/mol	0.00	5.52

Gaseous

Compound	**N10 AAt**	**N10 CCc**
EPh,E'Ph	SePh, SPh	SePh, SPh
B3LYP Energy (Hartree)	-3646.92620	-3646.93008
B3LYP Energy (kJ/mol)	-9575004.74	-9575014.93
B3LYP Energy (rel)* / kj/mol	10.19	0.00
Disperson Correction (Hatree)	-0.04342	-0.04183
B3LYP-D Energy (Hartree)	-3646.96962	-3646.97191
B3LYP-D Energy (kJ/mol)	-9575118.73	-9575124.74
B3LYP-D Energy (rel)* / kj/mol	6.01	0.00

Water

Compound	**N10 AAt**	**N10 CCc**
EPh,E'Ph	SePh, SPh	SePh, SPh
B3LYP Energy (Hartree)	-3647.157651	-3647.159322
B3LYP Energy (kJ/mol)	-9575612.41	-9575616.80
B3LYP Energy (rel)* / kj/mol	4.39	0.00
Disperson Correction (Hatree)	-0.04342	-0.04183
B3LYP-D Energy (Hartree)	-3647.20107	-3647.20115
B3LYP-D Energy (kJ/mol)	-9575726.41	-9575726.61
B3LYP-D Energy (rel)* / kj/mol	0.21	0.00

THF

Compound	**N10 AAt**	**N10 CCc**
EPh,E'Ph	SePh, SPh	SePh, SPh
B3LYP Energy (Hartree)	-3647.124034	-3647.126596
B3LYP Energy (kJ/mol)	-9575524.15	-9575530.88
B3LYP Energy (rel)* / kj/mol	6.73	0.00
Disperson Correction (Hatree)	-0.04342	-0.04183
B3LYP-D Energy (Hartree)	-3647.16745	-3647.16842
B3LYP-D Energy (kJ/mol)	-9575638.14	-9575640.69
B3LYP-D Energy (rel)* / kj/mol	2.55	0.00

Gaseous

Compound	**N11 AAt**	**N11 CCc**
EPh,E'Ph	TePh, SPh	TePh, SPh
B3LYP Energy (Hartree)	-1253.65689	-1253.65719

B3LYP Energy (kJ/mol)	-3291476.15	-3291476.97
B3LYP Energy (rel)* / kj/mol	0.81	0.00
Disperson Correction (Hatree)	-0.04378	-0.04249
B3LYP-D Energy (Hartree)	-1253.70067	-1253.69969
B3LYP-D Energy (kJ/mol)	-3291591.10	-3291588.53
B3LYP-D Energy (rel)* / kj/mol	0.00	2.57

Water

Compound	**N11 AAt**	**N11 CCc**
EPh,E'Ph	TePh, SPh	TePh, SPh
B3LYP Energy (Hartree)	-1253.893465	-1253.889792
B3LYP Energy (kJ/mol)	-3292097.29	-3292087.65
B3LYP Energy (rel)* / kj/mol	0.00	9.64
Disperson Correction (Hatree)	-0.04378	-0.04249
B3LYP-D Energy (Hartree)	-1253.93725	-1253.93229
B3LYP-D Energy (kJ/mol)	-3292212.24	-3292199.22
B3LYP-D Energy (rel)* / kj/mol	0.00	13.02

THF

Compound	**N11 AAt**	**N11 CCc**
EPh,E'Ph	TePh, SPh	TePh, SPh
B3LYP Energy (Hartree)	-1253.857462	-1253.855967
B3LYP Energy (kJ/mol)	-3292002.77	-3291998.84
B3LYP Energy (rel)* / kj/mol	0.00	3.93
Disperson Correction (Hatree)	-0.04378	-0.04249
B3LYP-D Energy (Hartree)	-1253.90124	-1253.89846
B3LYP-D Energy (kJ/mol)	-3292117.71	-3292110.41
B3LYP-D Energy (rel)* / kj/mol	0.00	7.30

Gaseous

Compound	**N12 AAc**	**N12 AAt**
EPh,E'Ph	TePh, SePh	TePh, SePh
B3LYP Energy (Hartree)	-3256.82390	-3256.82557
B3LYP Energy (kJ/mol)	-8550791.16	-8550795.54
B3LYP Energy (rel)* / kj/mol	4.38	0.00
Disperson Correction (Hatree)	-0.04500	-0.04458
B3LYP-D Energy (Hartree)	-3256.86890	-3256.87015
B3LYP-D Energy (kJ/mol)	-8550909.31	-8550912.58
B3LYP-D Energy (rel)* / kj/mol	3.27	0.00

Water

Compound	**N12 AAc**	**N12 AAt**
EPh,E'Ph	TePh, SePh	TePh, SePh
B3LYP Energy (Hartree)	-3257.062888	-3257.062564
B3LYP Energy (kJ/mol)	-8551418.61	-8551417.76
B3LYP Energy (rel)* / kj/mol	0.00	0.85

Disperson Correction (Hatree)	-0.04500	-0.04458
B3LYP-D Energy (Hartree)	-3257.10789	-3257.10714
B3LYP-D Energy (kJ/mol)	-8551536.76	-8551534.81
B3LYP-D Energy (rel)* / kj/mol	-1.95	0.00

THF		
Compound	**N12 AAc**	**N12 AAt**
EPh,E'Ph	TePh, SePh	TePh, SePh
B3LYP Energy (Hartree)	-3257.027913	-3257.026845
B3LYP Energy (kJ/mol)	-8551326.79	-8551323.98
B3LYP Energy (rel)* / kj/mol	0.00	2.81
Disperson Correction (Hatree)	-0.04500	-0.04458
B3LYP-D Energy (Hartree)	-3257.07291	-3257.07142
B3LYP-D Energy (kJ/mol)	-8551444.93	-8551441.03
B3LYP-D Energy (rel)* / kj/mol	-3.91	0.00

Adiabatic Ionisation Potentials

Table S9: Adiabatic ionisation potentials (atomic units and electron volts). Only the lowest energy conformers of the varying chemical compositions were considered. Energies are calculated at the B3LYP and B3LYP-D with differing solvents as approximated through PCM.

N7	Neutral Conformer	Monocation Conformer	Dication Conformer	First I.P. (e.V.)	Second I.P. (e.V.)
Gaseous	AB	CCc	CCc	6.55	10.12
Gaseous (Dispersion)	AAt	AAt	CCc	6.57	10.13
Water	CCt	CCc	CCc	5.18	5.79
Water (Dispersion)	AAt	AAt	CCc	5.20	5.80
THF	CCt	CCc	CCc	5.34	6.38
THF (Dispersion)	AAt	AAt	CCc	5.38	6.39
N8					
Gaseous	CCt	AAt	CCc	6.39	10.01
Gaseous (Dispersion)	AB	AAt	AAt	6.34	10.01
Water	AB	AAt	CCc	4.97	5.59
Water (Dispersion)	AB	AAt	AAt	4.93	5.56
THF	AB	AAt	AAt	5.15	6.20
THF (Dispersion)	AB	AAt	AAt	5.11	6.22
N9					
Gaseous	CCc	AAt	AAt	6.21	9.62
Gaseous (Dispersion)	CCc	AAt	AAt	6.13	9.63
Water	CCc	AAt	AAt	4.74	5.07
Water (Dispersion)	CCc	AAt	AAc	4.66	5.05
THF	CCc	AAt	AAt	4.95	5.75
THF (Dispersion)	CCc	AAt	AAc	4.86	5.70

N10					
Gaseous	BA	AAt	CCc	6.53	10.06
Gaseous (Dispersion)	BA	AAt	CCc	6.50	10.10
Water	BA	AAt	CCc	5.14	5.72
Water (Dispersion)	BA	AAt	CCc	5.10	5.75
THF	BA	AAt	CCc	5.31	6.31
THF (Dispersion)	BA	AAt	CCc	5.28	6.35
N11					
Gaseous	BA	AAt	CCc	6.48	9.99
Gaseous (Dispersion)	BA	AAt	AAt	6.45	10.00
Water	BA	AAt	AAt	5.03	5.50
Water (Dispersion)	BA	AAt	AAt	4.99	5.50
THF	BA	AAt	AAt	5.23	6.16
THF (Dispersion)	BA	AAt	AAt	5.19	6.16
N12					
Gaseous	BA	AAt	AAt	6.36	9.82
Gaseous (Dispersion)	BA	AAt	AAt	6.31	9.83
Water	BA	AAt	AAt	4.91	5.30
Water (Dispersion)	BA	AAt	AAt	4.86	5.31
THF	BA	AAt	AAt	5.11	5.93
THF (Dispersion)	BA	AAt	AAt	5.06	5.97

Computational Section continued for N13 – N16

Table S10 Results of *ab initio* MO Calculations performed on **N13-N16** evaluated at the B3LYP/6-31+G* level using X-ray and fully optimised geometries.

Compound	X...Y Expt.	(WBI)	X...Y Calc.	(WBI)
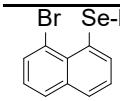 **N13**	3.114	0.05	3.172	0.05
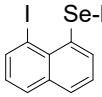 **N13**	3.252	0.06	3.336	0.05
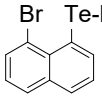 **N15**	3.191	0.07	3.266	0.07
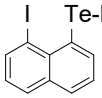 **N16**	3.426	0.08	3.427	0.08

To try and assess the possibility of direct X...E bonding interactions that would indicate an onset of 3c-4e bonding, density functional theory computations were performed for derivatives **N13-N16** at the B3LYP/6-31+G* level. The Wiberg bond index (WBI), which measures the covalent bond order, was calculated and increased from 0.05 for **5** to 0.08 for **8**, but indicates a very minor interaction taking place between the non-bonded atoms in these compounds (Table S10). For comparison, the fully covalent S-S single bond in naphtho(1,8-cd)(1,2-dithiole) has a WBI of 0.99 at the same level.

These results illustrate that more pronounced interactions could be expected as the neighbouring atoms become larger. Even stronger interactions can occur when one of the Se atoms carries an acceptor and indeed, when the "equatorial" Ph group on Se1 in 1,8-bis(phenylselanyl)naphthalene is replaced with Br, Se-Se distances as short as 2.516 Å have been observed. A B3LYP computation for the latter molecule from the X-ray structure affords a WBI of 0.55, suggesting a large extent of 3c-4e bonding in this case. Judging from the refined halogen-chalcogen distances, none of the species in the present study comes close to such a bonding situation.

Naph((E)PPh$_2$)(ER) compounds including N17

To try and assess the possibility of direct P···Se and E(2)···Se bonding interactions that would indicate an onset of 3c-4e bonding, density functional theory computations were performed for derivatives **N17** and **O,S** analogues at the B3LYP/6-31+G* level. For each compound both linear type arrangements [E(2)···E(1)-C and E(1)···P-C] were evaluated (Figure S29). The Wiberg bond index (WBI), which measures the covalent bond order, was calculated for each linear arrangement, both for the structures found in the solid and for the minima resulting from full geometry optimisations in the gas phase. WBI values of 0.02-0.04 are obtained throughout, indicating a very minor interaction between non-bonded atoms in these compounds. For comparison, the fully covalent S-S single bond in naphtho(1,8-cd)(1,2-dithiole) has a WBI of 0.99 at the same level. For **3S** and **3Se**, the aromatic π-stacking between phenyl groups at P and the chalcogen that is found in the solid is lost upon optimisation (due to the missing dispersion interaction at that level), but this affects the computed WBIs only slightly. When the "equatorial" Ph group on Se(1) in 1,8-bis(phenylselanyl)naphthalene is replaced with Br, Se-Se distances as short as 2.516 Å have been observed. A B3LYP computation for the latter molecule from the X-ray structure affords a WBI of 0.55, suggesting a large extent of 3c-4e bonding in this case. Judging from the refined

phosphorus-chalcogen and chalcogen-chalcogen distances, none of the species in the present study comes close to such a bonding situation.

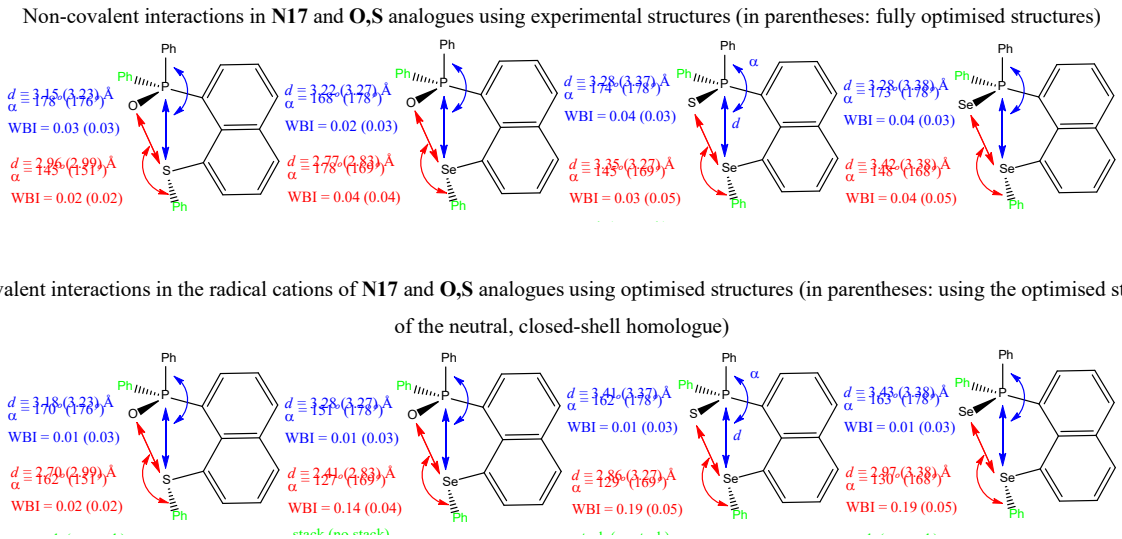

Figure S29 *DFT calculations performed on chalcogenides* **N17** *and O,S analogous, and their radical cations (B3LYP/6-31+G* level).*

Further calculations were performed on the radical cations of chalcogenides **2O**, **3O**, **3S**, and **3Se** (Figure 13). Whilst the Wiberg bond index values for the phosphorus-chalcogen interactions showed little change, the values for the E(2)···Se(1) interaction in the radical cations of selenium compounds **3O**, **3S**, and **3Se** increased to 0.14-0.19 indicating a greater interaction compared to the neutral species. This increase is a consequence of the nature of the HOMO in the latter species, which consists essentially of p-orbitals on E(2) and Se(1) in an antibonding combination (see Figure S30 for **3Se**). As MOs with the corresponding bonding combination are lower in energy, removal of an electron from the HOMO increases the net bond order between these atoms. No similar increase was observed for the O(1)···S(1) interaction in **2O** upon oxidation.

For each of the radical cations the adiabatic and vertical ionisation potentials were calculated. The values of 6.84-6.20 and 7.05-6.70 eV, respectively (Figure S30), are comparable to those of the known compound naphtho[1,8-*cd*]-1,2-dithiole, which has adiabatic and vertical IP values of 7.82 and 8.03 eV, respectively, computed at the same level. From previous unpublished work from the Woollins group it was shown that naphtho[1,8-*cd*]-1,2-dithiole can undergo one-electron oxidation and forms crystals of $[C_{10}H_6S_2^+]_3[BF_4^-]_3$ using electrocrystallisation techniques. Judging from the computed IP values, the four chalogenides **2O**, **3O**, **3S** and **3Se**, could exhibit similar electrochemical reactivity to naphtho[1,8-*cd*]-1,2-dithiole and may be able to form charge transfer compounds.

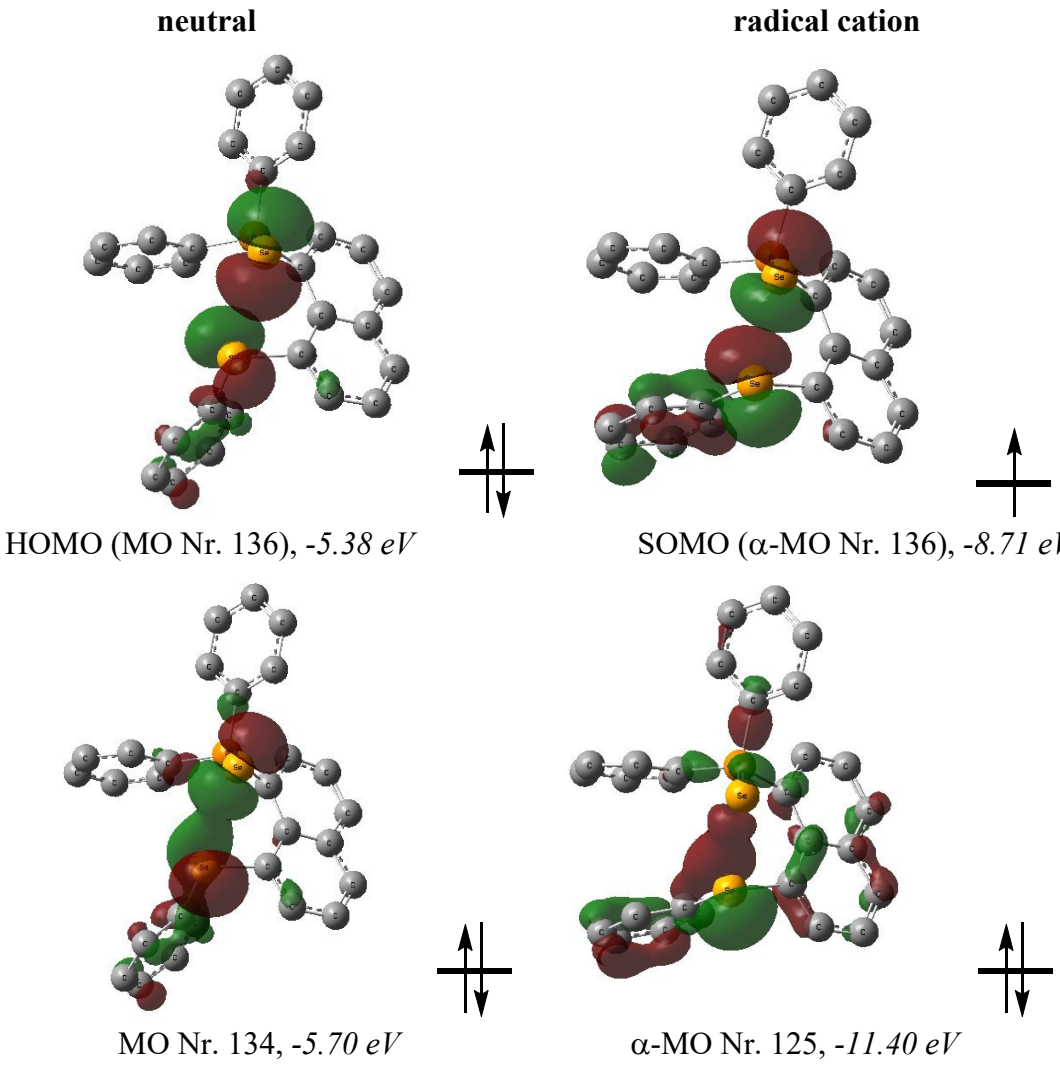

Figure S30 *Selected molecular orbitals of the neutral and radical cation species of* **N17** *(B3LYP level) showing bonding (bottom) and antibonding (top) combinations of p-orbitals on the Se atoms.*

Correlation of Wiburg Bond Indices to B3LYP-D3(BJ)/6-31+G(d) computed bond shortening

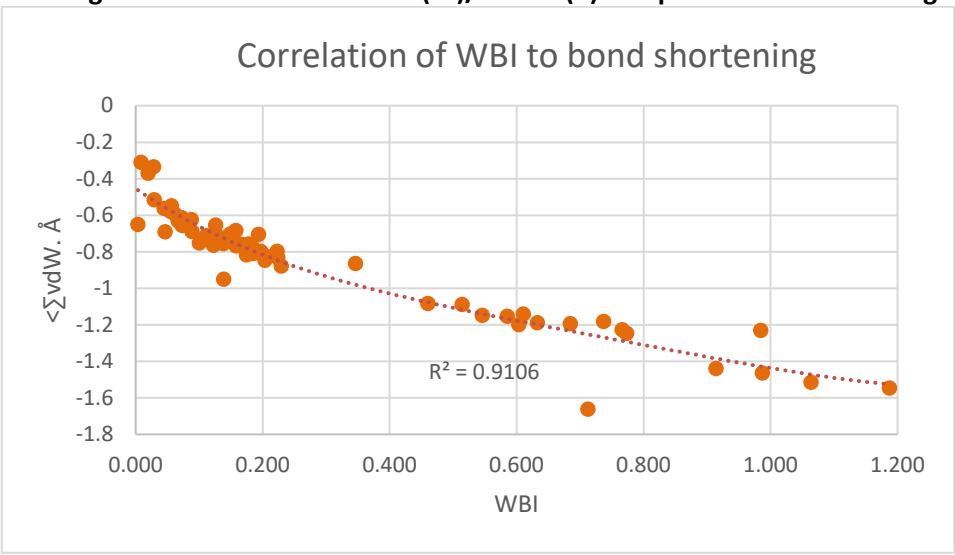

Figure S31. The degree of bond shortening expressed as *d* <∑vdW for E,E in Å fits to a fourth-order polynomial.

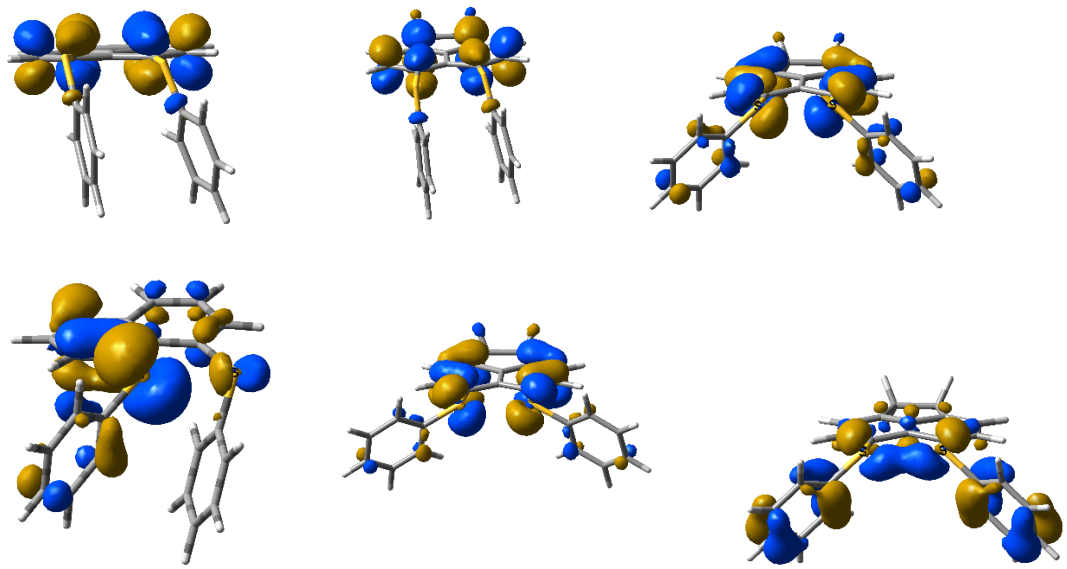

Figure S32. Molecular orbital diagrams of the HOMO (or SOMO) of the most stable **N1** conformers from neutral (left) to dication (right). A chalcogen-chalcogen interaction appears to be present at the HOMO for **N1**$^{2+}$.

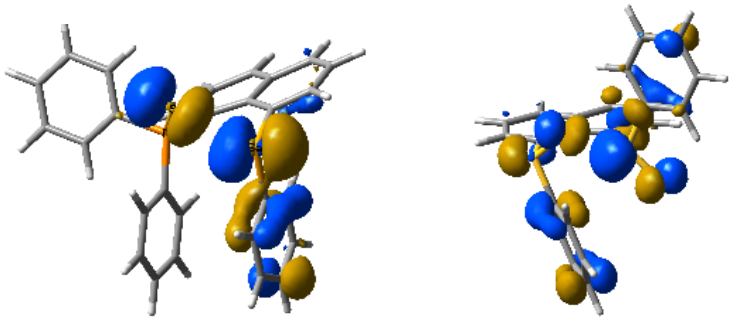

Figure S33. The SOMO of the monocations of **N17** and **N18**, the hemibond that develops by loss of the S*.

DFT modelling for neutral and oxidized N13 – **N16** (centre rows in Fig. 5, main paper). For the mixed halogen (Br, I) and PhE (Se, Te) compounds, the neutral conformations are all computed at the B3LYP-D3(BJ)/6-31+G(d)/PCM(CH_2Cl_2) level of theory to be in a B conformation (Table 3), which is in full agreement with all four crystal structures (CSD Refcodes: CIKPUI,[1] CUZDOR, CUZDUX and CUSFAF).[2] Upon 1*e* oxidation, the DFT results predict a C conformation for **N13**$^{+\bullet}$ and **N15**$^{+\bullet}$ (X = Br) but an A conformation for **N14**$^{+\bullet}$ and **N16**$^{+\bullet}$ (X = I). For these compounds, conformation C is always geometrically closer to B than A. No clear reason for these preferences could be found, but significantly it is the two iodides that induce the A conformations, with its expectation of preferred sigma E···X bonding. The WBI values for **N14**$^{+\bullet}$ (0.18) and **N16**$^{+\bullet}$ (0.19) are indeed slightly higher than those of **N13**$^{+\bullet}$ (0.07) and **N15**$^{+\bullet}$ (0.05), respectively. Upon removal of a second electron to afford dications, three adopt C conformations quite similar to **N13**$^{+\bullet}$ and **N15**$^{+\bullet}$, whereas in the case of **N16**$^{2+}$ (Te, I) there is a very clear preference for an A conformation. Evidently this favours Te–I σ-bond formation (WBI = 0.74).

DFT modelling for the remaining species (lowest two rows in Fig. 5, main article). The unsymmetrical PhSe/Ph_2P=S *peri*-substituted compound **N17** represents an interesting P(V)/Se(II) mixed-oxidation state exemplar. The E_p^{a1} is in the middle of the measured ranges for all the compounds. The geometry optimizations for neutral **N17**, by all methods employed, afford structures very close to the AA*c* molecular conformation also obtained from the SC-XRD experiment (CSD refcode: MUXGOC;[3] here conformation is defined on *one* of the PPh_2 rings). There is considerable distortion out of the $C_{10}H_6$ plane from steric constraints between the two large non-bonded substituents and the WBI of 0.03 indicates no bond between Se and P.[3] A dispersion-enhanced π-stacking interaction between the PhSe and one of the Ph_2P rings is observed but the overlap is poor (closest centroid to plane distance is 3.41 Å). Upon oxidation to the monocation, an incipient interaction develops between Se and the S bonded to P by rotation of the substituents relative to each other and the Se/S WBI increases to 0.21, while the π-stacking interaction also improves (3.32 Å). Upon the second oxidation, rotation completes to afford a C_3SeSP ring with an envelope conformation, and WBI values of 0.71 between Se and S with a bond length of 2.261 Å, whilst the P–S length has increased to 2.107 from 1.997 Å in the neutral molecule (a decrease in WBI from 1.32 to 0.97). The π-stacking interaction is also favourable in the dication ($d_{C\text{-}Pl}$ = 3.33 Å). To our knowledge, there is no experimental evidence for the isolation of such a cyclic dication despite the favourable geometry prediction. However, a cyclic neutral acenaphthene derivative containing a C_3Te_2O ring of generally similar conformation has been structurally characterized (CSD refcode WARPIQ – see Chart 5).[4]

The S(IV)/S(IV) *peri*-substituted disulfoxide **18** is by far the most difficult species to oxidize from this study, as may be expected from the higher oxidation states of both chalcogens. The neutral compound optimizes in a geometry close to that found in the SC-XRD (CSD refcode: MUWWIL),[3] where the closest non-bonded distance between the two S atoms is 3.086 Å with a negligible WBI. Importantly, the DFT-computed HOMO is still of the chalcogen-LP type, indicating that the RMO remains substituent-centred, even though the redox potential exceeds that of naphthalene itself (see above). The conformation is approximately AA*c* but the phenyl rings are far apart. Upon one and two electron oxidations, rotation to an AA*t* conformation facilitates an S···O interaction, with *d*(S···O) = 2.370 Å (WBI 0.14) in the monocation and *d*(S–O) = 1.658 Å (WBI 0.71). In the dication, the resultant C_3SOS ring with envelope conformation resembles that predicted for **N17**$^{2+}$ (main article, Fig. 5), and similarly may be compared to the neutral acenaphthene C_3Te_2O ring in WARPIQ.[3] The AA*t* conformation which is induced to form this covalent ring prevents any dispersion interaction between phenyl groups.

DFT modelling for N23, N23$^{+\bullet}$ and N23^{+2}

DFT Calculations on on **23**, **23**$^{+\bullet}$ and **23**$^{+2}$ to ascertain the origin of the small bond distance change on oxidation

DFT Calculations on 23, $23^{+\bullet}$ and 23^{+2}				
Neutrals		E(RB3LYP)	kJ.mol	D(S...S), Å
N18-dithiole_B3LYPD3bj-631G+d-PCMdcn	0 im fr	-1181.13	0	2.13666
			0	
	Naph-SPhx2			3.21698
	Acen-SPhx2			3.29063
Moncation		E(RB3LYP)	kJ.mol	D(S...S), Å
N18-dithiole+1_B3LYPD3bj-631G+d-PCMd	0 im fr	-1180.94	517.1132	2.08613
		IPa-I, eV	5.359424	2.4%
	Naph-SPhx2			2.87532
	Acen-SPhx2			2.94682
Dication		E(RB3LYP)	kJ.mol	D(S...S), Å
N18-dithiole2+_B3LYPD3bj-631G+d-PCMd	0 im fr	-1180.68	1187.267	2.05453
		IPa-II, eV	12.30498	3.8%
	Naph-SPhx2			
	Acen-SPhx2			2.59686

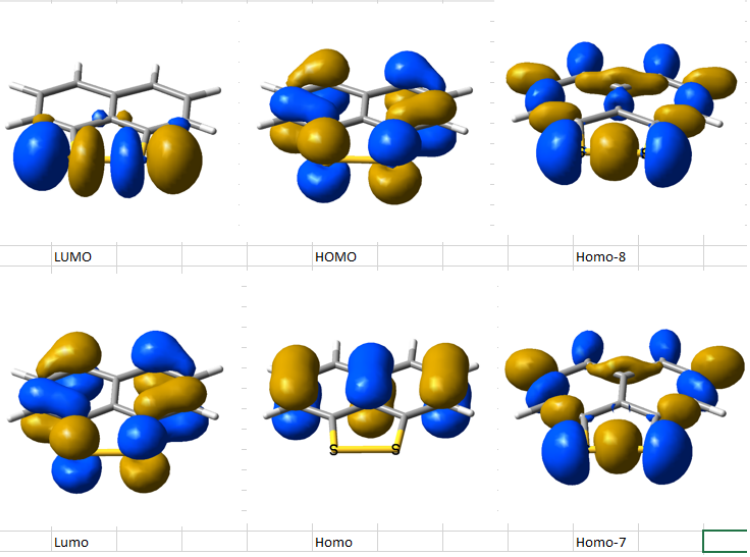

Pancake Bonding Analysis for [N23]BF_4.

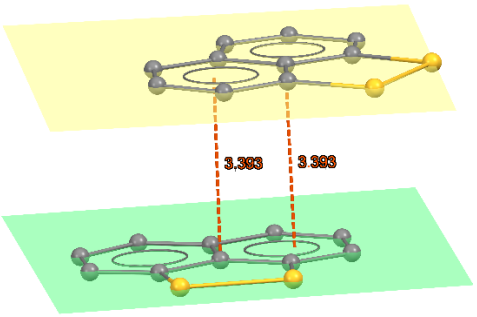

(a)

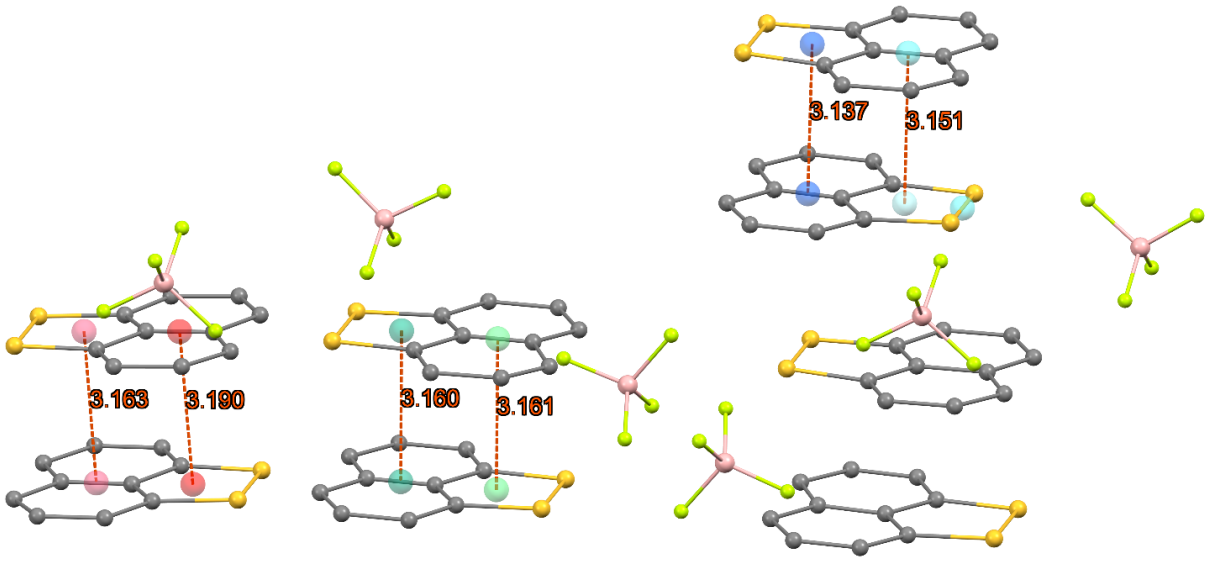

(b)

Figure S34. Experimental interplanar spacings in the crystal structures of (a) **N23** (DAQMUE) and (b) [**N23**]BF_4.

The SC-XRD structures of both neutral **N23** and oxidized rings in [**N23**]BF_4 have co-planar layers of $C_{10}H_6S_2$ rings, indicating significant inter-annular attractions. But the association of the former at a mean interplanar separation of 3.393 Å is significantly longer than the average value for the three independent dimers in the salt of 3.160(16) Å. Within the latter, there are stacks of alternating short-long separations, as shown in Fig. S34*b* at the right, with the longer separation of 3.385 Å closely matched to that of the neutral

system. Even more telling than the metrical separations in the two structures, however, are the strong differences in the overlap orientations of the atomic *p*-orbital components of the ring π-MOs. Thus, in neutral **N23**, the π-HOMO, as computed in a gas-phase B3LYPD3(BJ)/6-31+G(d) calculation (Fig. S35), shows the two rings totally out of register, and the HOMO-1 is homologous but with the contributions of the two rings exchanged. The LUMO is recognizably a combination of the LUMOs of the monomers (main article, Fig. 9).

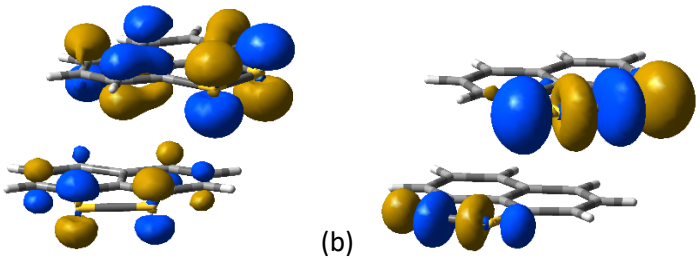

(a) (b)

Figure S35. (a) Out-of-register π-HOMO in the conventional π-stacked geometry of neutral **N23** (Refcode: DAQMUE). (b) LUMO of the same pair of stacked molecules.

In strong contrast, the closer-spaced dimers in the salt structure of [**N23**]BF_4 have the constituent atomic *p*-orbitals of the π-SOMOs in maximum overlap orientation (main article, Fig. 10). Using charge-compensated ion-pair models (discussed below), the interaction diagram shown in Fig. S36 can be computed, where two SOMOs, energy and topology shown at left of the diagram, can conceptually combine in- and out-of-phase to form the spin-paired SOMO-SOMO covalent bonding interaction. The question that needs to be answered, however, is to what extent that interaction contributes to the binding (i.e. to the closer spacing).

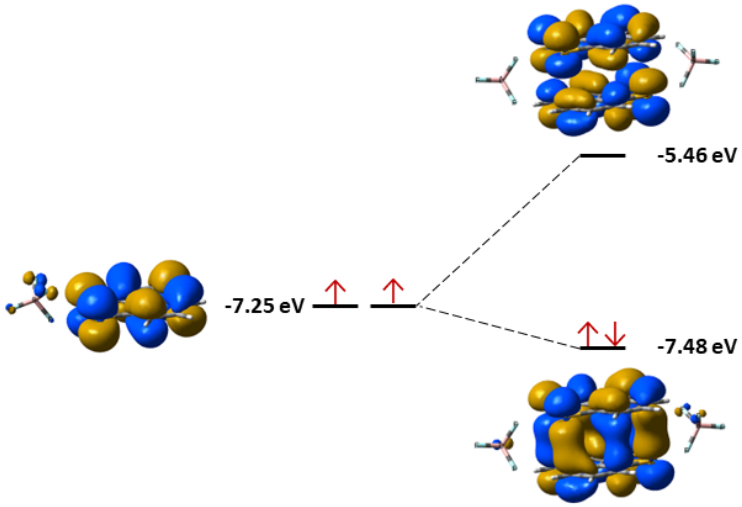

Figure S36. SOMO association by overlap in pancake-bonded dimer, with *e* pairing.

Following Cui *et al.*,[5] who have developed detailed models for the dimerization of $TCNE^{-\bullet}$ radical ions using high-level wavefunction theory (MR-AQCC) in an attempt to overcome the effects of Coulombic forces, we have also calculated two models, first an 'equatorial' model by optimizing a dimer plus two associated BF_4^- ions that are found at shortest separation to the sulfur atoms of the two radical cations, i.e. by optimizing charge-compensated ion pairs (Fig. S37a). Just as in the equatorial KTCNE radical ion pair, this form of association is still expected to have a significant Coulombic energy contribution (mutual attraction of two cation radicals to each of the anions, and repulsion expected to be strong between the cations and weaker between the anions, given the 1/*r* scaling of Coulombic energy. To improve on this, a second 'axial' model

was also developed where the anions are moved to above and below the cation dimer *which no longer corresponds to the crystal lattice*, but where the cross-coupling of the Coulombic attraction is minimized (Fig. S37c). Both models were optimized at our standard B3LYP-D3(BJ)/6-31+G(d) level of theory, albeit in a gas phase approximation, and the stability of the models checked by frequency calculations. In both models, the energy of the bound (singlet state) ion pairs are compared to single point calculations of the ion pairs (triplet state) separated to 10 Å by carrying the 'associated' anion with each cation (Fig. S37). Cui *et al.* scanned the separation distances in the K_2TCNE_2 models, and show convincingly that any effects attributable to pancake bonding fall away by the time 6 Å is reached, so that 10 Å seems a safe separation to minimize all interactions, including Coulombic, between the two ion pairs.

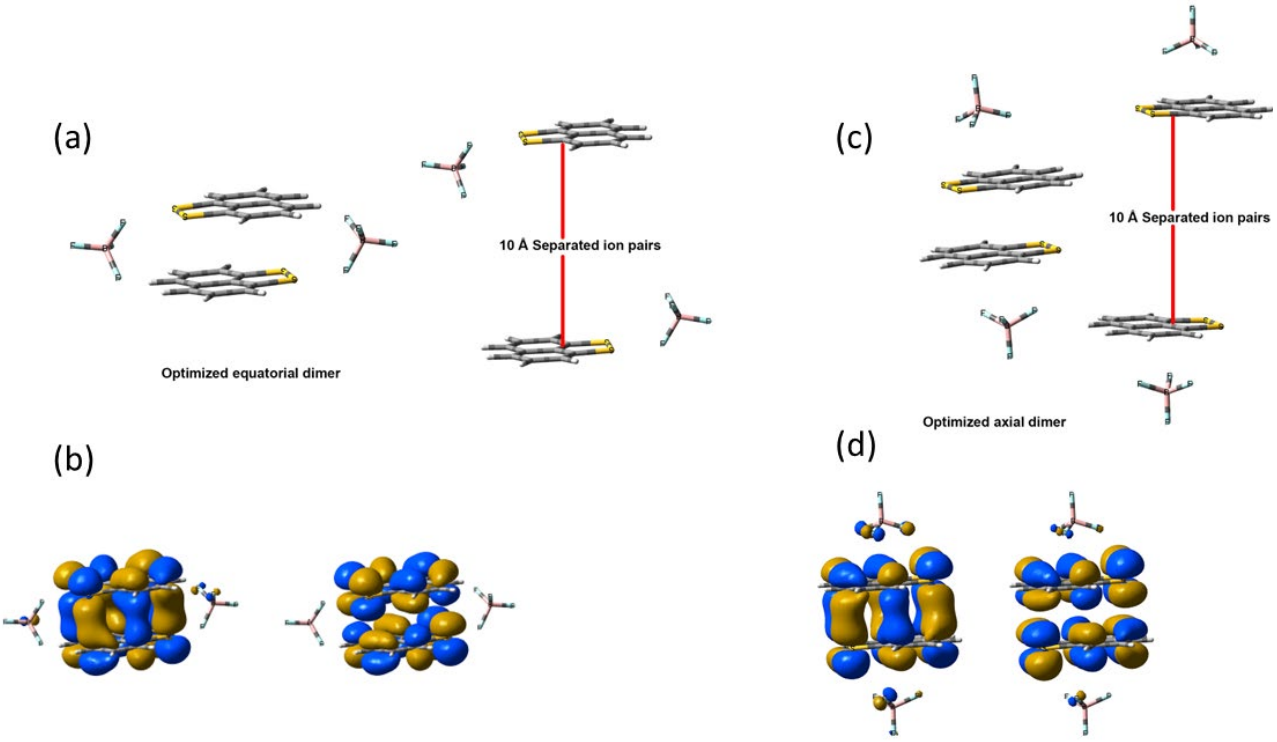

Figure S37. Geometries used for the gas-phase B3LYP-D3(BJ)/6-31+G(d) estimations of pancake bonding interaction energies for [(**N23**)BF_4]$_2$ ion-pair dimers. (a) Equatorial model, with bound state at the optimized separation of radical cations of 3.158 Å and separated to 10.0 Å. (b) The singlet HOMO (left) and LUMO (right) of the equatorial dimer model. (c) Axial model, with optimized bound state separation of 3.167 Å and (d) separated to 10.0 Å. (d) The singlet HOMO (left) and LUMO (right) of the axial dimer model.

For the 'equatorial' case, the raw interaction energy is computed to be −205 kJ/mol, with a HOMO-LUMO gap of 2.0 eV for the optimized dimer. This interaction energy, more than 49 kcal/mol, far exceeds the 7 – 11.5 kcal/mol magnitude expected for single-electron SOMO pancake bonding interactions.[5,6] Satisfyingly, the interaction energy in the axial model reduces to −99 kJ/mol, with a HOMO-LUMO gap in this model dimer of a very similar 1.98 eV, and a singlet-triplet gap of about 50 kJ/mol, computed by re-optimizing the axial model in the triplet state, where the ion pairs separate to about 3.7 Å. A BSSE correction has not been undertaken on this (improved) model, but the interaction energy magnitude of 24 kcal/mol still seems

excessive, indicating that full compensation of the large Coulombic energy may not have occurred. In the optimized dimer.

Further calculations are not warranted at this time, as Mou *et al.* have demonstrated the necessity of calibrating DFT methods against high-level wavefunction methods before they can be reliably used for pancake bonding estimates,[6] and the [(**N23**)BF_4]$_2$ system of cation radicals is intrinsically different from [KTCNE]$_2$. There is therefor no evidence that our standard B3LYP-D3(BJ)/6-31+G(d) is reliable for investigations beyond these estimates. It is to be hoped that a full treatment of the dimers of **N23**$^{+\bullet}$ and other related salts and charge transfer compounds from *peri*-substituted polycyclic aromatic hydrocarbons will be undertaken in due course.

Further References for the Computational Section

1. A. L. Fuller, F. R. Knight, A. M. Z. Slawin and J. D. Woollins, *Acta Crystallogr., Sect. E:Struct. Rep. Online*, 2007, **63**, o3855.
2. F. R. Knight, A. L. Fuller, M. Bühl, A. M. Z. Slawin, and J. D. Woollins, *Chem. Eur. J.*, 2010, **16**, 7605.
3. F. R. Knight, A. L. Fuller, M. Bühl, A. M. Z. Slawin, and J. D. Woollins, *Chem. Eur. J.*, 2010, **16**, 7617.
4. F. R. Knight, K. S. Athukorala Arachchige, R. A. M. Randall, M. Bühl, A. M. Z. Slawin and J. D. Woollins, *Dalton Trans.*, 2012, **41**, 3154.
5. Z-h. Cui, H. Lischka, T. Mueller, F. Plasser and M. Kertesz, *ChemPhysChem*, 2014, **15**, 165.
6. Z. Mou, Y-H. Tian and M. Kertesz, *Phys. Chem. Chem. Phys.*, 2017, **19**, 24761.

Section 3: Additional Solution Phase EPR Spectra

Under similar conditions to those reported for **A1**$^{+\bullet}$ by chemical oxidation with $NOBF_4$ in CH_2Cl_2.

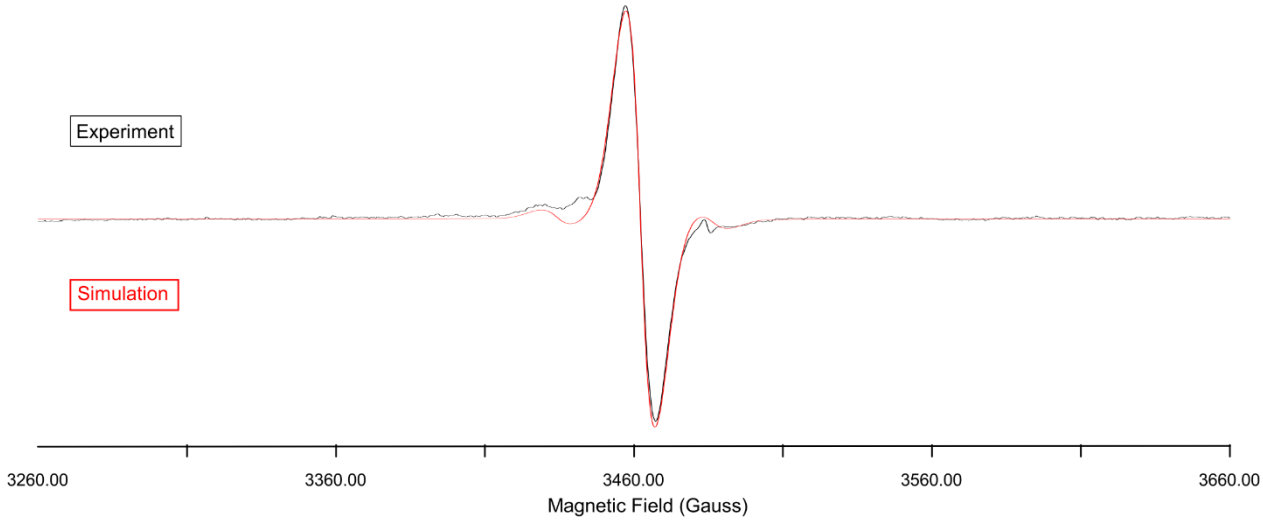

Figure S38. Solution EPR spectrum of **A4**$^{+\bullet}$

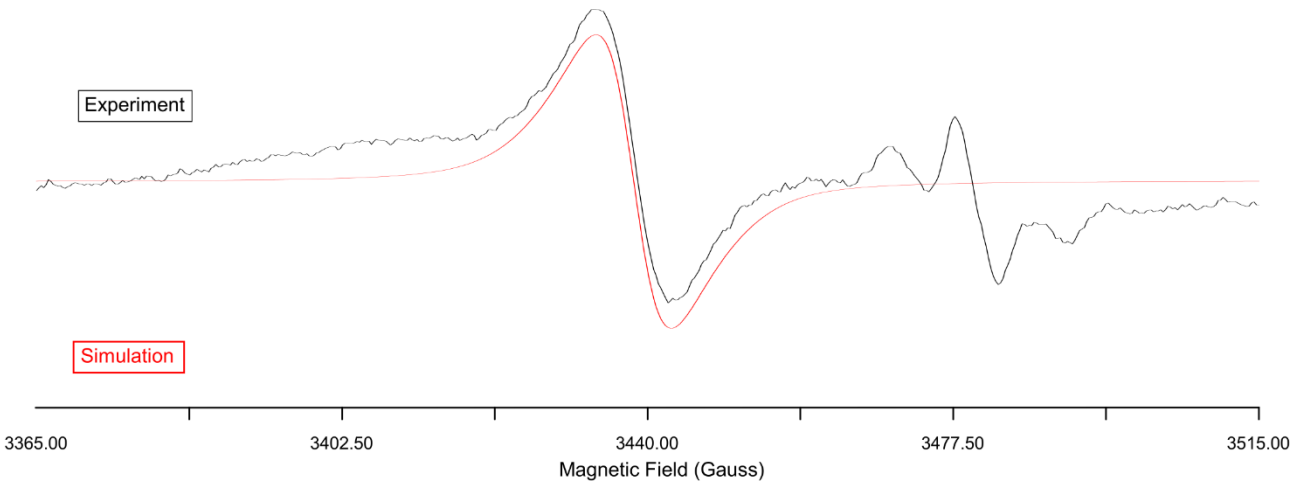

Figure S39. Solution EPR spectrum of **A4**$^{+\bullet}$

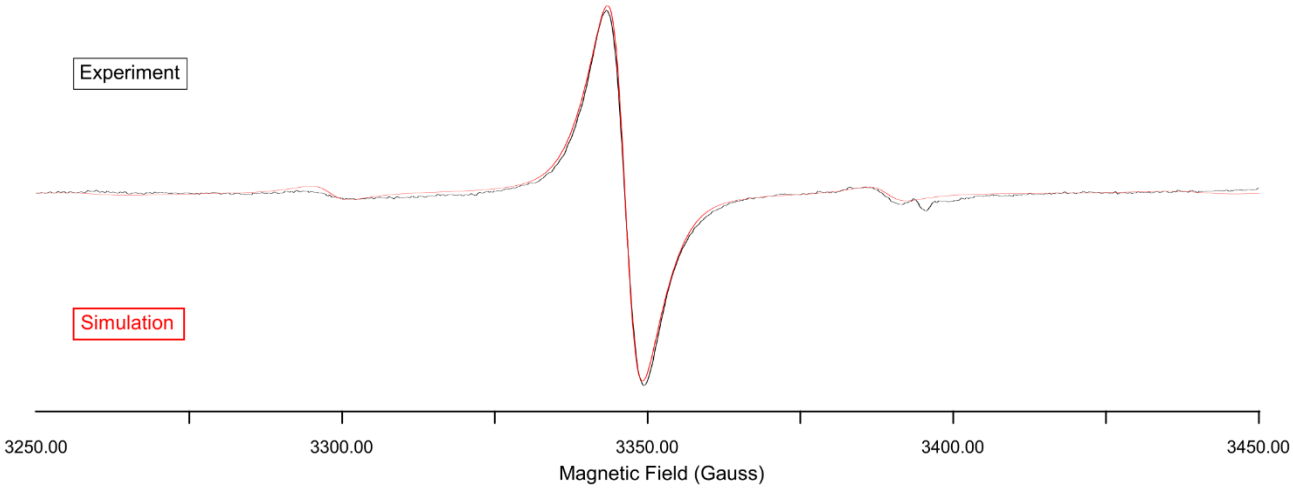

Figure S40. Sol Solution EPR spectrum of **A4**$^{+\bullet}$

Section 4: Detailed Crystallographic information

X-ray Crystallographic Structure determination on **A19**

Data Collection

A colorless platelet crystal of $C_{25}H_{23}BF_4O_2STe$ having approximate dimensions of 0.150 x 0.150 x 0.030 mm was mounted in a loop. All measurements were made on a Rigaku Saturn724 diffractometer Mo-Ka radiation.

Cell constants and an orientation matrix for data collection corresponded to a primitive triclinic cell with dimensions:

a = 11.7625(19) Å a = 83.26(3)°

b = 14.973(4) Å b = 71.08(2)°

c = 15.390(3) Å g = 68.25(2)°

V = 2381.4(10) Å^3

For Z = 4 and F.W. = 601.92, the calculated density is 1.679 g/cm^3. Based on a statistical analysis of intensity distribution, and the successful solution and refinement of the structure, the space group was determined to be:

P-1 (#2)

The data were collected at a temperature of -148 ± 1°C to a maximum 2q value of 57.9°.

Data Reduction

Of the 20303 reflections were collected, where 10339 were unique (R_{int} = 0.0847); equivalent reflections were merged. Data were collected and processed using CrystalClear (Rigaku). [1]

The linear absorption coefficient, m, for Mo-Ka radiation is 13.894 cm^{-1}. An empirical absorption correction was applied which resulted in transmission factors ranging from 0.757 to 0.959. The data were corrected for Lorentz and polarization effects.

Structure Solution and Refinement

The structure was solved by direct methods[2] and expanded using Fourier techniques. The non-hydrogen atoms were refined anisotropically. Hydrogen atoms were refined using the riding model. The final cycle of full-matrix least-squares refinement[3] on F^2 was based on 10339 observed reflections and 613 variable parameters and converged (largest parameter shift was 0.00 times its esd) with unweighted and weighted agreement factors of:

$$R1 = S \; ||Fo| - |Fc|| \; / \; S \; |Fo| = 0.0847$$

$$wR2 = [S (w (Fo^2 - Fc^2)^2)/ S \; w(Fo^2)^2]^{1/2} = 0.2033$$

The goodness of fit[4] was 1.09. Unit weights were used. The maximum and minimum peaks on the final difference Fourier map corresponded to 1.14 and -1.49 e$^-$/Å^3, respectively.

Neutral atom scattering factors were taken from International Tables for Crystallography (IT), Vol. C, Table 6.1.1.4 [5]. Anomalous dispersion effects were included in Fcalc[6]; the values for Df' and Df'' were those of Creagh and McAuley[7]. The values for the mass attenuation coefficients are those of Creagh and Hubbell[8]. All calculations were performed using the CrystalStructure[9] crystallographic software package except for refinement, which was performed using SHELXL Version 2018/3[10].

Further refinement was undertaken with SHELXL within the Olex2 v. 1.5 suite.[11]

Table 1 Crystal data and structure refinement for A19.

Identification code	A19
Empirical formula	$C_{25}H_{23}BF_4O_2STe$
Formula weight	601.90
Temperature/K	125.15
Crystal system	triclinic
Space group	P-1
a/Å	11.7625(19)
b/Å	14.972(4)
c/Å	15.390(3)
α/°	83.26(3)
β/°	71.08(2)
γ/°	68.25(2)
Volume/Å^3	2381.4(10)
Z	4
ρ_{calc}g/cm^3	1.679
μ/mm^{-1}	1.389
F(000)	1192.0
Crystal size/mm^3	0.15 × 0.15 × 0.03
Radiation	MoKα (λ = 0.71075)
2Θ range for data collection/°	2.798 to 50.498
Index ranges	-14 ≤ h ≤ 14, -17 ≤ k ≤ 17, -18 ≤ l ≤ 18
Reflections collected	18166
Independent reflections	8545 [R_{int} = 0.0839, R_{sigma} = 0.1415]
Data/restraints/parameters	8545/506/619
Goodness-of-fit on F^2	1.071
Final R indexes [I>=2σ (I)]	R_1 = 0.0758, wR_2 = 0.1447
Final R indexes [all data]	R_1 = 0.1284, wR_2 = 0.1740
Largest diff. peak/hole / e Å^{-3}	0.83/-1.22

Table 2 Fractional Atomic Coordinates (×10^4) and Equivalent Isotropic Displacement Parameters (Å^2×10^3) for A19. U_{eq} is defined as 1/3 of the trace of the orthogonalised U_{IJ} tensor.

Atom	*x*	*y*	*z*	U(eq)
Te1	9873.8(6)	8367.7(5)	3332.1(4)	43.1(2)
Te2	4852.4(6)	6913.3(5)	1746.0(4)	42.5(2)
S1	8957(2)	7841.8(17)	1998.7(17)	40.7(6)
S4	5987(2)	7388.1(17)	2960.6(17)	42.3(6)
F1	2086(7)	2256(5)	5033(5)	117(3)
F2	3057(7)	2940(6)	3828(5)	91(2)
F3	1238(8)	3841(5)	4866(5)	93(2)
F4	1192(7)	2862(5)	3905(6)	99(2)
F5	1671(9)	2592(10)	833(6)	173(5)
F6	2973(7)	2166(5)	-553(5)	90(2)
F7	3445(13)	1429(7)	644(9)	199(6)
F8	3538(7)	2866(5)	335(5)	101(2)
O1	10586(8)	8918(5)	4012(5)	72(2)
O2	3858(7)	6454(5)	1201(4)	58.3(19)
O3	4664(10)	2821(8)	1946(8)	116(3)

Table 2 Fractional Atomic Coordinates (×10^4) and Equivalent Isotropic Displacement Parameters (Å^2×10^3) for A19. U_{eq} is defined as 1/3 of the trace of the orthogonalised U_{IJ} tensor.

Atom	*x*	*y*	*z*	U(eq)
O4	212(9)	2070(8)	2687(7)	105(3)
C1	11021(8)	8731(6)	2089(6)	38(2)
C2	11962(9)	9085(7)	2094(7)	50(3)
C3	12699(10)	9381(7)	1282(7)	54(3)
C4	12540(10)	9308(7)	457(7)	50(2)
C5	11608(9)	8956(6)	454(6)	39(2)
C6	11518(10)	8962(6)	-442(7)	46(2)
C7	10614(10)	8685(6)	-560(7)	48(2)
C8	9790(9)	8350(6)	209(6)	43(2)
C9	9921(8)	8315(6)	1073(6)	36(2)
C10	10825(9)	8651(6)	1231(6)	38(2)
C11	13176(10)	9583(8)	-499(7)	62(3)
C12	12552(10)	9299(7)	-1131(7)	60(3)
C13	8267(9)	9640(7)	3449(6)	43(2)
C14	8464(11)	10523(7)	3261(7)	52(3)
C15	7397(12)	11354(7)	3354(7)	58(3)
C16	6179(11)	11306(8)	3644(7)	59(3)
C17	5987(10)	10450(8)	3847(7)	52(2)
C18	7018(10)	9603(7)	3772(6)	47(2)
C19	10688(11)	8559(8)	4898(7)	60(3)
C20	9977(9)	6585(6)	1976(7)	42(2)
C21	10905(10)	6147(7)	1178(7)	49(2)
C22	11626(11)	5180(7)	1213(8)	59(3)
C23	11434(11)	4672(8)	2030(8)	59(3)
C24	10518(10)	5121(8)	2819(8)	58(3)
C25	9768(9)	6095(7)	2803(7)	48(2)
C31	3791(9)	6557(6)	3060(6)	40(2)
C32	2804(9)	6248(7)	3126(7)	47(2)
C33	2111(9)	5925(7)	3984(7)	53(3)
C34	2506(9)	5900(7)	4728(7)	44(2)
C35	3524(9)	6193(6)	4654(6)	39(2)
C36	3825(10)	6111(6)	5468(6)	44(2)
C37	4843(10)	6324(6)	5516(7)	46(2)
C38	5525(10)	6685(6)	4714(7)	47(2)
C39	5210(8)	6821(6)	3892(6)	37(2)
C40	4207(9)	6540(6)	3826(6)	37(2)
C41	2016(10)	5591(7)	5706(7)	58(3)
C42	2881(11)	5746(7)	6200(7)	60(3)
C43	6423(9)	5576(6)	1546(6)	37(2)
C44	6145(10)	4744(7)	1648(7)	49(2)
C45	7160(11)	3877(7)	1515(7)	58(3)
C46	8371(11)	3841(8)	1325(7)	58(3)
C47	8673(11)	4677(8)	1217(7)	57(3)
C48	7658(9)	5565(7)	1337(7)	48(2)
C49	4114(11)	6491(9)	239(7)	71(4)

Table 2 Fractional Atomic Coordinates (×10^4) and Equivalent Isotropic Displacement Parameters (Å^2×10^3) for A19. U_{eq} is defined as 1/3 of the trace of the orthogonalised U_{IJ} tensor.

Atom	*x*	*y*	*z*	U(eq)
C50	4881(9)	8593(6)	3119(7)	41(2)
C51	3867(9)	8925(7)	3889(7)	45(2)
C52	3017(10)	9872(7)	3962(7)	50(2)
C53	3222(10)	10496(7)	3250(7)	46(2)
C54	4294(11)	10178(8)	2471(7)	57(3)
C55	5081(10)	9243(7)	2405(7)	48(2)
B1	1877(13)	2967(10)	4443(10)	57(3)
B2	2945(15)	2235(12)	334(10)	71(3)

Table 3 Anisotropic Displacement Parameters (Å^2×10^3) for A19. The Anisotropic displacement factor exponent takes the form: $-2\pi^2[h^2a^{*2}U_{11}+2hka^*b^*U_{12}+\ldots]$.

Atom	U_{11}	U_{22}	U_{33}	U_{23}	U_{13}	U_{12}
Te1	55.6(5)	44.4(4)	39.2(4)	5.9(3)	-20.2(3)	-25.3(4)
Te2	49.1(4)	43.8(4)	39.2(4)	1.3(3)	-16.3(3)	-19.4(3)
S1	43.1(15)	41.1(14)	41.4(14)	-0.8(12)	-11.9(12)	-19.2(12)
S4	41.4(15)	44.6(15)	44.3(14)	-4.9(12)	-12.2(12)	-18.4(13)
F1	103(6)	93(5)	100(6)	46(5)	-8(5)	-6(5)
F2	74(5)	126(6)	72(5)	-5(4)	-9(4)	-45(5)
F3	124(6)	67(4)	75(5)	-15(4)	-16(4)	-27(4)
F4	99(6)	79(5)	141(7)	-17(5)	-66(5)	-23(4)
F5	95(6)	332(14)	114(7)	-106(8)	18(5)	-109(7)
F6	111(6)	108(6)	59(4)	-3(4)	-14(4)	-59(5)
F7	290(13)	130(8)	266(14)	124(9)	-200(12)	-111(8)
F8	113(6)	109(6)	102(6)	-27(5)	-11(5)	-74(5)
O1	114(7)	92(6)	53(4)	21(4)	-52(5)	-68(5)
O2	71(5)	80(5)	39(4)	4(4)	-25(4)	-37(4)
O3	112(5)	121(5)	115(5)	0(3)	-38(4)	-37(3)
O4	100(4)	108(4)	105(4)	12(3)	-33(3)	-38(3)
C1	39(5)	34(5)	47(5)	6(4)	-19(4)	-16(4)
C2	52(6)	58(6)	54(6)	20(5)	-32(5)	-29(5)
C3	50(6)	56(7)	65(5)	9(6)	-19(5)	-31(6)
C4	49(6)	40(6)	53(5)	5(5)	-8(5)	-15(5)
C5	45(5)	28(5)	42(4)	1(4)	-13(4)	-9(4)
C6	61(6)	28(5)	45(5)	5(5)	-13(5)	-14(5)
C7	61(6)	33(5)	49(5)	6(5)	-24(5)	-11(5)
C8	50(6)	41(6)	45(5)	-4(5)	-22(4)	-15(5)
C9	38(5)	27(5)	43(5)	-2(4)	-15(4)	-8(4)
C10	48(5)	25(5)	44(4)	8(4)	-23(4)	-11(4)
C11	54(7)	52(7)	65(6)	8(6)	1(5)	-21(6)
C12	67(7)	46(6)	51(6)	9(5)	-3(5)	-18(6)
C13	56(5)	41(5)	29(5)	-3(4)	-10(4)	-16(5)
C14	68(6)	46(5)	50(6)	3(5)	-19(6)	-29(5)
C15	89(7)	40(5)	48(6)	-9(5)	-15(6)	-27(5)
C16	74(7)	55(6)	47(6)	-8(5)	-21(6)	-16(6)
C17	56(6)	61(6)	45(6)	-8(5)	-20(5)	-20(5)
C18	57(5)	55(5)	37(5)	-4(5)	-15(5)	-28(5)

Table 3 Anisotropic Displacement Parameters ($Å^2×10^3$) for A19. The Anisotropic displacement factor exponent takes the form: $-2\pi^2[h^2a^{*2}U_{11}+2hka^*b^*U_{12}+\ldots]$.

Atom	U_{11}	U_{22}	U_{33}	U_{23}	U_{13}	U_{12}
C19	76(8)	66(7)	42(6)	-9(5)	-26(6)	-21(6)
C20	56(6)	37(5)	44(5)	1(4)	-20(4)	-24(5)
C21	65(7)	42(5)	41(5)	-3(4)	-22(5)	-15(5)
C22	67(7)	43(5)	62(6)	-5(5)	-22(6)	-12(5)
C23	67(7)	41(6)	78(7)	10(5)	-32(5)	-24(5)
C24	53(7)	53(6)	75(7)	22(5)	-24(5)	-30(5)
C25	41(6)	49(5)	56(6)	10(5)	-8(5)	-27(5)
C31	44(5)	38(5)	46(5)	3(4)	-24(4)	-14(4)
C32	43(6)	50(6)	48(5)	11(5)	-19(5)	-16(5)
C33	43(6)	56(7)	61(6)	19(5)	-21(5)	-19(5)
C34	33(5)	40(5)	54(5)	10(5)	-14(4)	-9(4)
C35	44(5)	28(5)	42(4)	-2(4)	-15(4)	-9(4)
C36	57(6)	26(5)	40(5)	2(4)	-14(4)	-4(4)
C37	68(6)	28(5)	41(5)	-5(4)	-29(5)	-3(5)
C38	63(6)	37(5)	51(5)	-9(5)	-29(5)	-16(5)
C39	36(5)	37(5)	38(5)	-4(4)	-15(4)	-9(4)
C40	41(5)	32(5)	39(4)	-3(4)	-15(4)	-9(4)
C41	66(7)	40(6)	52(6)	5(5)	0(5)	-18(5)
C42	86(8)	42(6)	39(5)	0(5)	-4(5)	-23(6)
C43	57(5)	28(4)	33(5)	-5(4)	-19(4)	-15(4)
C44	61(6)	44(5)	49(6)	-7(5)	-15(5)	-26(4)
C45	80(6)	39(5)	52(7)	-5(5)	-19(6)	-16(5)
C46	71(6)	49(6)	52(7)	-2(5)	-35(6)	-5(5)
C47	58(6)	58(6)	44(6)	-6(5)	-14(5)	-6(5)
C48	53(5)	45(5)	48(6)	-5(5)	-18(5)	-17(4)
C49	83(9)	102(10)	40(5)	10(7)	-30(6)	-40(8)
C50	39(5)	38(5)	44(5)	-7(4)	-8(4)	-14(4)
C51	47(6)	50(5)	39(5)	-6(4)	-16(4)	-14(4)
C52	50(6)	42(5)	51(6)	-4(4)	-11(5)	-10(4)
C53	60(6)	42(5)	48(5)	-1(4)	-27(4)	-23(5)
C54	78(7)	49(5)	46(6)	2(5)	-18(5)	-25(5)
C55	48(6)	52(5)	51(6)	2(5)	-15(5)	-26(5)
B1	58(7)	52(6)	64(8)	-6(5)	-14(5)	-24(6)
B2	82(7)	92(9)	66(7)	35(8)	-35(6)	-61(7)

Table 4 Bond Lengths for A19.

Atom	Atom	Length/Å	Atom	Atom	Length/Å
Te1	O1	1.939(6)	C19	H19C	0.9800
Te1	C1	2.099(9)	C20	C21	1.385(13)
Te1	C13	2.103(10)	C20	C25	1.390(12)
Te2	O2	1.978(6)	C21	H21	0.9500
Te2	C31	2.130(9)	C21	C22	1.384(13)
Te2	C43	2.133(9)	C22	H22	0.9500
S1	C9	1.768(9)	C22	C23	1.390(14)
S1	C20	1.815(10)	C23	H23	0.9500
S4	C39	1.747(9)	C23	C24	1.376(15)

Table 4 Bond Lengths for A19.

Atom	Atom	Length/Å	Atom	Atom	Length/Å
S4	C50	1.779(10)	C24	H24	0.9500
F1	B1	1.320(14)	C24	C25	1.399(13)
F2	B1	1.393(14)	C25	H25	0.9500
F3	B1	1.362(15)	C31	C32	1.371(12)
F4	B1	1.386(14)	C31	C40	1.410(11)
F5	B2	1.371(17)	C32	H32	0.9500
F6	B2	1.371(15)	C32	C33	1.445(13)
F7	B2	1.244(15)	C33	H33	0.9500
F8	B2	1.367(14)	C33	C34	1.360(13)
O1	C19	1.432(10)	C34	C35	1.388(12)
O2	C49	1.411(11)	C34	C41	1.511(13)
O3	H3A	0.9796	C35	C36	1.390(12)
O3	H3B	0.8699	C35	C40	1.424(12)
O4	H4A	0.8701	C36	C37	1.374(13)
O4	H4B	0.8699	C36	C42	1.514(13)
C1	C2	1.395(11)	C37	H37	0.9500
C1	C10	1.436(12)	C37	C38	1.408(13)
C2	H2	0.9500	C38	H38	0.9500
C2	C3	1.401(13)	C38	C39	1.402(11)
C3	H3	0.9500	C39	C40	1.426(11)
C3	C4	1.364(13)	C41	H41A	0.9900
C4	C5	1.382(13)	C41	H41B	0.9900
C4	C11	1.507(13)	C41	C42	1.545(14)
C5	C6	1.416(12)	C42	H42A	0.9900
C5	C10	1.399(12)	C42	H42B	0.9900
C6	C7	1.344(12)	C43	C44	1.382(12)
C6	C12	1.533(13)	C43	C48	1.376(12)
C7	H7	0.9500	C44	H44	0.9500
C7	C8	1.438(13)	C44	C45	1.380(13)
C8	H8	0.9500	C45	H45	0.9500
C8	C9	1.381(11)	C45	C46	1.339(14)
C9	C10	1.427(11)	C46	H46	0.9500
C11	H11A	0.9900	C46	C47	1.402(14)
C11	H11B	0.9900	C47	H47	0.9500
C11	C12	1.567(14)	C47	C48	1.402(13)
C12	H12A	0.9900	C48	H48	0.9500
C12	H12B	0.9900	C49	H49A	0.9800
C13	C14	1.407(12)	C49	H49B	0.9800
C13	C18	1.410(13)	C49	H49C	0.9800
C14	H14	0.9500	C50	C51	1.362(13)
C14	C15	1.382(14)	C50	C55	1.400(12)
C15	H15	0.9500	C51	H51	0.9500
C15	C16	1.382(14)	C51	C52	1.392(13)
C16	H16	0.9500	C52	H52	0.9500
C16	C17	1.366(13)	C52	C53	1.373(12)
C17	H17	0.9500	C53	H53	0.9500

Table 4 Bond Lengths for A19.

Atom	Atom	Length/Å	Atom	Atom	Length/Å
C17	C18	1.377(13)	C53	C54	1.401(14)
C18	H18	0.9500	C54	H54	0.9500
C19	H19A	0.9800	C54	C55	1.356(13)
C19	H19B	0.9800	C55	H55	0.9500

Table 5 Bond Angles for A19.

Atom	Atom	Atom	Angle/˚	Atom	Atom	Atom	Angle/˚
O1	Te1	C1	90.3(3)	C32	C31	C40	121.2(8)
O1	Te1	C13	92.1(4)	C40	C31	Te2	119.2(6)
C1	Te1	C13	95.9(3)	C31	C32	C33	122.0(9)
O2	Te2	C31	88.1(3)	C34	C33	C32	117.4(9)
O2	Te2	C43	94.0(3)	C33	C34	C35	120.3(9)
C31	Te2	C43	95.3(3)	C33	C34	C41	130.9(9)
C9	S1	C20	101.8(4)	C35	C34	C41	108.8(8)
C39	S4	C50	101.0(4)	C34	C35	C36	113.5(8)
C19	O1	Te1	121.0(6)	C34	C35	C40	123.8(8)
C49	O2	Te2	118.8(6)	C36	C35	C40	122.7(8)
C2	C1	Te1	119.8(7)	C35	C36	C42	107.9(9)
C2	C1	C10	119.3(8)	C37	C36	C35	121.8(9)
C10	C1	Te1	120.9(6)	C37	C36	C42	130.3(9)
C1	C2	C3	121.2(9)	C36	C37	C38	116.9(8)
C4	C3	C2	120.7(9)	C39	C38	C37	122.8(9)
C3	C4	C5	117.9(9)	C38	C39	S4	120.3(7)
C3	C4	C11	131.5(10)	C38	C39	C40	120.2(8)
C5	C4	C11	110.6(9)	C40	C39	S4	119.4(6)
C4	C5	C6	111.3(9)	C31	C40	C35	115.1(8)
C4	C5	C10	125.1(9)	C31	C40	C39	129.4(8)
C10	C5	C6	123.6(8)	C35	C40	C39	115.4(8)
C5	C6	C12	109.6(9)	C34	C41	C42	104.4(8)
C7	C6	C5	119.0(9)	C36	C42	C41	105.4(8)
C7	C6	C12	131.4(9)	C44	C43	Te2	117.6(7)
C6	C7	C8	120.2(9)	C48	C43	Te2	120.0(7)
C9	C8	C7	120.2(8)	C48	C43	C44	122.4(9)
C8	C9	S1	119.5(7)	C45	C44	C43	117.8(10)
C8	C9	C10	121.1(8)	C46	C45	C44	121.2(10)
C10	C9	S1	119.5(7)	C45	C46	C47	121.8(10)
C5	C10	C1	115.7(8)	C46	C47	C48	117.8(10)
C5	C10	C9	115.9(8)	C43	C48	C47	118.9(9)
C9	C10	C1	128.3(8)	C51	C50	S4	124.5(7)
C4	C11	C12	105.1(8)	C51	C50	C55	118.1(9)
C6	C12	C11	103.1(8)	C55	C50	S4	117.4(8)
C14	C13	Te1	118.7(7)	C50	C51	C52	121.7(9)
C14	C13	C18	121.1(9)	C53	C52	C51	119.3(10)
C18	C13	Te1	120.0(7)	C52	C53	C54	119.7(10)
C15	C14	C13	118.0(10)	C55	C54	C53	119.6(10)
C16	C15	C14	120.2(10)	C54	C55	C50	121.5(10)

Table 5 Bond Angles for A19.

Atom	Atom	Atom	Angle/˚	Atom	Atom	Atom	Angle/˚
C17	C16	C15	121.7(11)	F1	B1	F2	108.4(11)
C16	C17	C18	120.3(10)	F1	B1	F3	112.3(11)
C17	C18	C13	118.5(9)	F1	B1	F4	112.3(11)
C21	C20	S1	121.7(7)	F3	B1	F2	110.1(10)
C21	C20	C25	122.3(9)	F3	B1	F4	108.4(11)
C25	C20	S1	116.0(8)	F4	B1	F2	105.0(11)
C22	C21	C20	118.1(10)	F5	B2	F6	105.8(11)
C21	C22	C23	120.7(11)	F7	B2	F5	108.4(13)
C24	C23	C22	120.4(10)	F7	B2	F6	111.0(15)
C23	C24	C25	120.1(10)	F7	B2	F8	113.4(12)
C20	C25	C24	118.2(10)	F8	B2	F5	110.8(14)
C32	C31	Te2	119.2(7)	F8	B2	F6	107.1(10)

Table 6 Hydrogen Bonds for A19.

D	H	A	d(D-H)/Å	d(H-A)/Å	d(D-A)/Å	D-H-A/°
O3	H3B	F8	0.87	2.38	3.152(13)	148.7
O4	H4A	F5	0.87	2.52	2.999(14)	115.5
O4	H4B	F4	0.87	2.35	3.030(13)	135.1
C18	H18	F1[1]	0.95	2.53	3.182(11)	125.8
C32	H32	O2	0.95	2.25	2.845(12)	119.9

[1]1-X,1-Y,1-Z

Table 7 Torsion Angles for A19.

A	B	C	D	Angle/˚	A	B	C	D	Angle/˚
Te1	C1	C2	C3	-176.6(7)	C18	C13	C14	C15	-3.4(14)
Te1	C1	C10	C5	177.1(6)	C20	S1	C9	C8	92.0(8)
Te1	C1	C10	C9	-1.7(13)	C20	S1	C9	C10	-87.7(8)
Te1	C13	C14	C15	-179.0(7)	C20	C21	C22	C23	-1.1(15)
Te1	C13	C18	C17	179.5(7)	C21	C20	C25	C24	-0.8(14)
Te2	C31	C32	C33	175.1(7)	C21	C22	C23	C24	0.3(16)
Te2	C31	C40	C35	-173.4(6)	C22	C23	C24	C25	0.2(16)
Te2	C31	C40	C39	6.7(14)	C23	C24	C25	C20	0.0(14)
Te2	C43	C44	C45	179.7(7)	C25	C20	C21	C22	1.3(14)
Te2	C43	C48	C47	179.4(7)	C31	C32	C33	C34	-2.6(15)
S1	C9	C10	C1	-5.1(13)	C32	C31	C40	C35	-0.6(13)
S1	C9	C10	C5	176.0(6)	C32	C31	C40	C39	179.5(9)
S1	C20	C21	C22	-178.7(7)	C32	C33	C34	C35	1.0(15)
S1	C20	C25	C24	179.2(7)	C32	C33	C34	C41	-179.0(10)
S4	C39	C40	C31	7.4(14)	C33	C34	C35	C36	-179.0(9)
S4	C39	C40	C35	-172.5(7)	C33	C34	C35	C40	0.7(15)
S4	C50	C51	C52	-178.5(7)	C33	C34	C41	C42	-179.7(11)
S4	C50	C55	C54	-179.3(8)	C34	C35	C36	C37	176.9(9)
C1	C2	C3	C4	-1.8(16)	C34	C35	C36	C42	-1.8(11)
C2	C1	C10	C5	-0.8(13)	C34	C35	C40	C31	-0.9(13)
C2	C1	C10	C9	-179.7(9)	C34	C35	C40	C39	179.0(9)
C2	C3	C4	C5	1.7(15)	C34	C41	C42	C36	-1.3(11)
C2	C3	C4	C11	178.8(10)	C35	C34	C41	C42	0.3(11)

Table 7 Torsion Angles for A19.

A	B	C	D	Angle/˚	A	B	C	D	Angle/˚
C3	C4	C5	C6	177.4(9)	C35	C36	C37	C38	3.7(14)
C3	C4	C5	C10	-1.3(15)	C35	C36	C42	C41	1.9(11)
C3	C4	C11	C12	179.7(11)	C36	C35	C40	C31	178.7(9)
C4	C5	C6	C7	-176.9(9)	C36	C35	C40	C39	-1.3(13)
C4	C5	C6	C12	3.6(11)	C36	C37	C38	C39	-0.5(14)
C4	C5	C10	C1	0.8(14)	C37	C36	C42	C41	-176.7(10)
C4	C5	C10	C9	179.8(9)	C37	C38	C39	S4	173.3(7)
C4	C11	C12	C6	4.8(11)	C37	C38	C39	C40	-3.6(14)
C5	C4	C11	C12	-3.0(12)	C38	C39	C40	C31	-175.7(9)
C5	C6	C7	C8	-2.6(14)	C38	C39	C40	C35	4.3(13)
C5	C6	C12	C11	-5.2(11)	C39	S4	C50	C51	11.0(9)
C6	C5	C10	C1	-177.7(8)	C39	S4	C50	C55	-169.7(7)
C6	C5	C10	C9	1.3(13)	C40	C31	C32	C33	2.3(15)
C6	C7	C8	C9	0.3(14)	C40	C35	C36	C37	-2.8(14)
C7	C6	C12	C11	175.4(10)	C40	C35	C36	C42	178.5(9)
C7	C8	C9	S1	-176.7(7)	C41	C34	C35	C36	1.0(11)
C7	C8	C9	C10	3.0(14)	C41	C34	C35	C40	-179.3(9)
C8	C9	C10	C1	175.1(9)	C42	C36	C37	C38	-177.9(9)
C8	C9	C10	C5	-3.7(13)	C43	C44	C45	C46	2.4(15)
C9	S1	C20	C21	-25.3(9)	C44	C43	C48	C47	0.4(14)
C9	S1	C20	C25	154.7(7)	C44	C45	C46	C47	-2.7(16)
C10	C1	C2	C3	1.4(15)	C45	C46	C47	C48	1.6(15)
C10	C5	C6	C7	1.8(14)	C46	C47	C48	C43	-0.5(14)
C10	C5	C6	C12	-177.7(9)	C48	C43	C44	C45	-1.3(14)
C11	C4	C5	C6	-0.3(12)	C50	S4	C39	C38	-95.3(8)
C11	C4	C5	C10	-178.9(9)	C50	S4	C39	C40	81.5(8)
C12	C6	C7	C8	176.8(9)	C50	C51	C52	C53	-1.6(14)
C13	C14	C15	C16	1.3(15)	C51	C50	C55	C54	0.1(14)
C14	C13	C18	C17	3.9(14)	C51	C52	C53	C54	-1.3(14)
C14	C15	C16	C17	0.2(16)	C52	C53	C54	C55	3.5(15)
C15	C16	C17	C18	0.3(16)	C53	C54	C55	C50	-2.9(15)
C16	C17	C18	C13	-2.3(14)	C55	C50	C51	C52	2.3(14)

Table 8 Hydrogen Atom Coordinates (Å×10^4) and Isotropic Displacement Parameters (Å^2×10^3) for A19.

Atom	*x*	*y*	*z*	U(eq)
H3A	4389.22	3383.56	2333.45	174
H3B	4232.06	2677.05	1655.27	174
H4A	714.86	1715.84	2204.99	157
H4B	608.8	2443.62	2728.84	157
H2	12105.21	9125.52	2658.45	60
H3	13316.73	9636.98	1305.89	64
H7	10518.17	8710.49	-1153.46	57
H8	9155.17	8151.61	121.9	52
H11A	14115.56	9230.24	-682.31	75
H11B	13014.09	10282.46	-536	75
H12A	12167.01	9857.58	-1487.65	72

Table 8 Hydrogen Atom Coordinates (Å×10^4) and Isotropic Displacement Parameters (Å^2×10^3) for A19.

Atom	*x*	*y*	*z*	U(eq)
H12B	13193.25	8775.12	-1559.9	72
H14	9304.78	10547.86	3074.6	62
H15	7501.18	11959.63	3219.32	70
H16	5456.25	11883.94	3702.97	71
H17	5139.31	10439.38	4041.17	63
H18	6890.63	9007.76	3933.22	56
H19A	11067.48	8922.13	5134.93	72
H19B	9831.06	8630.1	5319.78	72
H19C	11234.97	7877.21	4846.68	72
H21	11043.73	6499.12	622.94	58
H22	12258.51	4861.62	671.83	71
H23	11938.84	4009.83	2044.14	71
H24	10395.34	4768.75	3375.16	70
H25	9132.46	6412.33	3342.85	57
H32	2569.75	6246.55	2591.07	56
H33	1407.1	5737	4027.11	64
H37	5076.31	6231.7	6064.9	56
H38	6229.18	6843	4729.59	56
H41A	2097.48	4907.17	5729.75	70
H41B	1103.62	5988.98	5989.65	70
H42A	2363.27	6224.01	6701.67	72
H42B	3339.05	5134.94	6462.88	72
H44	5284.16	4766.58	1805.48	59
H45	6996.05	3295.41	1557.64	69
H46	9042.53	3232.15	1263.14	69
H47	9538.02	4643.32	1067.16	68
H48	7820.22	6148.92	1274.57	57
H49A	3551.38	6241.3	71.87	85
H49B	3956.06	7158.32	31.82	85
H49C	5013.66	6098.75	-55.91	85
H51	3736.51	8498.66	4388.16	54
H52	2303.04	10085.1	4497.97	61
H53	2639.65	11141.2	3286.25	55
H54	4468.28	10614.89	1991.18	69
H55	5782.65	9024.03	1863.07	58

X-ray Crystallographic Structure determination on A20

Data Collection

A colorless chip crystal of C26H25BF4O2SeTe having approximate dimensions of 0.150 x 0.090 x 0.060 mm was mounted in a loop. All measurements were made on a Rigaku Saturn724 diffractometer using graphite monochromated Mo-Ka radiation.

Cell constants and an orientation matrix for data collection corresponded to a primitive triclinic cell with dimensions:

a = 10.415(8) Å a = 61.44(3)o
b = 11.443(6) Å b = 84.01(4)o
c = 11.777(6) Å g = 88.75(4)o
V = 1225.4(13) Å3

For Z = 2 and F.W. = 662.85, the calculated density is 1.796 g/cm3. Based on a statistical analysis of intensity distribution, and the successful solution and refinement of the structure, the space group was determined to be:

P-1 (#2)

The data were collected at a temperature of -148 ± 1oC to a maximum 2q value of 58.3o.

Data Reduction

Of the 10562 reflections were collected, where 5326 were unique (Rint = 0.0617); equivalent reflections were merged. Data were collected and processed using CrystalClear (Rigaku). 1 The linear absorption coefficient, m, for Mo-Ka radiation is 27.524 cm-1. An empirical absorption correction was applied which resulted in transmission factors ranging from 0.389 to 0.848. The data were corrected for Lorentz and polarization effects.

Structure Solution and Refinement

The structure was solved by direct methods2 and expanded using Fourier techniques. The non-hydrogen atoms were refined anisotropically. Some hydrogen atoms were refined isotropically and the rest were refined using the riding model.The final cycle of full-matrix least-squares refinement3 on F2 was based on 5326 observed reflections and 340 variable parameters and converged (largest parameter shift was 0.00 times its esd) with unweighted and weighted agreement factors of:

$$R1 = S \; ||Fo| - |Fc|| \; / \; S \; |Fo| = 0.0981$$

$$wR2 = [S (w (Fo2 - Fc2)2)/ S w(Fo2)2]1/2 = 0.3485$$

The goodness of fit4 was 1.13. Unit weights were used. The maximum and minimum peaks on the final difference Fourier map corresponded to 1.72 and -6.24 e-/Å3, respectively.

Neutral atom scattering factors were taken from International Tables for Crystallography (IT), Vol. C, Table 6.1.1.4 5. Anomalous dispersion effects were included in Fcalc6; the values for Df' and Df'' were those of Creagh and McAuley7. The values for the mass attenuation coefficients are those of Creagh and Hubbell8. All calculations were performed using the CrystalStructure9 crystallographic software package except for refinement, which was performed using SHELXL Version 2018/3[10].

Further refinement was undertaken with SHELXL within the Olex2 v. 1.5 suite.[11]

Table 1 Crystal data and structure refinement for A20.

Identification code	A20
Empirical formula	$C_{26}H_{25}BF_4O_2SeTe$
Formula weight	662.83
Temperature/K	125.15
Crystal system	triclinic
Space group	P-1
a/Å	10.415(8)
b/Å	11.443(6)
c/Å	11.777(6)
α/°	61.44(3)
β/°	84.01(4)
γ/°	88.75(4)
Volume/Å^3	1225.4(13)
Z	2
ρ_{calc}g/cm^3	1.796
μ/mm^{-1}	2.752
F(000)	648.0
Crystal size/mm^3	0.15 × 0.09 × 0.06

Radiation	MoKα (λ = 0.71075)
2Θ range for data collection/°	4.054 to 50.5
Index ranges	-11 ≤ h ≤ 12, -13 ≤ k ≤ 12, -14 ≤ l ≤ 13
Reflections collected	9374
Independent reflections	4361 [R_{int} = 0.0587, R_{sigma} = 0.1155]
Data/restraints/parameters	4361/335/344
Goodness-of-fit on F^2	1.111
Final R indexes [I>=2σ (I)]	R_1 = 0.0680, wR_2 = 0.1615
Final R indexes [all data]	R_1 = 0.0867, wR_2 = 0.2161
Largest diff. peak/hole / e $Å^{-3}$	1.90/-3.59

Table 2 Fractional Atomic Coordinates (×10^4) and Equivalent Isotropic Displacement Parameters ($Å^2$×10^3) for A20. U_{eq} is defined as 1/3 of the trace of the orthogonalised U_{IJ} tensor.

Atom	*x*	*y*	*z*	U(eq)
Te1	8544.9(5)	1664.4(5)	3367.8(6)	33.5(3)
Se1	10254.6(9)	4050.4(9)	1776.6(9)	35.0(3)
F1	8579(7)	2575(8)	169(7)	78(2)
F2	6970(7)	1220(7)	1503(6)	66.1(18)
F3	6652(10)	2853(12)	-489(9)	74(4)
F5	7654(16)	1074(12)	-295(11)	109(5)
O1	7426(7)	216(7)	4737(7)	55.6(19)
O26	6226(10)	2065(10)	-2696(9)	82(3)
C1	9385(8)	1854(8)	4854(8)	27.9(17)
C2	9062(10)	903(9)	6105(10)	42(2)
C3	9548(11)	960(10)	7138(11)	49(2)
C4	10351(10)	1977(9)	6906(9)	37(2)
C5	10669(9)	2982(9)	5598(9)	34.0(18)
C6	11519(9)	3998(9)	5531(8)	32.2(18)
C7	11848(9)	5033(9)	4338(9)	37(2)
C8	11447(9)	5056(9)	3237(10)	39(2)
C9	10663(9)	4046(8)	3323(10)	36.5(19)
C10	10225(8)	2960(8)	4518(10)	33.9(18)
C11	11036(11)	2342(10)	7805(10)	49(2)
C12	11808(10)	3664(10)	6839(10)	46(2)
C13	7081(8)	3071(8)	3095(10)	35.3(19)
C14	6851(9)	4014(8)	1818(10)	39(2)
C15	5872(10)	4897(10)	1686(13)	55(3)
C16	5152(10)	4851(10)	2753(13)	55(3)
C17	5404(10)	3934(11)	3984(13)	55(3)
C18	6379(9)	3031(10)	4160(11)	46(2)
C19	11708(8)	3045(8)	1580(8)	31.1(18)
C20	12838(9)	2939(10)	2129(9)	42(2)
C21	13852(9)	2253(9)	1937(8)	37(2)
C22	13732(10)	1669(9)	1135(9)	42(2)
C23	12598(10)	1746(9)	611(9)	43(2)
C24	11592(9)	2462(8)	807(8)	35.2(19)
C25	6676(11)	-581(10)	4402(12)	56(3)

Table 2 Fractional Atomic Coordinates (×10^4) and Equivalent Isotropic Displacement Parameters (Å^2×10^3) for A20. U_{eq} is defined as 1/3 of the trace of the orthogonalised U_{IJ} tensor.

Atom	*x*	*y*	*z*	U(eq)
C26	4940(14)	1696(13)	-2200(15)	80(4)
B1	7476(16)	1897(17)	220(14)	45(3)
F3A	6910(30)	2100(30)	-620(30)	70(7)
F5A	8520(30)	740(30)	340(30)	66(7)
B1A	7700(40)	1610(50)	330(30)	45(3)

Table 3 Anisotropic Displacement Parameters (Å^2×10^3) for A20. The Anisotropic displacement factor exponent takes the form: $-2\pi^2[h^2a^{*2}U_{11}+2hka^*b^*U_{12}+\ldots]$.

Atom	U_{11}	U_{22}	U_{33}	U_{23}	U_{13}	U_{12}
Te1	29.0(5)	33.0(4)	40.4(5)	-19.7(3)	-0.1(3)	-2.0(3)
Se1	26.7(6)	37.3(6)	39.8(6)	-18.4(5)	1.4(4)	-0.2(4)
F1	55(4)	98(5)	76(5)	-39(4)	1(4)	-21(4)
F2	61(4)	91(5)	42(3)	-27(3)	-2(3)	-17(3)
F3	65(6)	81(7)	54(6)	-12(5)	-22(5)	16(5)
F5	185(15)	102(8)	85(8)	-79(7)	-36(9)	25(9)
O1	58(5)	44(4)	59(5)	-23(4)	7(4)	-21(3)
O26	73(6)	109(7)	58(6)	-36(6)	-5(5)	-4(5)
C1	28.8(19)	28.7(19)	28.0(19)	-14.8(12)	-3.9(10)	0.2(10)
C2	39(6)	40(5)	41(4)	-14(4)	2(4)	-2(4)
C3	46(6)	48(5)	58(6)	-30(5)	-2(5)	4(4)
C4	42(4)	49(4)	33(3)	-30(3)	-11(3)	5(3)
C5	25(5)	46(4)	42(4)	-31(4)	-2(4)	8(3)
C6	32(4)	46(3)	27(3)	-22(3)	-14(3)	4(3)
C7	38(6)	52(5)	29(4)	-26(4)	-8(4)	3(4)
C8	32(5)	42(5)	46(5)	-24(4)	4(4)	-4(4)
C9	26(5)	29(4)	51(5)	-18(3)	2(4)	3(3)
C10	26(5)	31(4)	51(5)	-25(3)	3(4)	1(3)
C11	53(5)	61(4)	42(4)	-30(3)	-12(3)	-2(3)
C12	40(6)	57(5)	56(5)	-38(5)	-5(4)	4(4)
C13	18(4)	35(4)	49(5)	-17(4)	-2(4)	-1(3)
C14	33(5)	35(4)	44(5)	-16(4)	2(4)	-5(3)
C15	34(6)	38(5)	84(7)	-24(5)	-5(5)	-1(4)
C16	28(6)	39(5)	100(7)	-36(5)	-1(5)	-1(4)
C17	29(6)	60(6)	83(7)	-43(5)	5(5)	-5(4)
C18	30(5)	54(6)	65(6)	-37(5)	6(4)	-4(4)
C19	26(4)	31(4)	36(5)	-17(4)	1(4)	-5(3)
C20	31(5)	64(6)	45(6)	-37(5)	-13(4)	2(4)
C21	35(4)	54(5)	26(4)	-19(4)	-18(4)	5(4)
C22	41(5)	46(5)	32(5)	-13(4)	-3(4)	8(4)
C23	53(6)	47(5)	28(5)	-17(4)	-15(4)	13(4)
C24	38(5)	39(5)	21(4)	-7(4)	-9(4)	1(4)
C25	53(7)	41(6)	73(8)	-26(6)	5(6)	-18(5)
C26	63(8)	64(8)	105(12)	-33(8)	-8(8)	3(6)
B1	52(7)	64(7)	33(5)	-32(5)	-10(4)	-1(4)

Table 3 Anisotropic Displacement Parameters ($Å^2×10^3$) for A20. The Anisotropic displacement factor exponent takes the form: $-2\pi^2[h^2a^{*2}U_{11}+2hka^*b^*U_{12}+\ldots]$.

Atom	U_{11}	U_{22}	U_{33}	U_{23}	U_{13}	U_{12}
F3A	74(10)	84(12)	55(8)	-32(8)	-23(7)	7(8)
F5A	73(10)	79(8)	49(11)	-32(8)	-13(7)	13(7)
B1A	52(7)	64(7)	33(5)	-32(5)	-10(4)	-1(4)

Table 4 Bond Lengths for A20.

Atom	Atom	Length/Å	Atom	Atom	Length/Å
Te1	Se1	2.960(2)	C11	C12	1.564(15)
Te1	O1	1.960(7)	C12	H12A	0.9900
Te1	C1	2.137(8)	C12	H12B	0.9900
Te1	C13	2.126(9)	C13	C14	1.413(13)
Se1	C9	1.911(10)	C13	C18	1.366(14)
Se1	C19	1.943(9)	C14	H14	0.9500
F1	B1	1.381(16)	C14	C15	1.386(13)
F1	B1A	1.38(2)	C15	H15	0.9500
F2	B1	1.376(15)	C15	C16	1.373(16)
F2	B1A	1.37(2)	C16	H16	0.9500
F3	B1	1.36(2)	C16	C17	1.373(16)
F5	B1	1.343(18)	C17	H17	0.9500
O1	C25	1.427(12)	C17	C18	1.391(14)
O26	C26	1.392(17)	C18	H18	0.9500
O26	H26	0.980(5)	C19	C20	1.377(12)
C1	C2	1.360(13)	C19	C24	1.376(12)
C1	C10	1.422(12)	C20	H20	0.9500
C2	H2	0.9500	C20	C21	1.366(13)
C2	C3	1.395(14)	C21	H21	0.9500
C3	H3	0.9500	C21	C22	1.410(13)
C3	C4	1.348(14)	C22	H22	0.9500
C4	C5	1.422(13)	C22	C23	1.371(13)
C4	C11	1.549(13)	C23	H23	0.9500
C5	C6	1.444(13)	C23	C24	1.384(13)
C5	C10	1.409(13)	C24	H24	0.9500
C6	C7	1.349(13)	C25	H25A	0.9800
C6	C12	1.463(12)	C25	H25B	0.9800
C7	H7	0.9500	C25	H25C	0.9800
C7	C8	1.391(13)	C26	H26A	0.9800
C8	H8	0.9500	C26	H26B	0.9800
C8	C9	1.387(13)	C26	H26C	0.9800
C9	C10	1.397(13)	F3A	B1A	1.34(5)
C11	H11A	0.9900	F5A	B1A	1.30(6)
C11	H11B	0.9900			

Table 5 Bond Angles for A20.

Atom	Atom	Atom	Angle/˚	Atom	Atom	Atom	Angle/˚
O1	Te1	Se1	166.4(2)	C9	C10	C5	114.1(8)
O1	Te1	C1	88.4(3)	C4	C11	C12	103.7(8)
O1	Te1	C13	91.6(3)	C6	C12	C11	107.0(8)
C1	Te1	Se1	79.3(2)	C14	C13	Te1	119.2(7)
C13	Te1	Se1	84.2(2)	C18	C13	Te1	119.1(7)
C13	Te1	C1	96.5(3)	C18	C13	C14	121.7(9)
C9	Se1	Te1	89.9(3)	C15	C14	C13	117.3(10)
C9	Se1	C19	97.8(4)	C16	C15	C14	121.3(11)
C19	Se1	Te1	94.2(3)	C15	C16	C17	120.3(10)
C25	O1	Te1	119.2(7)	C16	C17	C18	120.2(11)
C2	C1	Te1	117.5(7)	C13	C18	C17	119.2(11)
C2	C1	C10	122.5(8)	C20	C19	Se1	123.3(7)
C10	C1	Te1	120.0(6)	C24	C19	Se1	116.9(6)
C1	C2	C3	121.4(9)	C24	C19	C20	119.8(8)
C4	C3	C2	120.0(10)	C21	C20	C19	121.5(8)
C3	C4	C5	118.5(8)	C20	C21	C22	118.5(8)
C3	C4	C11	133.1(10)	C23	C22	C21	120.1(9)
C5	C4	C11	108.5(8)	C22	C23	C24	120.1(9)
C4	C5	C6	111.1(8)	C19	C24	C23	119.9(8)
C10	C5	C4	123.8(8)	F2	B1	F1	107.1(10)
C10	C5	C6	125.1(9)	F3	B1	F1	105.7(13)
C5	C6	C12	109.7(8)	F3	B1	F2	110.1(13)
C7	C6	C5	116.4(8)	F5	B1	F1	114.7(14)
C7	C6	C12	133.9(8)	F5	B1	F2	111.2(13)
C6	C7	C8	120.8(9)	F5	B1	F3	107.9(12)
C9	C8	C7	121.7(9)	F2	B1A	F1	107.6(16)
C8	C9	Se1	120.0(7)	F3A	B1A	F1	111(3)
C8	C9	C10	121.8(9)	F3A	B1A	F2	109(3)
C10	C9	Se1	118.0(6)	F5A	B1A	F1	97(3)
C5	C10	C1	113.8(8)	F5A	B1A	F2	114(4)
C9	C10	C1	132.1(9)	F5A	B1A	F3A	117(2)

Table 6 Hydrogen Bonds for A20.

D	H	A	d(D-H)/Å	d(H-A)/Å	d(D-A)/Å	D-H-A/°
C2	H2	O1	0.95	2.21	2.823(12)	120.9
C11	H11A	F5A[1]	0.99	2.40	3.19(3)	136.4
C24	H24	F1	0.95	2.38	3.287(12)	159.7
O26	H26	F3	0.980(5)	2.49(9)	3.203(16)	129(8)
O26	H26	F5	0.980(5)	2.07(3)	3.039(16)	169(9)
O26	H26	F3A	0.980(5)	1.76(7)	2.64(3)	147(10)

[1]2-X,-Y,1-Z

Table 7 Torsion Angles for A20.

A	B	C	D	Angle/˚	A	B	C	D	Angle/˚
Te1	C1	C2	C3	-178.9(7)	C6	C5	C10	C9	-1.0(13)
Te1	C1	C10	C5	177.8(6)	C6	C7	C8	C9	2.1(15)
Te1	C1	C10	C9	-0.1(13)	C7	C6	C12	C11	176.5(11)
Te1	C13	C14	C15	178.9(7)	C7	C8	C9	Se1	-174.9(7)
Te1	C13	C18	C17	-178.8(7)	C7	C8	C9	C10	0.6(14)
Se1	C9	C10	C1	-7.6(13)	C8	C9	C10	C1	176.8(9)
Se1	C9	C10	C5	174.5(6)	C8	C9	C10	C5	-1.1(12)
Se1	C19	C20	C21	-178.1(8)	C10	C1	C2	C3	-0.2(14)
Se1	C19	C24	C23	179.1(7)	C10	C5	C6	C7	3.6(13)
C1	C2	C3	C4	0.3(15)	C10	C5	C6	C12	-177.9(8)
C2	C1	C10	C5	-0.9(12)	C11	C4	C5	C6	0.3(12)
C2	C1	C10	C9	-178.8(9)	C11	C4	C5	C10	179.1(8)
C2	C3	C4	C5	0.8(15)	C12	C6	C7	C8	178.0(10)
C2	C3	C4	C11	179.4(11)	C13	C14	C15	C16	-0.4(14)
C3	C4	C5	C6	179.1(9)	C14	C13	C18	C17	0.5(14)
C3	C4	C5	C10	-2.0(14)	C14	C15	C16	C17	1.1(16)
C3	C4	C11	C12	-179.9(11)	C15	C16	C17	C18	-1.0(15)
C4	C5	C6	C7	-177.6(8)	C16	C17	C18	C13	0.2(15)
C4	C5	C6	C12	0.9(11)	C18	C13	C14	C15	-0.4(13)
C4	C5	C10	C1	2.0(12)	C19	C20	C21	C22	1.2(15)
C4	C5	C10	C9	-179.7(8)	C20	C19	C24	C23	1.5(14)
C4	C11	C12	C6	1.7(11)	C20	C21	C22	C23	-2.7(15)
C5	C4	C11	C12	-1.2(11)	C21	C22	C23	C24	3.6(15)
C5	C6	C7	C8	-4.0(14)	C22	C23	C24	C19	-3.0(15)
C5	C6	C12	C11	-1.7(10)	C24	C19	C20	C21	-0.7(15)
C6	C5	C10	C1	-179.4(8)					

Table 8 Hydrogen Atom Coordinates (Å×10^4) and Isotropic Displacement Parameters (Å^2×10^3) for A20.

Atom	*x*	*y*	*z*	U(eq)
H2	8494.48	184.35	6280.11	51
H3	9312.42	283.29	8005.26	59
H7	12360.54	5754.82	4248.44	44
H8	11716.21	5781.55	2406.08	47
H11A	11625.07	1635.67	8313.81	59
H11B	10400.47	2481.09	8412.3	59
H12A	11542.14	4386.51	7040.94	56
H12B	12746.41	3542.06	6906.21	56
H14	7346.01	4042	1080.64	47
H15	5695.83	5546.25	840.18	66
H16	4476.11	5456.46	2638.09	66
H17	4911.17	3916.72	4717.95	65
H18	6553.5	2394.5	5010.71	56
H20	12913.78	3351.94	2653.59	50
H21	14620.86	2172.18	2334.96	45
H22	14438.78	1219.86	957.99	50

Table 8 Hydrogen Atom Coordinates (Å×10^4) and Isotropic Displacement Parameters (Å^2×10^3) for A20.

Atom	*x*	*y*	*z*	U(eq)
H23	12502.83	1307.91	111.96	51
H24	10821.94	2550.51	409.33	42
H25A	7223.32	-858.01	3850.16	68
H25B	5965.39	-60.9	3929.71	68
H25C	6322.46	-1369.82	5195.83	68
H26A	4891.55	796.99	-1455.69	96
H26B	4454.55	1709.71	-2875.07	96
H26C	4568.6	2322.85	-1919.01	96
H26	6570(90)	1750(100)	-1860(50)	68

Table 9 Atomic Occupancy for A20.

Atom	*Occupancy*	Atom	*Occupancy*	Atom	*Occupancy*
F3	0.734(17)	F5	0.734(17)	B1	0.734(17)
F3A	0.266(17)	F5A	0.266(17)	B1A	0.266(17)

X-ray Crystallographic Structure determination on A21

Data Collection

A yellow prism crystal of C26H26BF4O2Te2 having approximate dimensions of 0.060 x 0.030 x 0.030 mm was mounted on a glass fiber. All measurements were made on a Rigaku Mercury70 diffractometer Mo-Ka radiation.

Cell constants and an orientation matrix for data collection corresponded to a primitive triclinic cell with dimensions:

a = 10.593(3) Å a = 61.571(14)o
b = 11.100(2) Å b = 85.183(18)o
c = 12.010(2) Å g = 87.92(2)o
V = 1237.4(5) Å3

For Z = 2 and F.W. = 712.49, the calculated density is 1.912 g/cm3. Based on a statistical analysis of intensity distribution, and the successful solution and refinement of the structure, the space group was determined to be:

P-1 (#2)

The data were collected at a temperature of -180 ± 1oC to a maximum 2q value of 50.7o.

Data Reduction

Of the 7940 reflections were collected, where 4389 were unique (Rint = 0.0215); equivalent reflections were merged. Data were collected and processed using CrystalClear (Rigaku). 1

The linear absorption coefficient, m, for Mo-Ka radiation is 24.106 cm-1. An empirical absorption correction was applied which resulted in transmission factors ranging from 0.779 to 0.930. The data were corrected for Lorentz and polarization effects.

Structure Solution and Refinement

The structure was solved by heavy-atom Patterson methods2 and expanded using Fourier techniques. The non-hydrogen atoms were refined anisotropically. Some hydrogen atoms were refined isotropically and the rest were refined using the riding model.The final cycle of full-matrix least-squares refinement3 on F2 was based on 4389 observed reflections and 322 variable parameters and converged (largest parameter shift

was 0.01 times its esd) with unweighted and weighted agreement factors of:

R1 = S ||Fo| - |Fc|| / S |Fo| = 0.0344

wR2 = [S (w (Fo2 - Fc2)2)/ S w(Fo2)2]1/2 = 0.0588

The goodness of fit4 was 1.02. Unit weights were used. The maximum and minimum peaks on the final difference Fourier map corresponded to 1.11 and -0.88 e-/Å3, respectively.

Neutral atom scattering factors were taken from International Tables for Crystallography (IT), Vol. C, Table 6.1.1.4 5. Anomalous dispersion effects were included in Fcalc6; the values for Df' and Df'' were those of Creagh and McAuley7. The values for the mass attenuation coefficients are those of Creagh and Hubbell8. All calculations were performed using the CrystalStructure9 crystallographic software package except for refinement, which was performed using SHELXL Version 2018/310.

Further refinement was undertaken with SHELXL within the Olex2 v. 1.5 suite.[11]

Table 1 Crystal data and structure refinement for A21.

Identification code	A21
Empirical formula	$C_{26}H_{25}BF_4O_2Te_2$
Formula weight	711.47
Temperature/K	93.15
Crystal system	triclinic
Space group	P-1
a/Å	10.593(3)
b/Å	11.100(2)
c/Å	12.010(2)
α/°	61.571(14)
β/°	85.183(18)
γ/°	87.92(2)
Volume/Å^3	1237.4(5)
Z	2
ρ_{calc}g/cm^3	1.909
μ/mm^{-1}	2.410
F(000)	684.0
Crystal size/mm^3	0.06 × 0.03 × 0.03
Radiation	MoKα (λ = 0.71075)
2Θ range for data collection/°	3.858 to 50.694
Index ranges	-12 ≤ h ≤ 10, -12 ≤ k ≤ 13, -13 ≤ l ≤ 14
Reflections collected	7940
Independent reflections	4389 [R_{int} = 0.0215, R_{sigma} = 0.0571]
Data/restraints/parameters	4389/1/322
Goodness-of-fit on F^2	1.035
Final R indexes [I>=2σ (I)]	R_1 = 0.0345, wR_2 = 0.0538
Final R indexes [all data]	R_1 = 0.0436, wR_2 = 0.0576
Largest diff. peak/hole / e Å^{-3}	1.10/-0.91

Table 2 Fractional Atomic Coordinates (×10^4) and Equivalent Isotropic Displacement Parameters (Å^2×10^3) for A21. U_{eq} is defined as 1/3 of the trace of the orthogonalised U_{IJ} tensor.

Atom	*x*	*y*	*z*	U(eq)
Te1	1502.1(2)	3457.3(2)	1533.2(2)	20.92(9)
Te2	-168.3(2)	932.2(3)	3238.5(2)	22.92(9)
F1	2181(3)	3826(3)	5416(3)	75.0(10)
F2	3149(3)	1980(3)	5476(2)	55.4(8)
F3	2988(2)	3862(3)	3586(2)	48.5(7)
F4	1277(2)	2586(3)	4649(3)	60.0(8)
O1	2598(3)	4930(3)	176(3)	33.2(7)
O26	3580(3)	2801(4)	7726(3)	54.5(9)
C1	666(3)	3238(4)	76(4)	19.9(9)
C2	1018(4)	4179(4)	-1159(4)	25.1(10)
C3	550(4)	4137(4)	-2211(4)	28.6(10)
C4	-278(4)	3131(4)	-1995(4)	25.2(10)
C5	-629(4)	2159(4)	-742(4)	21.0(9)
C6	-1481(4)	1164(4)	-685(4)	25.4(10)
C7	-1871(4)	110(4)	464(4)	26.7(10)
C8	-1454(4)	65(4)	1571(4)	27.0(10)
C9	-655(4)	1045(4)	1526(4)	22.2(9)
C10	-186(3)	2145(4)	345(4)	18.9(9)
C11	-922(4)	2800(4)	-2892(4)	33.4(11)
C12	-1770(4)	1551(4)	-2028(4)	29.1(10)
C13	2942(3)	1969(4)	1870(4)	21.3(9)
C14	3613(4)	1979(4)	817(4)	28.6(10)
C15	4599(4)	1052(5)	1012(5)	37.3(12)
C16	4899(4)	150(4)	2237(5)	40.4(12)
C17	4226(4)	152(4)	3276(4)	35.2(11)
C18	3238(4)	1065(4)	3094(4)	26.5(10)
C19	-1788(3)	1981(4)	3505(3)	18.6(9)
C20	-1738(4)	2512(4)	4338(4)	26.7(10)
C21	-2804(4)	3165(4)	4549(4)	30.6(10)
C22	-3891(4)	3273(4)	3959(4)	30.8(10)
C23	-3919(4)	2755(4)	3115(4)	34.6(11)
C24	-2869(4)	2106(4)	2887(4)	30.4(10)
C25	3402(4)	5639(4)	576(4)	39.6(12)
C26	4837(5)	3247(5)	7295(6)	71.0(18)
B1	2395(5)	3105(5)	4775(4)	25.6(11)

Table 3 Anisotropic Displacement Parameters (Å^2×10^3) for A21. The Anisotropic displacement factor exponent takes the form: $-2\pi^2[h^2a^{*2}U_{11}+2hka^*b^*U_{12}+\ldots]$.

Atom	U_{11}	U_{22}	U_{33}	U_{23}	U_{13}	U_{12}
Te1	20.57(17)	24.16(16)	21.42(16)	-13.21(13)	-4.52(12)	1.61(12)
Te2	19.79(17)	30.93(17)	17.50(15)	-11.15(13)	-1.67(12)	1.87(12)
F1	113(3)	67(2)	67(2)	-49.4(19)	-13(2)	9.2(19)
F2	57(2)	59.2(18)	36.6(17)	-11.9(15)	-8.3(15)	14.5(16)
F3	31.8(16)	60.7(18)	32.4(16)	-5.5(14)	2.5(13)	-10.9(14)

Table 3 Anisotropic Displacement Parameters ($Å^2×10^3$) for A21. The Anisotropic displacement factor exponent takes the form: $-2\pi^2[h^2a^{*2}U_{11}+2hka^*b^*U_{12}+\ldots]$.

Atom	U_{11}	U_{22}	U_{33}	U_{23}	U_{13}	U_{12}
F4	36.0(18)	97(2)	51.5(19)	-38.5(18)	3.9(15)	-24.0(16)
O1	40(2)	30.1(16)	28.6(17)	-12.4(14)	-2.3(15)	-14.0(14)
O26	48(2)	76(3)	46(2)	-34(2)	-2.4(19)	1(2)
C1	17(2)	23(2)	24(2)	-14(2)	-5.2(18)	5.3(18)
C2	24(2)	24(2)	27(2)	-12(2)	-4(2)	0.1(19)
C3	32(3)	30(2)	20(2)	-10(2)	-1(2)	2(2)
C4	24(2)	33(2)	20(2)	-14(2)	-9.2(19)	9(2)
C5	16(2)	28(2)	25(2)	-18(2)	-2.5(18)	3.7(18)
C6	17(2)	38(3)	32(3)	-25(2)	-6(2)	7(2)
C7	20(2)	32(2)	38(3)	-24(2)	-3(2)	0(2)
C8	22(2)	31(2)	30(3)	-17(2)	5(2)	-4(2)
C9	21(2)	28(2)	22(2)	-16(2)	-2.4(19)	1.5(19)
C10	15(2)	25(2)	22(2)	-15(2)	-3.6(18)	7.8(18)
C11	30(3)	52(3)	26(3)	-25(2)	-12(2)	3(2)
C12	26(3)	42(3)	32(3)	-27(2)	-12(2)	7(2)
C13	12(2)	23(2)	36(3)	-20(2)	-2.4(19)	-2.5(18)
C14	19(2)	33(2)	38(3)	-20(2)	-2(2)	-4(2)
C15	22(3)	43(3)	57(3)	-32(3)	-1(2)	-1(2)
C16	19(3)	30(3)	81(4)	-32(3)	-9(3)	4(2)
C17	27(3)	26(2)	51(3)	-14(2)	-16(2)	1(2)
C18	20(2)	27(2)	33(3)	-13(2)	-8(2)	-2.4(19)
C19	16(2)	20(2)	15(2)	-4.9(18)	2.8(17)	-2.8(17)
C20	19(2)	33(2)	27(2)	-14(2)	-5(2)	4(2)
C21	32(3)	32(2)	35(3)	-22(2)	-4(2)	0(2)
C22	25(3)	27(2)	38(3)	-15(2)	3(2)	0(2)
C23	17(3)	40(3)	51(3)	-24(3)	-13(2)	2(2)
C24	24(3)	36(3)	36(3)	-21(2)	-5(2)	-2(2)
C25	35(3)	33(3)	52(3)	-21(3)	-2(2)	-9(2)
C26	39(4)	40(3)	119(6)	-27(4)	0(4)	1(3)
B1	23(3)	35(3)	18(3)	-12(2)	-3(2)	-1(2)

Table 4 Bond Lengths for A21.

Atom	Atom	Length/Å	Atom	Atom	Length/Å
Te1	Te2	3.0769(10)	C11	C12	1.540(6)
Te1	O1	1.990(3)	C12	H12A	0.9900
Te1	C1	2.142(3)	C12	H12B	0.9900
Te1	C13	2.122(4)	C13	C14	1.394(5)
Te2	C9	2.107(3)	C13	C18	1.384(5)
Te2	C19	2.126(4)	C14	H14	0.9500
F1	B1	1.352(5)	C14	C15	1.392(6)
F2	B1	1.395(5)	C15	H15	0.9500
F3	B1	1.373(5)	C15	C16	1.386(6)
F4	B1	1.386(5)	C16	H16	0.9500
O1	C25	1.432(4)	C16	C17	1.385(6)

Table 4 Bond Lengths for A21.

Atom	Atom	Length/Å	Atom	Atom	Length/Å
O26	C26	1.405(6)	C17	H17	0.9500
O26	H26	0.981(5)	C17	C18	1.385(5)
C1	C2	1.374(5)	C18	H18	0.9500
C1	C10	1.432(5)	C19	C20	1.387(5)
C2	H2	0.9500	C19	C24	1.383(5)
C2	C3	1.417(5)	C20	H20	0.9500
C3	H3	0.9500	C20	C21	1.390(5)
C3	C4	1.357(5)	C21	H21	0.9500
C4	C5	1.398(5)	C21	C22	1.374(5)
C4	C11	1.510(5)	C22	H22	0.9500
C5	C6	1.425(5)	C22	C23	1.387(5)
C5	C10	1.417(5)	C23	H23	0.9500
C6	C7	1.358(5)	C23	C24	1.382(5)
C6	C12	1.514(5)	C24	H24	0.9500
C7	H7	0.9500	C25	H25A	0.9800
C7	C8	1.414(5)	C25	H25B	0.9800
C8	H8	0.9500	C25	H25C	0.9800
C8	C9	1.381(5)	C26	H26A	0.9800
C9	C10	1.423(5)	C26	H26B	0.9800
C11	H11A	0.9900	C26	H26C	0.9800
C11	H11B	0.9900			

Table 5 Bond Angles for A21.

Atom	Atom	Atom	Angle/˚	Atom	Atom	Atom	Angle/˚
O1	Te1	Te2	167.91(7)	C10	C9	Te2	119.8(2)
O1	Te1	C1	88.09(13)	C5	C10	C1	114.6(3)
O1	Te1	C13	91.94(14)	C5	C10	C9	114.9(3)
C1	Te1	Te2	81.49(11)	C9	C10	C1	130.4(3)
C13	Te1	Te2	83.29(10)	C4	C11	C12	105.0(3)
C13	Te1	C1	96.84(13)	C6	C12	C11	105.4(3)
C9	Te2	Te1	85.36(11)	C14	C13	Te1	117.6(3)
C9	Te2	C19	96.35(14)	C18	C13	Te1	120.8(3)
C19	Te2	Te1	97.85(10)	C18	C13	C14	121.5(4)
C25	O1	Te1	116.4(2)	C15	C14	C13	118.7(4)
C2	C1	Te1	116.9(3)	C16	C15	C14	119.8(4)
C2	C1	C10	120.3(3)	C17	C16	C15	120.9(4)
C10	C1	Te1	122.7(3)	C16	C17	C18	119.8(4)
C1	C2	C3	122.6(4)	C13	C18	C17	119.2(4)
C4	C3	C2	118.9(4)	C20	C19	Te2	118.0(3)
C3	C4	C5	119.0(3)	C24	C19	Te2	121.1(3)
C3	C4	C11	131.6(4)	C24	C19	C20	121.0(3)
C5	C4	C11	109.4(3)	C19	C20	C21	118.5(4)
C4	C5	C6	111.7(3)	C22	C21	C20	121.1(4)
C4	C5	C10	124.6(3)	C21	C22	C23	119.6(4)
C10	C5	C6	123.7(4)	C24	C23	C22	120.3(4)

Table 5 Bond Angles for A21.

Atom	Atom	Atom	Angle/˚	Atom	Atom	Atom	Angle/˚
C5	C6	C12	108.2(4)	C23	C24	C19	119.5(4)
C7	C6	C5	119.2(3)	F1	B1	F2	108.6(3)
C7	C6	C12	132.7(4)	F1	B1	F3	113.0(4)
C6	C7	C8	118.8(3)	F1	B1	F4	111.4(4)
C9	C8	C7	122.4(4)	F3	B1	F2	108.9(4)
C8	C9	Te2	119.2(3)	F3	B1	F4	108.2(3)
C8	C9	C10	121.0(3)	F4	B1	F2	106.6(4)

Table 6 Hydrogen Bonds for A21.

D	H	A	d(D-H)/Å	d(H-A)/Å	d(D-A)/Å	D-H-A/°
C2	H2	O1	0.95	2.17	2.809(4)	123.1
C20	H20	F4	0.95	2.40	3.255(5)	148.9
O26	H26	F1	0.981(5)	1.986(13)	2.958(5)	170(6)

Table 7 Torsion Angles for A21.

A	B	C	D	Angle/˚	A	B	C	D	Angle/˚
Te1	C1	C2	C3	179.0(3)	C6	C5	C10	C9	0.1(5)
Te1	C1	C10	C5	-179.2(3)	C6	C7	C8	C9	-0.7(6)
Te1	C1	C10	C9	0.4(6)	C7	C6	C12	C11	-175.3(4)
Te1	C13	C14	C15	177.3(3)	C7	C8	C9	Te2	176.9(3)
Te1	C13	C18	C17	-176.8(3)	C7	C8	C9	C10	-1.3(6)
Te2	C9	C10	C1	3.7(6)	C8	C9	C10	C1	-178.1(4)
Te2	C9	C10	C5	-176.7(2)	C8	C9	C10	C5	1.6(5)
Te2	C19	C20	C21	-178.2(3)	C10	C1	C2	C3	1.2(6)
Te2	C19	C24	C23	177.9(3)	C10	C5	C6	C7	-2.1(6)
C1	C2	C3	C4	0.0(6)	C10	C5	C6	C12	177.9(3)
C2	C1	C10	C5	-1.5(5)	C11	C4	C5	C6	-0.2(5)
C2	C1	C10	C9	178.2(4)	C11	C4	C5	C10	179.0(4)
C2	C3	C4	C5	-0.8(6)	C12	C6	C7	C8	-177.7(4)
C2	C3	C4	C11	-179.1(4)	C13	C14	C15	C16	-0.5(6)
C3	C4	C5	C6	-178.8(3)	C14	C13	C18	C17	0.1(5)
C3	C4	C5	C10	0.4(6)	C14	C15	C16	C17	0.4(6)
C3	C4	C11	C12	-178.5(4)	C15	C16	C17	C18	0.0(6)
C4	C5	C6	C7	177.1(3)	C16	C17	C18	C13	-0.3(6)
C4	C5	C6	C12	-2.9(5)	C18	C13	C14	C15	0.2(5)
C4	C5	C10	C1	0.7(5)	C19	C20	C21	C22	0.7(6)
C4	C5	C10	C9	-179.0(4)	C20	C19	C24	C23	-0.8(6)
C4	C11	C12	C6	-4.6(4)	C20	C21	C22	C23	-1.7(6)
C5	C4	C11	C12	3.1(5)	C21	C22	C23	C24	1.4(6)
C5	C6	C7	C8	2.4(6)	C22	C23	C24	C19	-0.2(6)
C5	C6	C12	C11	4.6(4)	C24	C19	C20	C21	0.5(6)
C6	C5	C10	C1	179.8(3)					

Table 8 Hydrogen Atom Coordinates (Å×10^4) and Isotropic Displacement Parameters (Å^2×10^3) for A21.

Table 7 Torsion Angles for A21.

A	B	C	D	Angle/˚	A	B	C	D	Angle/˚		
Atom				***x***					***y***	***z***	**U(eq)**
H2				1597.47					4884.32	-1312.51	30
H3				811.74					4802.14	-3053.62	34
H7				-2413.09					-584.28	521.99	32
H8				-1734.37					-666.4	2375.05	32
H11A				-289.05					2577.49	-3421.37	40
H11B				-1436.74					3583.99	-3456.61	40
H12A				-2675.24					1787.92	-2151.75	35
H12B				-1569.39					783.83	-2215.01	35
H14				3402.7					2607.61	-18.31	34
H15				5064.1					1036.7	307.11	45
H16				5574.97					-477.29	2365.75	48
H17				4441.15					-470.53	4110.94	42
H18				2769.25					1070.14	3802.09	32
H20				-992.36					2430.49	4755.66	32
H21				-2780.35					3543.29	5109.06	37
H22				-4619.86					3701.18	4129.36	37
H23				-4662.63					2845.97	2691.45	42
H24				-2888.82					1748.41	2309.94	37
H25A				4064.3					5017.97	1063.4	48
H25B				2897.4					5954.66	1108.67	48
H25C				3793.02					6428.5	-171.26	48
H26A				5397.71					2450.42	7560.02	85
H26B				5086.48					3820.32	7657.41	85
H26C				4904.95					3779.82	6366.12	85
H26				3160(60)					3050(70)	6950(40)	150(30)

X-ray Crystallographic Structure determination on A22

Data Collection

A colorless prism crystal of $C_{48}H_{36}B_2F_8OSe_2Te_2 \cdot 1.7CH_2Cl_2$ having approximate dimensions of 0.050 x 0.050 x 0.050 mm was mounted in a loop. All measurements were made on a Rigaku Mercury70 diffractometer Mo-Ka radiation.

Cell constants and an orientation matrix for data collection corresponded to a primitive monoclinic cell with dimensions:

a = 12.11690 Å
b = 19.87480 Å b = 95.19600o
c = 20.93930 Å
V = 5021.90086 Å3

For Z = 4 and F.W. = 1300.47, the calculated density is 1.720 g/cm3. The reflection conditions of:

h0l: h+l = 2n
0k0: k = 2n

uniquely determine the space group to be:
P21/n (#14)
The data were collected at a temperature of -180 ± 1oC to a maximum 2q value of 50.7o.
Data Reduction
Of the 31003 reflections were collected, where 9151 were unique (Rint = 0.1050); equivalent reflections

were merged. Data were collected and processed using CrystalClear (Rigaku). 1
The linear absorption coefficient, m, for Mo-Ka radiation is 27.833 cm-1. An empirical absorption correction was applied which resulted in transmission factors ranging from 0.476 to 0.870. The data were corrected for Lorentz and polarization effects.

Structure Solution and Refinement

The structure was solved by direct methods2 and expanded using Fourier techniques. The non-hydrogen atoms were refined anisotropically. Hydrogen atoms were refined using the riding model. The final cycle of full-matrix least-squares refinement3 on F2 was based on 9151 observed reflections and 622 variable parameters and converged (largest parameter shift was 0.00 times its esd) with unweighted and weighted agreement factors of:
R1 = S ||Fo| - |Fc|| / S |Fo| = 0.0884
wR2 = [S (w (Fo2 - Fc2)2)/ S w(Fo2)2]1/2 = 0.2646
The goodness of fit4 was 1.05. Unit weights were used. The maximum and minimum peaks on the final difference Fourier map corresponded to 1.58 and -1.10 e-/Å3, respectively.
Neutral atom scattering factors were taken from International Tables for Crystallography (IT), Vol. C, Table 6.1.1.4 5. Anomalous dispersion effects were included in Fcalc6; the values for Df' and Df'' were those of Creagh and McAuley7. The values for the mass attenuation coefficients are those of Creagh and Hubbell8. All calculations were performed using the CrystalStructure9 crystallographic software package except for refinement, which was performed using SHELXL Version 2018/310.

Further refinement was undertaken with SHELXL within the Olex2 v. 1.5 suite.[11]

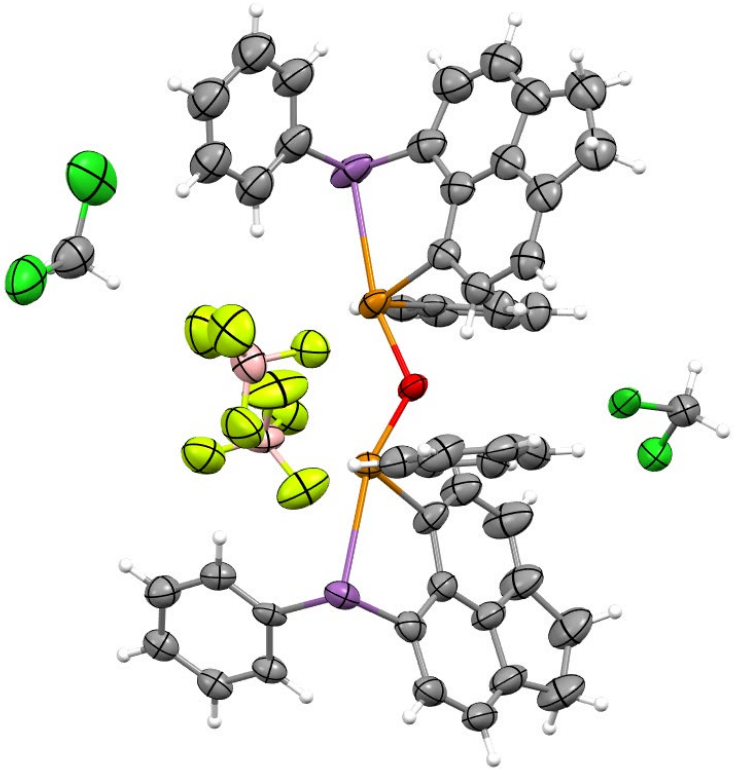

Figure S41. Displacement ellipsoids (40%) plot of the asymmetric unit of the structure of **A22**, showing the location of the two CH_2Cl_2 solvent molecules, when refined to 0.5 occupancy (the total solvent content corresponds more closely to an occupancy of 0.85, but this did not refine well).

During the refinement, the two CH_2Cl_2 solvents of crystallization, which are well separated from the cations and anions in the lattice, could be located but did not refine well. Employment of a solvent mask indicated an overall occupancy of 1.7 CH_2Cl_2 per asymmetric unit, but it did not prove possible to reliably assign this to the two location. In view of the limited data quality, the decision was taken to reserve the data for refining the cation and anions of the chemical unit, and the solvents were treated via the successful solvent mask.

Table 1 Crystal data and structure refinement for A22.

Identification code	A22
Empirical formula	$C_{48}H_{36}B_2F_8OSe_2Te_2 \cdot 1.7CH_2Cl_2$
Formula weight	1359.91
Temperature/K	93.15
Crystal system	monoclinic
Space group	$P2_1/n$
a/Å	12.117(3)
b/Å	19.875(5)
c/Å	20.939(5)
α/°	90
β/°	95.196(7)
γ/°	90
Volume/Å^3	5022(2)
Z	4
ρ_{calc}g/cm^3	1.799
μ/mm^{-1}	2.674
F(000)	2344.0
Crystal size/mm^3	0.05 × 0.05 × 0.05
Radiation	MoKα (λ = 0.71075)
2Θ range for data collection/°	3.744 to 50.68
Index ranges	-14 ≤ h ≤ 14, -23 ≤ k ≤ 14, -25 ≤ l ≤ 23
Reflections collected	30990
Independent reflections	9146 [R_{int} = 0.1053, R_{sigma} = 0.1052]
Data/restraints/parameters	9146/976/713
Goodness-of-fit on F^2	1.038
Final R indexes [I>=2σ (I)]	R_1 = 0.0781, wR_2 = 0.2064
Final R indexes [all data]	R_1 = 0.1150, wR_2 = 0.2312
Largest diff. peak/hole / e Å^{-3}	1.64/-0.83

Table 2 Fractional Atomic Coordinates (×10^4) and Equivalent Isotropic Displacement Parameters (Å^2×10^3) for A22. U_{eq} is defined as 1/3 of the trace of the orthogonalised U_{IJ} tensor.

Atom	*x*	*y*	*z*	U(eq)
Te1	189.3(5)	2091.8(3)	8091.0(3)	47.7(2)
Te2	1484.3(6)	3696.3(4)	8203.2(3)	55.1(2)
Se1	-1086.3(9)	852.7(6)	7831.2(5)	56.8(3)
Se2	2354(7)	5091(3)	8108(5)	67.7(18)
F1	-957(6)	3464(4)	8001(3)	82(2)
F2	-1310(11)	3827(6)	6993(5)	146(4)
F3	-2089(8)	2818(5)	7352(5)	131(4)
F4	-2650(7)	3868(6)	7594(5)	126(3)
F5	1603(7)	1896(4)	6968(4)	104(3)
F6	2880(8)	2624(5)	6618(4)	104(3)
F7	1267(11)	2990(5)	6967(5)	149(4)
F8	1296(7)	2421(4)	6018(4)	97(2)
O1	1176(5)	2782(3)	8508(3)	51.5(16)
C1	1423(9)	1379(6)	8348(5)	60(3)
C2	2497(10)	1565(7)	8489(6)	76(3)

Table 2 Fractional Atomic Coordinates (×10^4) and Equivalent Isotropic Displacement Parameters (Å^2×10^3) for A22. U_{eq} is defined as 1/3 of the trace of the orthogonalised U_{IJ} tensor.

Atom	*x*	*y*	*z*	U(eq)
C3	3362(12)	1122(8)	8728(8)	98(5)
C4	3130(12)	474(7)	8782(7)	89(4)
C5	2016(11)	236(6)	8624(5)	69(3)
C6	1916(13)	-459(6)	8717(6)	79(3)
C7	889(14)	-745(6)	8571(5)	83(3)
C8	24(13)	-345(6)	8311(5)	79(3)
C9	169(10)	345(6)	8214(4)	61(2)
C10	1164(9)	662(6)	8387(3)	60(2)
C11	3820(15)	-119(8)	9045(8)	106(5)
C12	3005(14)	-727(8)	8995(8)	107(5)
C13	-632(10)	2037(5)	8943(5)	56(2)
C14	-6(13)	1941(6)	9515(5)	81(3)
C15	-447(14)	1978(7)	10082(6)	84(4)
C16	-1531(14)	2120(6)	10089(6)	86(3)
C17	-2173(13)	2210(7)	9520(7)	85(3)
C18	-1761(11)	2180(6)	8925(6)	70(3)
C19	-840(8)	755(5)	6932(4)	48(2)
C20	-417(8)	168(5)	6712(5)	54(2)
C21	-341(8)	102(6)	6050(5)	58(2)
C22	-695(8)	616(6)	5635(5)	59(2)
C23	-1141(11)	1196(6)	5877(5)	71(3)
C24	-1181(9)	1270(6)	6531(5)	60(2)
C31	1303(8)	4107(6)	9123(5)	58(2)
C32	771(7)	3715(6)	9551(5)	65(3)
C33	712(9)	3932(7)	10176(6)	72(3)
C34	1200(20)	4544(10)	10424(9)	66(4)
C35	1680(20)	4916(10)	9997(10)	64(5)
C36	2150(20)	5523(11)	10311(12)	74(5)
C37	2684(18)	5912(10)	9921(12)	66(5)
C38	2755(19)	5788(10)	9318(12)	65(5)
C39	2325(17)	5231(9)	9022(8)	58(4)
C40	1770(20)	4730(10)	9367(9)	59(4)
C41	1250(20)	4864(12)	11079(10)	81(5)
C42	1840(20)	5484(13)	11001(12)	86(6)
C43	3220(9)	3494(5)	8393(5)	51(2)
C44	3641(9)	3325(6)	9014(5)	61(3)
C45	4742(10)	3168(7)	9126(6)	72(3)
C46	5408(9)	3180(6)	8627(6)	65(3)
C47	4971(10)	3338(6)	8022(6)	68(3)
C48	3849(9)	3487(6)	7911(5)	60(2)
C49	930(30)	5420(20)	7600(15)	80(7)
C50	906(15)	6248(9)	8050(10)	52(4)
C51	-63(17)	6608(11)	7903(11)	70(5)
C52	-941(17)	6266(11)	7517(11)	69(5)
C53	-900(15)	5600(10)	7373(9)	59(4)

Table 2 Fractional Atomic Coordinates (×10^4) and Equivalent Isotropic Displacement Parameters (Å^2×10^3) for A22. U_{eq} is defined as 1/3 of the trace of the orthogonalised U_{IJ} tensor.

Atom	*x*	*y*	*z*	U(eq)
C54	83(14)	5240(9)	7541(8)	46(4)
B1	-1792(14)	3466(10)	7504(7)	84(3)
B2	1730(15)	2484(7)	6605(8)	74(3)
Se2A	2322(11)	5035(5)	7940(6)	77(3)
C50A	890(30)	6110(20)	7739(17)	88(7)
C51A	-80(30)	6467(16)	7561(19)	95(8)
C52A	-900(30)	6076(17)	7170(20)	99(8)
C53A	-860(30)	5394(17)	7099(18)	93(7)
C54A	150(30)	5065(19)	7299(17)	93(8)
C34A	1250(30)	4599(13)	10293(12)	73(6)
C35A	1740(30)	4939(12)	9846(11)	58(5)
C36A	2220(20)	5578(12)	10088(14)	64(6)
C37A	2710(20)	5928(13)	9652(15)	66(6)
C38A	2780(20)	5766(13)	9058(15)	69(6)
C39A	2330(30)	5189(13)	8810(10)	66(5)
C40A	1810(30)	4741(11)	9219(11)	57(5)
C41A	1430(30)	4991(13)	10924(12)	72(6)
C42A	1990(30)	5609(13)	10786(13)	68(6)
C49A	971(15)	5565(9)	7874(8)	43(4)

Table 3 Anisotropic Displacement Parameters (Å^2×10^3) for A22. The Anisotropic displacement factor exponent takes the form: $-2\pi^2[h^2a^{*2}U_{11}+2hka^*b^*U_{12}+\ldots]$.

Atom	U_{11}	U_{22}	U_{33}	U_{23}	U_{13}	U_{12}
Te1	44.7(4)	43.9(4)	55.8(4)	-0.7(3)	11.7(3)	-3.8(3)
Te2	44.1(4)	48.4(4)	72.4(5)	15.1(3)	3.4(3)	-6.2(3)
Se1	59.8(7)	54.8(7)	57.9(6)	-14.0(5)	17.6(5)	-13.0(5)
Se2	45.5(18)	32.7(19)	124(5)	18(2)	1(3)	-5.9(12)
F1	62(4)	87(6)	96(4)	-6(4)	1(3)	1(4)
F2	158(10)	176(11)	106(6)	7(6)	26(6)	-26(8)
F3	111(7)	113(7)	157(8)	-21(6)	-51(6)	-1(5)
F4	59(5)	152(9)	167(8)	4(7)	3(5)	19(5)
F5	94(6)	86(5)	141(6)	25(5)	61(5)	17(5)
F6	108(6)	104(7)	104(5)	-7(5)	29(4)	-36(5)
F7	216(12)	71(6)	181(8)	-14(5)	140(8)	19(7)
F8	87(5)	89(6)	115(5)	0(4)	13(4)	-17(5)
O1	50(4)	41(4)	62(4)	10(3)	-4(3)	-7(3)
C1	44(5)	54(5)	82(7)	21(5)	4(5)	5(4)
C2	53(6)	60(7)	117(9)	11(6)	12(6)	4(5)
C3	51(7)	72(7)	168(14)	17(8)	6(8)	11(5)
C4	80(7)	65(6)	123(10)	7(7)	7(7)	17(5)
C5	87(6)	44(5)	76(7)	9(5)	13(6)	5(4)
C6	118(8)	47(6)	72(7)	12(5)	16(7)	8(5)
C7	141(9)	49(7)	58(7)	0(5)	12(7)	-12(6)
C8	119(9)	62(6)	54(6)	-7(5)	7(6)	-23(6)

Table 3 Anisotropic Displacement Parameters ($Å^2×10^3$) for A22. The Anisotropic displacement factor exponent takes the form: $-2\pi^2[h^2a^{*2}U_{11}+2hka^*b^*U_{12}+\ldots]$.

Atom	U_{11}	U_{22}	U_{33}	U_{23}	U_{13}	U_{12}
C9	81(6)	63(6)	39(5)	-2(4)	12(5)	-10(5)
C10	73(6)	51(5)	57(6)	2(4)	6(5)	3(4)
C11	108(9)	88(9)	122(11)	28(9)	5(9)	23(7)
C12	125(10)	63(8)	134(12)	24(8)	18(9)	19(7)
C13	70(5)	41(6)	58(5)	-15(4)	17(4)	-13(5)
C14	118(9)	73(9)	53(5)	2(5)	13(5)	-9(7)
C15	125(9)	73(9)	56(5)	8(5)	15(6)	-21(8)
C16	148(10)	40(7)	77(6)	1(5)	56(6)	-1(8)
C17	95(9)	63(8)	104(7)	8(7)	50(6)	13(7)
C18	80(6)	54(7)	79(6)	-4(5)	29(5)	3(6)
C19	44(5)	41(5)	60(5)	-14(3)	11(4)	-15(4)
C20	53(6)	50(5)	59(5)	-12(4)	11(4)	-4(5)
C21	46(6)	65(7)	65(5)	-18(4)	15(4)	-6(5)
C22	51(6)	68(6)	58(5)	-12(4)	9(4)	-12(5)
C23	81(8)	61(7)	70(5)	1(5)	7(5)	-2(6)
C24	62(7)	46(6)	73(5)	-5(4)	15(5)	-1(5)
C31	46(5)	54(5)	75(6)	-6(4)	12(4)	12(4)
C32	58(7)	60(6)	76(6)	2(4)	1(5)	1(5)
C33	56(7)	85(7)	76(6)	8(5)	7(5)	13(5)
C34	46(8)	81(7)	70(7)	1(5)	1(6)	26(6)
C35	54(9)	68(7)	71(6)	-2(5)	1(6)	19(6)
C36	67(9)	81(8)	73(8)	-7(6)	2(7)	16(6)
C37	59(8)	66(8)	71(7)	-12(6)	1(6)	20(6)
C38	61(8)	65(8)	67(7)	-13(6)	-3(7)	3(6)
C39	50(7)	53(7)	70(7)	-6(6)	1(7)	7(6)
C40	47(8)	59(7)	70(7)	-1(5)	0(6)	8(6)
C41	81(10)	92(9)	73(7)	1(6)	18(7)	25(7)
C42	83(10)	92(9)	82(8)	-12(7)	5(7)	16(7)
C43	54(5)	33(5)	65(5)	-2(4)	5(4)	-7(4)
C44	45(5)	69(8)	71(5)	9(5)	8(4)	2(5)
C45	59(6)	78(9)	77(6)	3(6)	2(5)	12(6)
C46	43(5)	60(7)	93(6)	-8(5)	11(4)	0(5)
C47	56(5)	69(8)	80(6)	-14(5)	18(5)	-5(6)
C48	58(5)	51(7)	72(6)	1(5)	13(4)	-11(5)
C49	75(9)	80(9)	84(11)	14(8)	8(8)	3(7)
C50	59(7)	40(6)	57(8)	9(6)	12(6)	-7(5)
C51	73(8)	63(8)	74(9)	7(7)	7(7)	11(6)
C52	71(8)	59(7)	75(9)	17(6)	0(7)	10(6)
C53	54(7)	61(7)	62(8)	12(6)	11(6)	4(6)
C54	49(7)	42(7)	47(7)	12(6)	13(5)	-5(5)
B1	67(8)	107(9)	75(8)	-8(7)	5(5)	7(6)
B2	91(7)	46(7)	92(7)	-12(5)	41(6)	-1(6)
Se2A	52(3)	95(5)	85(4)	48(3)	11(3)	-6(3)
C50A	87(9)	83(9)	96(12)	10(8)	8(8)	1(7)
C51A	91(10)	87(10)	107(12)	8(8)	8(8)	5(7)

Table 3 Anisotropic Displacement Parameters ($Å^2×10^3$) for A22. The Anisotropic displacement factor exponent takes the form: $-2\pi^2[h^2a^{*2}U_{11}+2hka^*b^*U_{12}+\ldots]$.

Atom	U_{11}	U_{22}	U_{33}	U_{23}	U_{13}	U_{12}
C52A	93(10)	94(9)	107(12)	9(8)	4(8)	6(7)
C53A	85(9)	93(9)	100(12)	10(8)	9(8)	-5(7)
C54A	93(10)	91(10)	94(12)	1(8)	0(8)	2(7)
C34A	66(10)	81(8)	71(8)	1(6)	7(7)	8(7)
C35A	45(9)	61(8)	66(7)	1(5)	-2(7)	16(7)
C36A	62(10)	67(8)	66(8)	0(6)	11(7)	8(7)
C37A	62(10)	70(9)	68(8)	1(6)	11(7)	6(7)
C38A	68(10)	69(8)	71(8)	-2(7)	17(7)	0(7)
C39A	66(5)	66(5)	67(5)	0.3(10)	6.0(11)	0.1(10)
C40A	50(10)	57(7)	64(7)	1(6)	3(7)	9(7)
C41A	70(10)	74(9)	72(8)	7(6)	10(7)	14(8)
C42A	68(10)	74(9)	61(8)	-1(7)	8(7)	11(7)
C49A	47(6)	37(6)	46(7)	17(5)	8(6)	-4(5)

Table 4 Bond Lengths for A22.

Atom	Atom	Length/Å	Atom	Atom	Length/Å
Te1	Se1	2.9321(14)	C33	H33A	0.9500
Te1	O1	1.972(6)	C33	C34	1.43(2)
Te1	C1	2.094(10)	C33	C34A	1.49(2)
Te1	C13	2.123(10)	C34	C35	1.33(2)
Te2	Se2	2.978(5)	C34	C41	1.51(2)
Te2	O1	1.973(6)	C35	C36	1.46(2)
Te2	C31	2.121(11)	C35	C40	1.38(2)
Te2	C43	2.143(11)	C36	C37	1.34(3)
Te2	Se2A	2.918(9)	C36	C42	1.53(3)
Se1	C9	1.938(12)	C37	H37	0.9500
Se1	C19	1.944(9)	C37	C38	1.30(2)
Se2	C39	1.937(15)	C38	H38	0.9500
Se2	C49A	1.95(2)	C38	C39	1.35(2)
F1	B1	1.384(16)	C39	C40	1.43(2)
F2	B1	1.45(2)	C41	H41A	0.9900
F3	B1	1.37(2)	C41	H41B	0.9900
F4	B1	1.338(19)	C41	C42	1.44(3)
F5	B2	1.409(17)	C42	H42A	0.9900
F6	B2	1.419(19)	C42	H42B	0.9900
F7	B2	1.406(16)	C43	C44	1.394(14)
F8	B2	1.299(17)	C43	C48	1.319(15)
C1	C2	1.360(16)	C44	H44	0.9500
C1	C10	1.462(15)	C44	C45	1.369(15)
C2	H2	0.9500	C45	H45	0.9500
C2	C3	1.423(17)	C45	C46	1.376(17)
C3	H3	0.9500	C46	H46	0.9500
C3	C4	1.33(2)	C46	C47	1.365(16)
C4	C5	1.439(19)	C47	H47	0.9500

Table 4 Bond Lengths for A22.

Atom	Atom	Length/Å	Atom	Atom	Length/Å
C4	C11	1.519(19)	C47	C48	1.390(16)
C5	C6	1.403(16)	C48	H48	0.9500
C5	C10	1.392(16)	C49	Se2A	1.93(4)
C6	C7	1.38(2)	C49	C50A	1.41(5)
C6	C12	1.49(2)	C49	C54A	1.30(5)
C7	H7	0.9500	C50	H50	0.9500
C7	C8	1.387(19)	C50	C51	1.39(2)
C8	H8	0.9500	C50	C49A	1.41(3)
C8	C9	1.400(17)	C51	H51	0.9500
C9	C10	1.379(16)	C51	C52	1.45(3)
C11	H11A	0.9900	C52	H52	0.9500
C11	H11B	0.9900	C52	C53	1.36(3)
C11	C12	1.56(2)	C53	H53	0.9500
C12	H12A	0.9900	C53	C54	1.41(2)
C12	H12B	0.9900	C54	H54	0.9500
C13	C14	1.371(16)	C54	C49A	1.39(2)
C13	C18	1.394(16)	Se2A	C39A	1.848(16)
C14	H14	0.9500	C50A	H50A	0.9500
C14	C15	1.348(18)	C50A	C51A	1.39(3)
C15	H15	0.9500	C51A	H51A	0.9500
C15	C16	1.34(2)	C51A	C52A	1.45(3)
C16	H16	0.9500	C52A	H52A	0.9500
C16	C17	1.375(19)	C52A	C53A	1.36(3)
C17	H17	0.9500	C53A	H53A	0.9500
C17	C18	1.385(17)	C53A	C54A	1.41(2)
C18	H18	0.9500	C54A	H54A	0.9500
C19	C20	1.369(14)	C34A	C35A	1.34(2)
C19	C24	1.364(14)	C34A	C41A	1.53(2)
C20	H20	0.9500	C35A	C36A	1.47(2)
C20	C21	1.403(14)	C35A	C40A	1.38(2)
C21	H21	0.9500	C36A	C37A	1.33(3)
C21	C22	1.384(16)	C36A	C42A	1.51(3)
C22	H22	0.9500	C37A	H37A	0.9500
C22	C23	1.388(16)	C37A	C38A	1.30(3)
C23	H23	0.9500	C38A	H38A	0.9500
C23	C24	1.383(15)	C38A	C39A	1.35(2)
C24	H24	0.9500	C39A	C40A	1.42(2)
C31	C32	1.388(16)	C41A	H41C	0.9900
C31	C40	1.438(18)	C41A	H41D	0.9900
C31	C40A	1.409(19)	C41A	C42A	1.45(3)
C32	H32	0.9500	C42A	H42C	0.9900
C32	C33	1.386(16)	C42A	H42D	0.9900
C33	H33	0.9500			

Table 5 Bond Angles for A22.

Atom	Atom	Atom	Angle/˚	Atom	Atom	Atom	Angle/˚
O1	Te1	Se1	162.78(17)	C34	C35	C40	124.6(16)
O1	Te1	C1	88.1(4)	C40	C35	C36	126.1(17)
O1	Te1	C13	88.6(3)	C35	C36	C42	105.5(17)
C1	Te1	Se1	80.3(3)	C37	C36	C35	113.0(19)
C1	Te1	C13	97.3(4)	C37	C36	C42	141.6(19)
C13	Te1	Se1	80.4(2)	C38	C37	C36	124.4(19)
O1	Te2	Se2	163.2(3)	C37	C38	C39	123(2)
O1	Te2	C31	91.3(4)	C38	C39	Se2	122.1(14)
O1	Te2	C43	88.8(3)	C38	C39	C40	121.2(16)
O1	Te2	Se2A	168.6(3)	C40	C39	Se2	116.7(11)
C31	Te2	Se2	76.7(4)	C35	C40	C31	120.3(15)
C31	Te2	C43	94.8(4)	C35	C40	C39	112.1(13)
C31	Te2	Se2A	83.6(4)	C39	C40	C31	127.6(14)
C43	Te2	Se2	80.8(3)	C42	C41	C34	103.8(17)
C43	Te2	Se2A	81.6(4)	C41	C42	C36	108.5(15)
C9	Se1	Te1	88.8(3)	C44	C43	Te2	119.3(8)
C9	Se1	C19	99.5(4)	C48	C43	Te2	119.0(8)
C19	Se1	Te1	98.0(3)	C48	C43	C44	121.5(11)
C39	Se2	Te2	91.7(5)	C45	C44	C43	118.9(11)
C39	Se2	C49A	95.0(9)	C44	C45	C46	119.7(11)
C49A	Se2	Te2	99.5(6)	C47	C46	C45	120.2(11)
Te1	O1	Te2	128.5(3)	C46	C47	C48	119.7(11)
C2	C1	Te1	121.3(9)	C43	C48	C47	119.9(11)
C2	C1	C10	117.3(10)	C50A	C49	Se2A	111(3)
C10	C1	Te1	121.4(8)	C54A	C49	Se2A	123(3)
C1	C2	C3	124.6(13)	C54A	C49	C50A	127(4)
C4	C3	C2	118.4(14)	C51	C50	C49A	120.4(18)
C3	C4	C5	120.0(12)	C50	C51	C52	116.5(19)
C3	C4	C11	132.1(15)	C53	C52	C51	122.8(17)
C5	C4	C11	107.7(13)	C52	C53	C54	119.2(18)
C6	C5	C4	112.5(12)	C49A	C54	C53	119.3(17)
C10	C5	C4	122.2(11)	F1	B1	F2	103.8(13)
C10	C5	C6	125.3(13)	F3	B1	F1	109.4(14)
C5	C6	C12	108.7(13)	F3	B1	F2	114.1(13)
C7	C6	C5	117.6(13)	F4	B1	F1	114.8(13)
C7	C6	C12	133.6(13)	F4	B1	F2	100.3(14)
C6	C7	C8	119.2(12)	F4	B1	F3	113.8(14)
C7	C8	C9	121.1(13)	F5	B2	F6	107.9(13)
C8	C9	Se1	117.7(9)	F7	B2	F5	103.5(11)
C10	C9	Se1	120.3(9)	F7	B2	F6	106.8(12)
C10	C9	C8	121.9(12)	F8	B2	F5	112.2(12)
C5	C10	C1	117.2(10)	F8	B2	F6	110.4(11)
C9	C10	C1	128.1(10)	F8	B2	F7	115.6(14)
C9	C10	C5	114.7(11)	C49	Se2A	Te2	97.1(12)
C4	C11	C12	104.6(13)	C39A	Se2A	Te2	86.2(8)
C6	C12	C11	106.4(12)	C39A	Se2A	C49	102.8(15)

Table 5 Bond Angles for A22.

Atom	Atom	Atom	Angle/˚	Atom	Atom	Atom	Angle/˚
C14	C13	Te1	118.5(9)	C51A	C50A	C49	118(3)
C14	C13	C18	121.1(11)	C50A	C51A	C52A	114(3)
C18	C13	Te1	120.0(8)	C53A	C52A	C51A	125(2)
C15	C14	C13	122.0(15)	C52A	C53A	C54A	118(3)
C16	C15	C14	119.1(13)	C49	C54A	C53A	118(3)
C15	C16	C17	119.7(12)	C33	C34A	C41A	128.2(18)
C16	C17	C18	123.5(14)	C35A	C34A	C33	123.5(17)
C17	C18	C13	114.6(12)	C35A	C34A	C41A	108.2(17)
C20	C19	Se1	120.4(8)	C34A	C35A	C36A	112.4(17)
C24	C19	Se1	117.1(8)	C34A	C35A	C40A	126.2(17)
C24	C19	C20	122.3(9)	C40A	C35A	C36A	121.3(18)
C19	C20	C21	118.1(10)	C35A	C36A	C42A	105.7(18)
C22	C21	C20	120.5(10)	C37A	C36A	C35A	114(2)
C21	C22	C23	119.5(10)	C37A	C36A	C42A	141(2)
C24	C23	C22	119.9(11)	C38A	C37A	C36A	127(2)
C19	C24	C23	119.6(10)	C37A	C38A	C39A	121(2)
C32	C31	Te2	117.6(8)	C38A	C39A	Se2A	118.9(17)
C32	C31	C40	116.5(12)	C38A	C39A	C40A	119.1(18)
C32	C31	C40A	129.2(13)	C40A	C39A	Se2A	121.9(15)
C40	C31	Te2	125.6(11)	C31	C40A	C39A	133.4(18)
C40A	C31	Te2	113.1(11)	C35A	C40A	C31	109.1(16)
C33	C32	C31	120.1(12)	C35A	C40A	C39A	117.6(16)
C32	C33	C34	123.5(14)	C42A	C41A	C34A	106.9(18)
C32	C33	C34A	111.8(14)	C41A	C42A	C36A	106.7(16)
C33	C34	C41	132.1(17)	C50	C49A	Se2	117.8(13)
C35	C34	C33	114.9(15)	C54	C49A	Se2	120.8(14)
C35	C34	C41	113.0(17)	C54	C49A	C50	121.4(17)
C34	C35	C36	109.2(16)				

Table 6 Torsion Angles for A22.

A	B	C	D	Angle/˚	A	B	C	D	Angle/˚
Te1	C1	C2	C3	173.6(11)	C33	C34	C41	C42	-179(2)
Te1	C1	C10	C5	-173.6(8)	C33	C34A	C35A	C36A	-179(3)
Te1	C1	C10	C9	6.6(8)	C33	C34A	C35A	C40A	1(6)
Te1	C13	C14	C15	172.2(10)	C33	C34A	C41A	C42A	180(3)
Te1	C13	C18	C17	-172.3(8)	C34	C35	C36	C37	178(2)
Te2	C31	C32	C33	174.5(5)	C34	C35	C36	C42	-2(3)
Te2	C31	C40	C35	-174.1(19)	C34	C35	C40	C31	2(4)
Te2	C31	C40	C39	9(3)	C34	C35	C40	C39	180(3)
Te2	C31	C40A	C35A	-175(2)	C34	C41	C42	C36	-1(3)
Te2	C31	C40A	C39A	7(5)	C35	C34	C41	C42	-1(3)
Te2	C43	C44	C45	177.1(9)	C35	C36	C37	C38	3(4)
Te2	C43	C48	C47	-178.2(9)	C35	C36	C42	C41	2(3)
Te2	Se2A	C39A	C38A	173(3)	C36	C35	C40	C31	178(2)
Te2	Se2A	C39A	C40A	-11(3)	C36	C35	C40	C39	-4(4)

Table 6 Torsion Angles for A22.

A	B	C	D	Angle/˚	A	B	C	D	Angle/˚
Se1	C9	C10	C1	3.1(7)	C36	C37	C38	C39	-3(4)
Se1	C9	C10	C5	-176.6(7)	C37	C36	C42	C41	-178(3)
Se1	C19	C20	C21	174.8(6)	C37	C38	C39	Se2	175.6(18)
Se1	C19	C24	C23	-172.8(9)	C37	C38	C39	C40	-1(4)
Se2	C39	C40	C31	5(4)	C38	C39	C40	C31	-178(2)
Se2	C39	C40	C35	-172.7(19)	C38	C39	C40	C35	4(4)
C1	C2	C3	C4	4(2)	C40	C31	C32	C33	0.1(14)
C2	C1	C10	C5	6.0(11)	C40	C35	C36	C37	1(4)
C2	C1	C10	C9	-173.8(9)	C40	C35	C36	C42	-179(3)
C2	C3	C4	C5	-2(2)	C41	C34	C35	C36	2(3)
C2	C3	C4	C11	-176.3(16)	C41	C34	C35	C40	178(3)
C3	C4	C5	C6	-179.2(14)	C42	C36	C37	C38	-178(3)
C3	C4	C5	C10	3(2)	C43	C44	C45	C46	0.1(19)
C3	C4	C11	C12	176.9(18)	C44	C43	C48	C47	-3.0(17)
C4	C5	C6	C7	-178.9(12)	C44	C45	C46	C47	-1.0(19)
C4	C5	C6	C12	3.7(16)	C45	C46	C47	C48	0.0(18)
C4	C5	C10	C1	-4.6(15)	C46	C47	C48	C43	2.0(18)
C4	C5	C10	C9	175.2(10)	C48	C43	C44	C45	1.9(17)
C4	C11	C12	C6	-0.3(18)	C49	Se2A	C39A	C38A	-91(3)
C5	C4	C11	C12	2.4(17)	C49	Se2A	C39A	C40A	86(3)
C5	C6	C7	C8	3.3(18)	C49	C50A	C51A	C52A	-8(4)
C5	C6	C12	C11	-1.9(17)	C50	C51	C52	C53	9(3)
C6	C5	C10	C1	177.7(10)	C51	C50	C49A	Se2	-179.3(15)
C6	C5	C10	C9	-2.5(14)	C51	C50	C49A	C54	1(2)
C6	C7	C8	C9	-2.2(18)	C51	C52	C53	C54	-7(3)
C7	C6	C12	C11	-178.8(15)	C52	C53	C54	C49A	2.7(16)
C7	C8	C9	Se1	178.8(9)	C53	C54	C49A	Se2	-179.2(12)
C7	C8	C9	C10	-1.6(15)	C53	C54	C49A	C50	0.3(15)
C8	C9	C10	C1	-176.5(9)	Se2A	C49	C50A	C51A	-176(2)
C8	C9	C10	C5	3.7(11)	Se2A	C49	C54A	C53A	177(2)
C10	C1	C2	C3	-6.1(18)	Se2A	C39A	C40A	C31	6(6)
C10	C5	C6	C7	-1.0(18)	Se2A	C39A	C40A	C35A	-172(3)
C10	C5	C6	C12	-178.4(12)	C50A	C49	C54A	C53A	-2(2)
C11	C4	C5	C6	-3.9(17)	C50A	C51A	C52A	C53A	14(5)
C11	C4	C5	C10	178.2(11)	C51A	C52A	C53A	C54A	-14(5)
C12	C6	C7	C8	179.9(15)	C52A	C53A	C54A	C49	7(4)
C13	C14	C15	C16	-0.6(18)	C54A	C49	C50A	C51A	3(2)
C14	C13	C18	C17	-0.3(12)	C34A	C35A	C36A	C37A	-180(3)
C14	C15	C16	C17	1(2)	C34A	C35A	C36A	C42A	1(4)
C15	C16	C17	C18	-2(2)	C34A	C35A	C40A	C31	-1(5)
C16	C17	C18	C13	1.1(17)	C34A	C35A	C40A	C39A	177(4)
C18	C13	C14	C15	0.1(14)	C34A	C41A	C42A	C36A	-3(4)
C19	C20	C21	C22	-0.5(11)	C35A	C34A	C41A	C42A	4(4)
C20	C19	C24	C23	2.5(16)	C35A	C36A	C37A	C38A	2(5)
C20	C21	C22	C23	-0.9(12)	C35A	C36A	C42A	C41A	1(3)
C21	C22	C23	C24	3.1(16)	C36A	C35A	C40A	C31	179(3)

Table 6 Torsion Angles for A22.

A	B	C	D	Angle/˚	A	B	C	D	Angle/˚
C22	C23	C24	C19	-3.9(17)	C36A	C35A	C40A	C39A	-2(5)
C24	C19	C20	C21	-0.3(14)	C36A	C37A	C38A	C39A	0(5)
C31	C32	C33	C34	-1.7(14)	C37A	C36A	C42A	C41A	-177(4)
C31	C32	C33	C34A	0.9(18)	C37A	C38A	C39A	Se2A	173(3)
C32	C31	C40	C35	0(3)	C37A	C38A	C39A	C40A	-3(5)
C32	C31	C40	C39	-178(2)	C38A	C39A	C40A	C31	-178(3)
C32	C31	C40A	C35A	2(4)	C38A	C39A	C40A	C35A	4(5)
C32	C31	C40A	C39A	-177(3)	C40A	C31	C32	C33	-2(2)
C32	C33	C34	C35	3(3)	C40A	C35A	C36A	C37A	0(5)
C32	C33	C34	C41	-179(2)	C40A	C35A	C36A	C42A	-179(3)
C32	C33	C34A	C35A	-1(4)	C41A	C34A	C35A	C36A	-3(4)
C32	C33	C34A	C41A	-176(3)	C41A	C34A	C35A	C40A	177(3)
C33	C34	C35	C36	-180(2)	C42A	C36A	C37A	C38A	180(4)
C33	C34	C35	C40	-3(4)	C49A	C50	C51	C52	-5(3)

Table 7 Hydrogen Atom Coordinates (Å×10^4) and Isotropic Displacement Parameters (Å^2×10^3) for A22.

Atom	*x*	*y*	*z*	U(eq)
H2	2683.53	2022.22	8424.06	91
H3	4087.36	1287.18	8845.11	117
H7	774.7	-1209.46	8647.59	99
H8	-679.69	-543.45	8195.36	94
H11A	4108.02	-37.96	9495.99	128
H11B	4453.21	-198.91	8786.83	128
H12A	3274.67	-1080.46	8714.32	128
H12B	2935.73	-922.61	9424.13	128
H14	761.41	1844.81	9510.88	97
H15	1.4	1904.97	10471.93	101
H16	-1851.4	2157.86	10484.65	103
H17	-2941.06	2298.51	9535.34	102
H18	-2211.13	2250.78	8534.92	84
H20	-180.86	-183.92	6999.61	64
H21	-44.84	-298.12	5885.85	69
H22	-631.96	572.82	5188.03	70
H23	-1419.66	1542.23	5592.96	85
H24	-1443.41	1677.24	6700.27	72
H32	447.01	3298	9414.52	78
H33	325.03	3659.36	10454.51	87
H33A	368.29	3684.33	10491.84	87
H37	3037.02	6305.82	10096.23	79
H38	3126.82	6104.11	9073.45	78
H41A	499.87	4952.36	11207.16	98
H41B	1656.3	4573.2	11405.47	98
H42A	2521.87	5496.03	11302	103
H42B	1371.36	5871.46	11095.54	103
H44	3172.87	3319.08	9354.44	74

Table 7 Hydrogen Atom Coordinates (Å×10^4) and Isotropic Displacement Parameters (Å^2×10^3) for A22.

Atom	*x*	*y*	*z*	U(eq)
H45	5044.52	3050.5	9545.55	86
H46	6174.61	3078.45	8704.8	78
H47	5431.41	3346.4	7678.41	81
H48	3536.38	3583.66	7488.89	72
H50	1529.6	6461.6	8270.77	62
H51	-145.13	7057.16	8047.35	84
H52	-1573.88	6517.83	7357.52	82
H53	-1526.96	5381.16	7161.1	70
H54	138.61	4778.92	7428.27	55
H50A	1518.87	6336.77	7948.47	106
H51A	-199.04	6920.48	7682.77	114
H52A	-1506.3	6309.66	6956.79	118
H53A	-1487.02	5149.74	6918.81	112
H54A	248.63	4600.4	7214.88	112
H37A	3047.52	6340.71	9791.56	79
H38A	3157.22	6056.58	8791.12	82
H41C	703.4	5091.57	11089.21	87
H41D	1878.64	4725.06	11249.81	87
H42C	2694.08	5649.07	11063.13	81
H42D	1520.39	6003.15	10863	81

Table 8 Atomic Occupancy for A22.

Atom	*Occupancy*	Atom	*Occupancy*	Atom	*Occupancy*
Se2	0.57(2)	H33	0.57(2)	H33A	0.43(2)
C34	0.57(2)	C35	0.57(2)	C36	0.57(2)
C37	0.57(2)	H37	0.57(2)	C38	0.57(2)
H38	0.57(2)	C39	0.57(2)	C40	0.57(2)
C41	0.57(2)	H41A	0.57(2)	H41B	0.57(2)
C42	0.57(2)	H42A	0.57(2)	H42B	0.57(2)
C49	0.43(2)	C50	0.57(2)	H50	0.57(2)
C51	0.57(2)	H51	0.57(2)	C52	0.57(2)
H52	0.57(2)	C53	0.57(2)	H53	0.57(2)
C54	0.57(2)	H54	0.57(2)	Se2A	0.43(2)
C50A	0.43(2)	H50A	0.43(2)	C51A	0.43(2)
H51A	0.43(2)	C52A	0.43(2)	H52A	0.43(2)
C53A	0.43(2)	H53A	0.43(2)	C54A	0.43(2)
H54A	0.43(2)	C34A	0.43(2)	C35A	0.43(2)
C36A	0.43(2)	C37A	0.43(2)	H37A	0.43(2)
C38A	0.43(2)	H38A	0.43(2)	C39A	0.43(2)
C40A	0.43(2)	C41A	0.43(2)	H41C	0.43(2)
H41D	0.43(2)	C42A	0.43(2)	H42C	0.43(2)
H42D	0.43(2)	C49A	0.57(2)		

Table 9 Solvent masks information for A22.

Number	X	Y	Z	Volume	Electron count	Content
1	-0.951	0.000	0.000	444.6	142.1	3.4 CH2Cl2
2	-0.757	0.500	0.500	444.6	142.1	3.4 CH2Cl2

X-ray Crystallographic Structure determination on $[N23]BF_4$

Data Collection

A red needle crystal of $C_{10}H_6BF_4S_2$ having approximate dimensions of 0.200 x 0.060 x 0.010 mm was mounted in a loop. All measurements were made on a Rigaku Saturn724 diffractometer using multi-layer mirror monochromated Mo-Ka radiation.

Cell constants and an orientation matrix for data collection corresponded to a primitive orthorhombic cell with dimensions:

a = 10.11690 Å
b = 6.60720 Å
c = 46.90380 Å
V = 3135.25551 Å3

For Z = 12 and F.W. = 277.08, the calculated density is 1.761 g/cm3. Based on the reflection conditions of:

h0l: h+l = 2n

packing considerations, a statistical analysis of intensity distribution, and the successful solution and refinement of the structure, the space group was determined to be:

Pmn21 (#31)

The data were collected at a temperature of -179 ± 1oC to a maximum 2q value of 54.2o.

Data Reduction

Of the 16907 reflections were collected, where 5414 were unique (Rint = 0.0623); equivalent reflections were merged. Data were collected and processed using CrystalClear (Rigaku). 1

The linear absorption coefficient, m, for Mo-Ka radiation is 5.337 cm-1. The data were corrected for Lorentz and polarization effects.

Structure Solution and Refinement

The structure was solved by direct methods2 and expanded using Fourier techniques. The non-hydrogen atoms were refined anisotropically. Hydrogen atoms were refined using the riding model. The final cycle of full-matrix least-squares refinement3 on F2 was based on 5413 observed reflections and 507 variable parameters and converged (largest parameter shift was 0.03 times its esd) with unweighted and weighted agreement factors of:

$R1 = S ||Fo| - |Fc|| / S |Fo| = 0.0697$

$wR2 = [S (w (Fo2 - Fc2)2)/ S w(Fo2)2]1/2 = 0.1738$

The goodness of fit4 was 1.15. Unit weights were used. The maximum and minimum peaks on the final difference Fourier map corresponded to 0.86 and -0.62 e-/Å3, respectively. The final Flack parameter 5 was 0.60(17).

Neutral atom scattering factors were taken from International Tables for Crystallography (IT), Vol. C, Table 6.1.1.4 6. Anomalous dispersion effects were included in Fcalc7; the values for Df' and Df'' were those of Creagh and McAuley8. The values for the mass attenuation coefficients are those of Creagh and Hubbell9. All calculations were performed using the CrystalStructure10 crystallographic software package except for refinement, which was performed using SHELXL Version 2018/311.

Further refinement was undertaken with SHELXL within the Olex2 v. 1.5 suite.[11]

Table 1 Crystal data and structure refinement for $[N23]BF_4$.

Identification code	$[N23]BF_4$
Empirical formula	$C_{10}H_6BF_4S_2$
Formula weight	277.08
Temperature/K	93.25
Crystal system	orthorhombic
Space group	$Pmn2_1$
a/Å	10.1169(9)
b/Å	6.6072(6)
c/Å	46.904(4)
α/°	90
β/°	90
γ/°	90
Volume/$Å^3$	3135.3(5)
Z	12
$\rho_{calc}g/cm^3$	1.761
μ/mm^{-1}	0.534
F(000)	1668.0
Crystal size/mm^3	0.2 × 0.06 × 0.01
Radiation	MoKα (λ = 0.71069)
2Θ range for data collection/°	6.226 to 54.178
Index ranges	-8 ≤ h ≤ 12, -8 ≤ k ≤ 5, -57 ≤ l ≤ 60
Reflections collected	16895
Independent reflections	5411 [R_{int} = 0.0612, R_{sigma} = 0.0381]
Data/restraints/parameters	5411/607/506
Goodness-of-fit on F^2	1.151
Final R indexes [I>=2σ (I)]	R_1 = 0.0698, wR_2 = 0.1561
Final R indexes [all data]	R_1 = 0.0779, wR_2 = 0.1614
Largest diff. peak/hole / e $Å^{-3}$	0.77/-0.67
Flack parameter	0.4(2)

Table 2 Fractional Atomic Coordinates (×10^4) and Equivalent Isotropic Displacement Parameters ($Å^2$×10^3) for $[N23]BF_4$. U_{eq} is defined as 1/3 of the trace of the orthogonalised U_{IJ} tensor.

Atom	*x*	*y*	*z*	U(eq)
S1	-1012(3)	-4669(4)	-3644.6(6)	18.7(6)
C1	-1172(12)	-4869(16)	-4013(2)	17(2)
C2	0	-4900(20)	-4167(3)	16(3)
C3	0	-5060(20)	-4465(3)	15(3)
C4	-1243(12)	-5162(18)	-4602(2)	26(3)
C5	-2412(13)	-5039(18)	-4450(3)	24(2)
C6	-2412(13)	-4900(16)	-4151(2)	19(2)
S2	-1009(3)	-9942(4)	-4529.3(5)	17.0(6)
C7	-1224(13)	-9729(17)	-4166(2)	18(2)
C8	0	-9670(20)	-4013(3)	18(3)
C9	0	-9470(20)	-3704(3)	16(3)

Table 2 Fractional Atomic Coordinates (×10^4) and Equivalent Isotropic Displacement Parameters (Å^2×10^3) for [N23]BF_4. U_{eq} is defined as 1/3 of the trace of the orthogonalised U_{IJ} tensor.

Atom	*x*	*y*	*z*	U(eq)
C10	-1244(11)	-9377(17)	-3562(2)	17(2)
C11	-2412(11)	-9452(15)	-3726(2)	17(2)
C12	-2404(13)	-9644(16)	-4020(2)	20(2)
S3	-3984(3)	-2969(4)	-5346.3(5)	15.6(6)
C13	-3820(10)	-3340(15)	-5709(2)	11.5(19)
C14	-5000	-3490(20)	-5861(3)	12(3)
C15	-5000	-3840(20)	-6162(3)	15(3)
C16	-3755(12)	-4094(17)	-6296(2)	19(2)
C17	-2604(12)	-3854(17)	-6148(2)	20(2)
C18	-2577(11)	-3535(16)	-5845(2)	14(2)
S4	-3987(3)	-8649(4)	-6161.0(5)	11.7(5)
C19	-3810(10)	-8286(16)	-5799(2)	12.5(19)
C20	-5000	-8120(20)	-5645(3)	12(3)
C21	-5000	-7780(20)	-5351(3)	14(3)
C22	-3769(12)	-7600(17)	-5214(2)	19(2)
C23	-2594(11)	-7798(16)	-5366(2)	18(2)
C24	-2583(11)	-8126(15)	-5658(2)	12.9(19)
S5	-1008(3)	-2653(4)	-7821.1(5)	14.4(5)
C25	-1204(11)	-2281(17)	-7456(2)	19(2)
C26	0	-2090(30)	-7300(3)	20(3)
C27	0	-1690(20)	-7006(4)	19(3)
C28	-1257(12)	-1489(17)	-6870(2)	19(2)
C29	-2425(12)	-1702(15)	-7028(2)	17(2)
C30	-2418(12)	-2060(17)	-7314(2)	20(2)
S6	-1009(3)	-6908(4)	-7015.3(5)	15.6(5)
C31	-1194(11)	-7362(16)	-7378(2)	15(2)
C32	0	-7510(20)	-7524(3)	13(3)
C33	0	-7850(20)	-7830(3)	15(3)
C34	-1245(11)	-8018(16)	-7966(2)	17(2)
C35	-2414(11)	-7810(15)	-7813(2)	16(2)
C36	-2427(11)	-7497(16)	-7516(2)	16(2)
B1	0	-1870(30)	-5283(4)	22(3)
F1	0	-1109(14)	-5559.7(19)	22(2)
F2	-1131(7)	-3016(10)	-5241.6(14)	24.7(16)
F3	0	-171(16)	-5095(2)	29(2)
B2	-5000	-1250(30)	-4583(4)	20(3)
F4	-5000	-2022(15)	-4300.9(19)	21(2)
F5	-3866(8)	-53(11)	-4625.2(17)	34(2)
F6	-5000	-2864(15)	-4778(2)	25(2)
B3	0	-7560(30)	-6246(4)	18(3)
F7	0	-6594(12)	-5983(2)	17(2)
F8	-1144(7)	-8755(11)	-6270.4(16)	29.0(17)
F9	0	-6071(17)	-6468.2(19)	27(2)
B4	-5000	-8020(30)	-6928(4)	23(3)
F10	-5000	-9447(16)	-6710(2)	30(2)

Table 2 Fractional Atomic Coordinates (×10^4) and Equivalent Isotropic Displacement Parameters (Å^2×10^3) for [N23]BF$_4$. U$_{eq}$ is defined as 1/3 of the trace of the orthogonalised U$_{IJ}$ tensor.

Atom	*x*	*y*	*z*	U(eq)
F11	-3893(8)	-6795(12)	-6899.2(16)	32.3(18)
F12	-5000	-9037(15)	-7187.6(19)	22(2)
B5	0	-4240(30)	-8577(4)	25(4)
F13	0	-3352(15)	-8845(2)	26(2)
F14	0	-2637(19)	-8377(2)	41(3)
F15	-1118(8)	-5394(12)	-8545.4(16)	33.3(19)
B6	-5000	-3780(30)	-7884(4)	21(3)
F16	-5000	-4556(15)	-7609(2)	26(2)
F17	-3870(8)	-2593(11)	-7929.5(15)	32.1(18)
F18	-5000	-5394(15)	-8080(2)	29(2)

Table 3 Anisotropic Displacement Parameters (Å^2×10^3) for [N23]BF$_4$. The Anisotropic displacement factor exponent takes the form: -2π^2[h^{2}a*^{2}U$_{11}$+2hka*b*U$_{12}$+…].

Atom	U$_{11}$	U$_{22}$	U$_{33}$	U$_{23}$	U$_{13}$	U$_{12}$
S1	14.3(13)	20.3(14)	21.5(14)	-0.8(10)	1.0(13)	0.5(11)
C1	17(2)	16(2)	17(2)	0.1(13)	-0.4(13)	-0.1(14)
C2	16(3)	15(3)	16(3)	0.0(14)	0	0
C3	15(3)	14(4)	16(3)	1(2)	0	0
C4	24(3)	27(4)	26(3)	1(2)	-2(2)	-2(2)
C5	23(3)	24(3)	24(3)	1(2)	-2(2)	-1(3)
C6	18(2)	18(3)	20(2)	0.1(14)	-0.3(13)	0.5(14)
S2	11.3(13)	21.7(15)	18.1(13)	-2.2(10)	-1.7(13)	0.9(11)
C7	18(2)	17(3)	18(2)	0.2(13)	0.3(13)	0.0(14)
C8	18(3)	18(3)	18(3)	-0.3(14)	0	0
C9	16(3)	16(3)	16(3)	0.0(14)	0	0
C10	17(2)	17(2)	17(2)	0.7(14)	1.7(13)	0.7(14)
C11	16(3)	16(3)	19(3)	0(2)	4(2)	1(2)
C12	18(3)	20(3)	22(3)	-1(2)	1(2)	-1(2)
S3	9.6(12)	19.1(16)	18.2(12)	-2.8(10)	0.0(12)	-0.6(10)
C13	12(2)	11(2)	12(2)	-0.3(13)	-0.3(13)	-0.5(13)
C14	12(3)	12(3)	12(3)	0.0(14)	0	0
C15	16(3)	15(4)	14(3)	1(3)	0	0
C16	19(3)	19(3)	18(3)	0(2)	1(2)	2(2)
C17	20(3)	20(3)	21(3)	0(2)	2(2)	0(2)
C18	13(2)	13(2)	14(2)	0.5(13)	0.6(13)	0.1(14)
S4	9.1(10)	12.8(12)	13.3(10)	-1.7(8)	0.1(10)	2.4(10)
C19	13(2)	12(2)	13(2)	0.2(13)	0.0(13)	-0.4(13)
C20	12(3)	12(3)	13(3)	0.1(14)	0	0
C21	14(3)	14(3)	15(3)	0.1(14)	0	0
C22	20(3)	19(3)	19(3)	0(2)	-1(2)	0(2)
C23	17(3)	19(3)	20(3)	-1(2)	-2(2)	0(2)
C24	11(3)	11(3)	17(3)	-1(2)	0(2)	1(2)
S5	13.7(12)	12.7(14)	16.7(12)	-1.8(10)	-1.3(12)	0.2(10)
C25	20(3)	19(3)	18(3)	0(2)	1(2)	-2(2)

Table 3 Anisotropic Displacement Parameters ($Å^2×10^3$) for [N23]BF_4. The Anisotropic displacement factor exponent takes the form: $-2\pi^2[h^2a^{*2}U_{11}+2hka^*b^*U_{12}+\ldots]$.

Atom	U_{11}	U_{22}	U_{33}	U_{23}	U_{13}	U_{12}
C26	20(4)	20(4)	21(4)	1(3)	0	0
C27	19(4)	17(4)	19(3)	2(3)	0	0
C28	20(3)	18(3)	20(3)	-2(2)	0(2)	2(2)
C29	17(2)	16(2)	17(2)	0.9(14)	0.8(13)	0.6(14)
C30	19(3)	20(3)	21(3)	2(2)	-1(2)	0(2)
S6	12.9(12)	14.9(14)	19.0(12)	-0.4(10)	0.3(12)	0.3(10)
C31	15(3)	14(3)	15(3)	1(2)	1(2)	-1(2)
C32	13(3)	13(4)	14(3)	-1(3)	0	0
C33	15(3)	14(3)	15(3)	0.1(14)	0	0
C34	17(3)	15(3)	17(3)	0(2)	-2(2)	0(2)
C35	15(3)	15(3)	17(3)	0(2)	-3(2)	-2(2)
C36	15(3)	15(3)	19(3)	-2(2)	0(2)	2(2)
B1	21(4)	22(4)	22(4)	-0.4(14)	0	0
F1	17(5)	28(5)	21(4)	-6(4)	0	0
F2	17(4)	32(4)	25(3)	5(3)	-1(3)	-10(3)
F3	21(6)	37(6)	29(5)	-7(4)	0	0
B2	13(7)	30(9)	18(6)	6(5)	0	0
F4	18(5)	34(6)	10(4)	-1(3)	0	0
F5	20(4)	42(5)	40(5)	10(3)	3(4)	-7(3)
F6	24(6)	35(6)	16(4)	7(4)	0	0
B3	17(4)	19(4)	18(4)	-2(2)	0	0
F7	19(5)	12(4)	21(4)	-5(3)	0	0
F8	17(4)	37(4)	33(4)	-9(3)	-4(3)	-9(3)
F9	22(5)	46(6)	14(4)	2(4)	0	0
B4	15(6)	31(6)	21(5)	-6(4)	0	0
F10	31(6)	36(6)	24(5)	-7(4)	0	0
F11	19(4)	50(5)	28(4)	-11(3)	2(3)	-11(3)
F12	11(4)	40(6)	14(4)	-4(4)	0	0
B5	25(4)	25(4)	25(4)	0.3(14)	0	0
F13	18(5)	37(6)	24(5)	9(4)	0	0
F14	31(7)	65(7)	26(5)	-8(5)	0	0
F15	23(4)	52(5)	26(4)	15(3)	-2(3)	-6(3)
B6	13(7)	34(9)	18(6)	1(6)	0	0
F16	23(5)	34(6)	21(4)	5(4)	0	0
F17	28(4)	36(4)	32(4)	1(3)	2(3)	-16(3)
F18	29(6)	38(6)	20(5)	-2(4)	0	0

Table 4 Bond Lengths for [N23]BF_4.

Atom	Atom	Length/Å	Atom	Atom	Length/Å
S1	$S1^1$	2.048(6)	S5	$S5^1$	2.039(6)
S1	C1	1.741(11)	S5	C25	1.739(11)
C1	C2	1.388(14)	C25	C26	1.428(14)
C1	C6	1.411(16)	C25	C30	1.405(16)
C2	C3	1.40(2)	C26	C27	1.40(2)

Table 4 Bond Lengths for $[N23]BF_4$.

Atom	Atom	Length/Å	Atom	Atom	Length/Å
C3	C4[1]	1.412(14)	C27	C28[1]	1.429(14)
C3	C4	1.412(14)	C27	C28	1.429(14)
C4	H4	0.9500	C28	H28	0.9500
C4	C5	1.383(17)	C28	C29	1.402(16)
C5	H5	0.9500	C29	H29	0.9500
C5	C6	1.406(16)	C29	C30	1.363(15)
C6	H6	0.9500	C30	H30	0.9500
S2	S2[1]	2.042(6)	S6	S6[1]	2.041(6)
S2	C7	1.722(12)	S6	C31	1.738(10)
C7	C8	1.432(15)	C31	C32	1.392(13)
C7	C12	1.378(17)	C31	C36	1.408(15)
C8	C9	1.46(2)	C32	C33	1.45(2)
C9	C10	1.425(13)	C33	C34	1.416(13)
C9	C10[1]	1.425(13)	C33	C34[1]	1.416(13)
C10	H10	0.9500	C34	H34	0.9500
C10	C11	1.412(16)	C34	C35	1.389(16)
C11	H11	0.9500	C35	H35	0.9500
C11	C12	1.383(15)	C35	C36	1.409(15)
C12	H12	0.9500	C36	H36	0.9500
S3	S3[2]	2.055(6)	B1	F1	1.39(2)
S3	C13	1.729(10)	B1	F2	1.387(13)
C13	C14	1.393(12)	B1	F2[1]	1.387(13)
C13	C18	1.415(15)	B1	F3	1.42(2)
C14	C15	1.43(2)	B2	F4	1.416(19)
C15	C16[2]	1.418(14)	B2	F5	1.409(13)
C15	C16	1.418(13)	B2	F5[2]	1.409(13)
C16	H16	0.9500	B2	F6	1.40(2)
C16	C17	1.366(16)	B3	F7	1.39(2)
C17	H17	0.9500	B3	F8	1.407(12)
C17	C18	1.437(15)	B3	F8[1]	1.407(12)
C18	H18	0.9500	B3	F9	1.43(2)
S4	S4[2]	2.049(5)	B4	F10	1.39(2)
S4	C19	1.725(10)	B4	F11[2]	1.389(14)
C19	C20	1.410(13)	B4	F11	1.389(14)
C19	C24	1.409(15)	B4	F12	1.39(2)
C20	C21	1.40(2)	B5	F13	1.39(2)
C21	C22[2]	1.407(14)	B5	F14	1.42(2)
C21	C22	1.407(14)	B5	F15	1.372(14)
C22	H22	0.9500	B5	F15[1]	1.372(14)
C22	C23	1.394(16)	B6	F16	1.39(2)
C23	H23	0.9500	B6	F17[2]	1.403(13)
C23	C24	1.387(15)	B6	F17	1.403(13)
C24	H24	0.9500	B6	F18	1.41(2)

[1]-X,+Y,+Z; [2]-1-X,+Y,+Z

Table 5 Bond Angles for $[N23]BF_4$.

Atom	Atom	Atom	Angle/˚	Atom	Atom	Atom	Angle/˚
C1	S1	S1[1]	95.3(4)	C27	C26	C25[1]	121.4(7)
C2	C1	S1	115.9(9)	C27	C26	C25	121.4(7)
C2	C1	C6	121.5(11)	C26	C27	C28	117.1(8)
C6	C1	S1	122.5(9)	C26	C27	C28[1]	117.1(8)
C1	C2	C1[1]	117.4(14)	C28	C27	C28[1]	125.8(15)
C1[1]	C2	C3	121.3(7)	C29	C28	C27	120.3(11)
C1	C2	C3	121.3(7)	C30	C29	C28	122.2(11)
C2	C3	C4[1]	117.1(7)	C29	C30	C25	119.3(11)
C2	C3	C4	117.1(7)	C31	S6	S6[1]	96.2(4)
C4	C3	C4[1]	125.8(14)	C32	C31	S6	113.6(8)
C5	C4	C3	121.7(11)	C32	C31	C36	122.5(9)
C4	C5	C6	121.2(11)	C36	C31	S6	123.9(8)
C5	C6	C1	117.2(11)	C31	C32	C31[1]	120.4(13)
C7	S2	S2[1]	97.2(4)	C31[1]	C32	C33	119.8(7)
C8	C7	S2	112.9(10)	C31	C32	C33	119.8(7)
C12	C7	S2	127.2(10)	C34	C33	C32	117.2(7)
C12	C7	C8	119.8(11)	C34[1]	C33	C32	117.2(7)
C7[1]	C8	C7	119.7(15)	C34[1]	C33	C34	125.6(14)
C7	C8	C9	120.1(7)	C35	C34	C33	121.1(10)
C7[1]	C8	C9	120.1(7)	C34	C35	C36	122.2(10)
C10[1]	C9	C8	118.0(7)	C31	C36	C35	117.1(10)
C10	C9	C8	118.0(7)	F1	B1	F3	107.1(14)
C10[1]	C9	C10	124.0(14)	F2	B1	F1	109.1(10)
C11	C10	C9	118.8(10)	F2[1]	B1	F1	109.1(10)
C12	C11	C10	122.8(11)	F2[1]	B1	F2	111.1(14)
C7	C12	C11	120.3(12)	F2[1]	B1	F3	110.2(10)
C13	S3	S3[2]	95.5(4)	F2	B1	F3	110.2(10)
C14	C13	S3	115.4(8)	F5[2]	B2	F4	109.4(10)
C14	C13	C18	121.8(9)	F5	B2	F4	109.5(10)
C18	C13	S3	122.8(8)	F5[2]	B2	F5	109.1(14)
C13	C14	C13[2]	118.1(13)	F6	B2	F4	109.8(14)
C13[2]	C14	C15	121.0(6)	F6	B2	F5[2]	109.5(10)
C13	C14	C15	121.0(6)	F6	B2	F5	109.5(10)
C16[2]	C15	C14	117.2(8)	F7	B3	F8	109.3(9)
C16	C15	C14	117.2(8)	F7	B3	F8[1]	109.3(9)
C16	C15	C16[2]	125.3(15)	F7	B3	F9	109.4(13)
C17	C16	C15	121.2(11)	F8	B3	F8[1]	110.8(14)
C16	C17	C18	122.5(11)	F8	B3	F9	109.1(9)
C13	C18	C17	116.1(10)	F8[1]	B3	F9	109.1(9)
C19	S4	S4[2]	96.0(4)	F11[2]	B4	F10	108.9(10)
C20	C19	S4	115.3(8)	F11	B4	F10	108.9(10)
C24	C19	S4	124.2(8)	F11	B4	F11[2]	107.6(15)
C24	C19	C20	120.4(9)	F11	B4	F12	111.5(10)
C19[2]	C20	C19	117.4(13)	F11[2]	B4	F12	111.5(10)
C21	C20	C19	121.3(6)	F12	B4	F10	108.4(15)
C21	C20	C19[2]	121.3(7)	F13	B5	F14	106.6(15)

Table 5 Bond Angles for $[N23]BF_4$.

Atom	Atom	Atom	Angle/˚	Atom	Atom	Atom	Angle/˚
C20	C21	C22	117.7(7)	F15	B5	F13	109.5(10)
C20	C21	C22[2]	117.7(7)	F15[1]	B5	F13	109.5(10)
C22	C21	C22[2]	124.5(14)	F15	B5	F14	110.0(10)
C23	C22	C21	120.8(10)	F15[1]	B5	F14	110.0(10)
C24	C23	C22	121.9(11)	F15	B5	F15[1]	111.0(16)
C23	C24	C19	117.8(10)	F16	B6	F17	110.4(10)
C25	S5	S5[1]	96.6(4)	F16	B6	F17[2]	110.4(10)
C26	C25	S5	114.8(9)	F16	B6	F18	109.2(14)
C30	C25	S5	125.5(9)	F17	B6	F17[2]	109.1(15)
C30	C25	C26	119.5(10)	F17[2]	B6	F18	108.8(10)
C25	C26	C25[1]	117.2(14)	F17	B6	F18	108.8(10)

[1]-X,+Y,+Z; [2]-1-X,+Y,+Z

Table 6 Hydrogen Bonds for $[N23]BF_4$.

D	H	A	d(D-H)/Å	d(H-A)/Å	d(D-A)/Å	D-H-A/°
C18	H18	F2	0.95	2.45	3.204(13)	136.2
C24	H24	F7	0.95	2.34	3.189(12)	147.9
C24	H24	F8	0.95	2.50	3.245(13)	135.4
C30	H30	F17	0.95	2.51	3.257(14)	135.7
C34	H34	F15	0.95	2.61	3.226(12)	122.5
C36	H36	F11	0.95	2.53	3.285(14)	136.2
C36	H36	F12	0.95	2.35	3.192(13)	147.6

Table 7 Torsion Angles for $[N23]BF_4$.

A	B	C	D	Angle/˚	A	B	C	D	Angle/˚
S1[1]	S1	C1	C2	-1.5(10)	S4[2]	S4	C19	C20	-0.4(9)
S1[1]	S1	C1	C6	-178.6(9)	S4[2]	S4	C19	C24	-179.4(9)
S1	C1	C2	C1[1]	3.0(19)	S4	C19	C20	C19[2]	0.8(18)
S1	C1	C2	C3	180.0(11)	S4	C19	C20	C21	-178.7(11)
S1	C1	C6	C5	179.1(8)	S4	C19	C24	C23	178.8(8)
C1	C2	C3	C4	1(2)	C19	C20	C21	C22[2]	179.1(12)
C1[1]	C2	C3	C4[1]	-1(2)	C19[2]	C20	C21	C22	-179.1(12)
C1[1]	C2	C3	C4	177.5(13)	C19	C20	C21	C22	0(2)
C1	C2	C3	C4[1]	-177.5(13)	C19[2]	C20	C21	C22[2]	0(2)
C2	C1	C6	C5	2.2(17)	C20	C19	C24	C23	-0.1(16)
C2	C3	C4	C5	2(2)	C20	C21	C22	C23	-1.3(19)
C3	C4	C5	C6	-3.1(19)	C21	C22	C23	C24	1.6(17)
C4[1]	C3	C4	C5	-179.7(11)	C22[2]	C21	C22	C23	-180.0(9)
C4	C5	C6	C1	0.7(17)	C22	C23	C24	C19	-0.9(15)
C6	C1	C2	C1[1]	-179.9(8)	C24	C19	C20	C19[2]	179.8(8)
C6	C1	C2	C3	-3(2)	C24	C19	C20	C21	0.3(19)
S2[1]	S2	C7	C8	-1.0(10)	S5[1]	S5	C25	C26	0.9(10)

Table 7 Torsion Angles for $[N23]BF_4$.

A	B	C	D	Angle/°	A	B	C	D	Angle/°
$S2^1$	S2	C7	C12	-180.0(10)	$S5^1$	S5	C25	C30	177.5(10)
S2	C7	C8	$C7^1$	1.9(19)	S5	C25	C26	$C25^1$	-2(2)
S2	C7	C8	C9	179.2(11)	S5	C25	C26	C27	177.1(12)
S2	C7	C12	C11	-179.4(8)	S5	C25	C30	C29	-177.6(9)
C7	C8	C9	C10	1(2)	$C25^1$	C26	C27	$C28^1$	0(2)
$C7^1$	C8	C9	C10	178.7(12)	C25	C26	C27	$C28^1$	-178.9(13)
$C7^1$	C8	C9	$C10^1$	-1(2)	C25	C26	C27	C28	0(2)
C7	C8	C9	$C10^1$	-178.7(12)	$C25^1$	C26	C27	C28	178.9(13)
C8	C7	C12	C11	1.7(17)	C26	C25	C30	C29	-1.2(17)
C8	C9	C10	C11	-1.0(19)	C26	C27	C28	C29	0.5(19)
C9	C10	C11	C12	1.1(17)	C27	C28	C29	C30	-1.4(17)
$C10^1$	C9	C10	C11	179.0(9)	$C28^1$	C27	C28	C29	179.3(10)
C10	C11	C12	C7	-1.4(17)	C28	C29	C30	C25	1.8(17)
C12	C7	C8	$C7^1$	-179.0(9)	C30	C25	C26	$C25^1$	-178.6(9)
C12	C7	C8	C9	-2(2)	C30	C25	C26	C27	0(2)
$S3^2$	S3	C13	C14	0.2(9)	$S6^1$	S6	C31	C32	-1.0(9)
$S3^2$	S3	C13	C18	-178.2(8)	$S6^1$	S6	C31	C36	-178.8(9)
S3	C13	C14	$C13^2$	-0.4(18)	S6	C31	C32	$C31^1$	2.0(19)
S3	C13	C14	C15	-178.6(11)	S6	C31	C32	C33	-178.8(10)
S3	C13	C18	C17	179.5(8)	S6	C31	C36	C35	178.1(8)
C13	C14	C15	C16	2(2)	$C31^1$	C32	C33	$C34^1$	0.1(19)
C13	C14	C15	$C16^2$	176.2(12)	C31	C32	C33	$C34^1$	-179.1(12)
$C13^2$	C14	C15	$C16^2$	-2(2)	C31	C32	C33	C34	-0.1(19)
$C13^2$	C14	C15	C16	-176.2(12)	$C31^1$	C32	C33	C34	179.1(12)
C14	C13	C18	C17	1.2(16)	C32	C31	C36	C35	0.5(16)
C14	C15	C16	C17	-5.0(19)	C32	C33	C34	C35	1.7(18)
C15	C16	C17	C18	6.3(18)	C33	C34	C35	C36	-2.3(17)
$C16^2$	C15	C16	C17	-178.7(10)	$C34^1$	C33	C34	C35	-179.4(9)
C16	C17	C18	C13	-4.2(16)	C34	C35	C36	C31	1.1(15)
C18	C13	C14	$C13^2$	178.1(8)	C36	C31	C32	$C31^1$	179.8(9)
C18	C13	C14	C15	-0.2(19)	C36	C31	C32	C33	-1.0(19)

^{1}-X,+Y,+Z; ^{2}-1-X,+Y,+Z

Table 8 Hydrogen Atom Coordinates (Å×10^4) and Isotropic Displacement Parameters (Å^2×10^3) for $[N23]BF_4$.

Atom	*x*	*y*	*z*	U(eq)
H4	-1276.41	-5321.04	-4802.69	31
H5	-3229.41	-5047.2	-4549.47	28
H6	-3213.77	-4830.41	-4045.52	22
H10	-1285.91	-9267.21	-3360.14	21
H11	-3238.87	-9366.05	-3631.04	20
H12	-3215.44	-9717.24	-4121.08	24
H16	-3721.52	-4436.33	-6492.89	23
H17	-1790.84	-3900.31	-6249.05	24

Table 8 Hydrogen Atom Coordinates (Å×10^4) and Isotropic Displacement Parameters (Å^2×10^3) for [N23]BF$_4$.

Atom	*x*	*y*	*z*	U(eq)
H18	-1770.42	-3458.75	-5741.72	16
H22	-3737.78	-7341.09	-5014.41	23
H23	-1776.53	-7704.81	-5267.54	22
H24	-1775.37	-8239.09	-5760.47	15
H28	-1301.18	-1209.59	-6671.74	23
H29	-3249.85	-1592.94	-6932.48	20
H30	-3226.21	-2159.18	-7416.64	24
H34	-1281.67	-8276.32	-8165.14	20
H35	-3230.96	-7882.44	-7912.45	19
H36	-3232.36	-7380.83	-7413.56	20

References to the Crystallographic Section

(1) CrystalClear: Data Collection and Processing Software, Rigaku Corporation (1998-2015). Tokyo 196-8666, Japan.

(2) SHELXS97: Sheldrick, G. M. (2008). Acta Cryst. A64, 112-122.

(3) Least Squares function minimized: (SHELXL Version 2018/3)

Sw(Fo2-Fc2)2 where w = Least Squares weights.

(4) Goodness of fit is defined as:

[Sw(Fo2-Fc2)2/(No-Nv)]1/2

where: No = number of observations

Nv = number of variables

(5) International Tables for Crystallography, Vol.C (1992). Ed. A.J.C. Wilson, Kluwer Academic Publishers, Dordrecht, Netherlands, Table 6.1.1.4, pp. 572.

(6) Ibers, J. A. & Hamilton, W. C.; Acta Crystallogr., 17, 781 (1964).

(7) Creagh, D. C. & McAuley, W.J .; "International Tables for Crystallography", Vol C, (A.J.C. Wilson, ed.), Kluwer Academic Publishers, Boston, Table 4.2.6.8, pages 219-222 (1992).

(8) Creagh, D. C. & Hubbell, J.H..; "International Tables for Crystallography", Vol C, (A.J.C. Wilson, ed.), Kluwer Academic Publishers, Boston, Table 4.2.4.3, pages 200-206 (1992).

(9) CrystalStructure 4.3: Crystal Structure Analysis Package, Rigaku Corporation (2000-2019). Tokyo 196-8666, Japan.

(10) SHELXL Version 2018/3: Sheldrick, G. M. (2008). Acta Cryst. A64, 112-122.

(11) L . J. Bourhis, O. V. Dolomanov, R. J. Gildea, J. A. K. Howard, H. Puschmann, *Acta Crystallogr., Sect. A: Found. Crystallogr*. 2015, A**71**, 59.